

Electronic Supporting Information for

Access to luminescent mesophases of gold(I) chiral complexes by thermal or mechanic stimuli. The role of the tertiary carbon

*María Barcenilla,^a César L. Folcia,^b Josu Ortega,^b Jesús Etxebarria,^b Silverio Coco,^{*a} and Pablo Espinet.^{*a}*

^a IU CINQUIMA/Química Inorgánica, Facultad de Ciencias, Universidad de Valladolid, 47071 Valladolid, Castilla y León, Spain. Department of Physics, University of the Basque Country, UPV/EHU, 48080 Bilbao, Spain.

* E-mail addresses: silverio.coco@uva.es; espinet@qi.uva.es

Table of Contents

Experimental section	Page S2
¹H NMR spectra	Page S10
¹³C{¹H} NMR spectra	Page S16
¹⁹F NMR spectra	Page S21
MALDI-TOF mass spectra	Page S25
POM textures	Page S31
DSC scans	Page S34
UV-Visible and luminescence data	Page S38
X-ray diffraction diagrams	Page S51
References	Page S53

EXPERIMENTAL SECTION

General Considerations. General procedures are as reported before.¹ Elemental analyses were performed by the “Servicio de análisis elemental, CACTI, Universidad de Vigo”. IR spectra were recorded on a Perkin-Elmer Frontier spectrometer coupled to a Pike GladiATR-210 accessory. NMR spectra were recorded on Varian 500 instruments in CDCl₃. MALDI-TOF MS was performed using a Bruker Daltonics autoflex speed instrument equipped with nitrogen laser (340 nm). Positive-ion mode spectra were recorded using the reflective mode. The accelerating voltage was 19 kV. The analytical sample was obtained by mixing the dichloromethane or tetrahydrofuran solution of the sample (1 mg/mL) and a solution of the matrix in the same solvent (DCTB, 10 mg/mL) in a 1/5 (vol/vol) ratio. The prepared solution of the sample and the matrix (0.5 μL) was loaded on the MALDI plate and allowed to dry at 23°C before the plate was inserted into the vacuum chamber of the MALDI instrument. UV/Vis absorption spectra were obtained by means of a Shimadzu UV-2550 spectrophotometer, in dichloromethane ($\sim 1 \times 10^{-5}$ M).

Luminescence spectra were recorded with a Perkin-Elmer LS-55 spectrofluorimeter. Emission and excitation spectra at 298 K were measured in deoxygenated CH₂Cl₂ solutions in quartz tubes and in the mesophase by means of a remote fiber optic accessory with the sample placed between two quartz plates, and the Mettler FP-82HT hot stage. The emission spectrum of the ground phase was recorded at 298 K by means of the remote fiber optic probe, at the same time that the sample was being crushed on a quartz plate. Lifetime measurements in solution were carried out on a Edinburgh instrument (FLS980 spectrometer) at the LTI services of the University of Burgos. In mesophase, lifetime measurements were recorded on a Jobin-Yvon Horiba Fluorolog 3-22 Tau-3 spectrofluorimeter at the University of La Rioja.

Microscopy studies were carried out on a Leica DMRB microscope equipped with a Mettler FP82HT hot stage and a Mettler FP90 central processor, at a heating rate of 10 °C min⁻¹. DSC was

performed using a DSC Q20 from TA Instruments with samples (2–5 mg) sealed in aluminum pans and a scanning rate of 10 °C/min under a nitrogen atmosphere.

Specific rotations were measured using a Perkin-Elmer 343 polarimeter at 589 nm.

The X-ray diffraction diagrams were recorded using a Stoe Stadivari goniometer equipped with a Genix3D microfocus generator (Xenocs) and a Dectris Pilatus 100K detector. Temperature control was achieved using a nitrogen-gas Cryostream controller (Oxford Cryosystems) allowing for a temperature control of about 0.1 °C. Lindemann capillaries of diameter 0.6 μm were utilized. The exposure time was 2 minutes and the samples were continuously rotated during the measurements to reduce texture effects. Monochromatic Cu-Kα radiation ($\lambda = 1.5418 \text{ \AA}$) was used.

Literature methods were used to prepare $[\text{CNC}_6\text{H}_4\text{O}(\text{O})\text{CC}_6\text{H}_4\text{OC}_n\text{H}_{2n+1}\text{-}p]$ ($n = 6, 8, 10$),^{1,2} and $[\text{AuCl}(\text{tht})]$ (tht = tetrahydrothiophene).³ The new chiral isocyanide ligand was prepared from the chiral nitro precursor, as reported for similar isocyanides.⁴

The chiral chain was introduced in the corresponding phenol derivatives, using the Mitsunobu reaction with (S)-2-octanol (Aldrich), triphenylphosphine, and diethyl azodicarboxylate to give the (R)-2-octyl derivative.⁵

Only example procedures are described, as the syntheses were similar for the rest of the compounds. Yields, IR, and analytical data are given for all the gold complexes.

Preparation of (R)-1-(2-octyloxy)-2,3,5,6-tetrafluorobenzene

Diethyl azodicarboxylate (0.83 g, 5 mmol) were added slowly to a solution of 2,3,5,6-tetrafluorophenol (0.83 g, 5 mmol) and triphenylphosphine (1.64 g, 6.2 mmol) in 50 mL of tetrahydrofuran, with stirring and under nitrogen atmosphere. A solution of (S)-2-octanol (0.8 mL, 6.2 mmol) in 10 mL of tetrahydrofuran was then added dropwise. After reacting for 20 h at room temperature, the reaction mixture was evaporated to dryness. The residue was chromatographed (silica gel, hexane as eluent) and the hexane was evaporated to obtain the product as a colorless

liquid. Yield: 0.9 g, 65 %. ^1H NMR (CDCl_3 , 500 MHz): δ_1 6.76 (m, 1H, Ar), δ_2 4.39 (m, 1H, CH), δ_3 1.69 (m, 2H, O-CH- CH_2), δ_4 1.44 (m, 2H, O-CH- CH_2 - CH_2), δ_5 1.30 (m, 6H, CH_2), δ_6 1.30 (d, 3H, CH- CH_3 , $J = 6.16$ Hz), δ_7 0.89 (t, 3H, CH_3 , $J = 6.99$ Hz). ^{19}F NMR (CDCl_3): δ_1 -140.48 (m, *Ortho*), δ_2 -156.06 (m, *Meta*). ^{13}C $\{^1\text{H}\}$ NMR (CDCl_3 , 126 MHz): 146.25 (dm, *Ortho*- C_{Ar} , $^1J_{\text{C-F}} = 246$ Hz), 141.69 (dm, *Meta*- C_{Ar} , $^1J_{\text{C-F}} = 246$ Hz), 137.37 (tt, C_{Ar} -O CH_2 , $^2J_{\text{C-F}} = 12$ Hz, $^3J_{\text{C-F}} = 4$ Hz), 99.28 (t, H- C_{Ar} , $^2J_{\text{C-F}} = 23$ Hz), 81.90 (CH), 36.73, 31.70, 29.15, 25.13, 22.51 (CH_2), 19.91 (CH- CH_3), 13.91 (CH_3). $[\alpha]_{589}^{25}$ (CHCl_3): 14.0 deg $\text{cm}^2 \text{g}^{-1}$.

Preparation of 4-Isocyanophenyl 4-((*R*)-2-octyloxybenzoate)

To a solution of 4-{4-((*R*)-2-octyloxybenzoyloxy)N-phenyl}formamide (1.40 g, 3.79 mmol), prepared by reaction of the amine with formic acid, and triethylamine (1.06 mL, 7.58 mmol) in 50 ml of CH_2Cl_2 was added dropwise a solution of triphosgene (0.38 g, 1.26 mmol) in 5 ml of CH_2Cl_2 under nitrogen. The mixture was stirred for 1h and then the solvent was removed on a rotary evaporator. The resulting residue was chromatographed (silica gel, CH_2Cl_2 /hexane, 1:1 as eluent) and the solvent was evaporated to obtain the product as a cream solid. Yield: 1.1 g, 82 %. ^1H NMR (CDCl_3 , 500 MHz): δ_1 8.09 (d, 2H, O(O)C-Ar, AA' part of AA'XX' spin system, $N = J_{\text{AX}} + J_{\text{AX}'} = 8.88$ Hz, $J_{\text{AA}'} \approx J_{\text{XX}'}$), δ_2 7.42 (d, 2H, CN-Ar, AA' part of AA'XX' spin system, $N = J_{\text{AX}} + J_{\text{AX}'} = 8.84$ Hz, $J_{\text{AA}'} \approx J_{\text{XX}'}$), δ_3 7.22 (d, 2H, CN-Ar, XX' part of AA'XX' spin system, $N = J_{\text{AX}} + J_{\text{AX}'} = 8.84$ Hz, $J_{\text{AA}'} \approx J_{\text{XX}'}$), δ_4 6.94 (d, 2H, O(O)C-Ar, XX' part of AA'XX' spin system, $N = J_{\text{AX}} + J_{\text{AX}'} = 8.88$ Hz, $J_{\text{AA}'} \approx J_{\text{XX}'}$), δ_5 4.47 (m, 1H, CH), δ_6 1.68 (m, 2H, O-CH- CH_2), δ_7 1.50-1.20 (m, 8H, CH_2), δ_8 1.33 (d, 3H, CH- CH_3 , $J = 6.13$ Hz), δ_9 0.87 (t, 3H, CH_3 , $J = 6.76$ Hz). ^{13}C $\{^1\text{H}\}$ NMR (CDCl_3 , 126 MHz): 164.39 ($\text{C}\equiv\text{N}$), 164.29 ($\text{C}=\text{O}$), 163.10 (C_{Ar} -O), 151.33 (C_{Ar} -O-C(O)), 132.42, 127.56 (C_{Ar} -H), 123.89 ($\text{C}\equiv\text{N}$ - C_{Ar}), 123.03 (C_{Ar} -H), 120.36 (O(O)C- C_{Ar}), 115.28 (C_{Ar} -H), 74.21 (Ar-O-CH), 36.25 (CH- CH_2), 31.73, 29.18, 25.38, 22.55 (CH_2), 19.55 (CH- CH_3), 14.04 (CH_2 - CH_3). IR (cm^{-1}): $\nu(\text{C}\equiv\text{N})$: 2122; $\nu(\text{C}=\text{O})$: 1733. Anal. calcd (%) for $\text{C}_{22}\text{H}_{25}\text{NO}_3$: C, 75.19; H, 7.17; N, 3.99. Found: C, 74.99; H, 7.32; N, 3.92. MALDI-TOF MS: m/z 352.1921 $[\text{M}+\text{H}]^+$ (calcd 352.1907 for $\text{C}_{22}\text{H}_{26}\text{NO}_3$). $[\alpha]_{589}^{25}$ (CHCl_3): 12.0 deg $\text{cm}^2 \text{g}^{-1}$.

Preparation of [Au(C₆F₄OR¹)(C≡NC₆H₄O(O)CC₆H₄OR²)] (R¹ = C₆H₁₃, C₈H₁₇, C₁₀H₂₁, (R)-2-Octyl; R² = C₆H₁₃, C₈H₁₇, C₁₀H₂₁, (R)-2-Octyl)

To a solution of HC₆F₄OR¹ (0.312 mmol) in 25 mL of dried diethyl ether was added a solution of n-butyllithium 1.6 M in hexane (0.194 mL, 0.312 mmol) at -78 °C, under nitrogen. After stirring for one hour at -50 °C, solid [AuCl(tht)] (0.96 g, 0.312 mmol) was added at -78 °C and the reaction mixture was slowly brought to room temperature (3 h). Then, a few drops of water were added and the solution was filtered in air through anhydrous MgSO₄. C≡NC₆H₄O(O)CC₆H₄OR² (0.312 mmol). was added to the solution obtained. After stirring for 15 min, the solvent was removed on a rotary evaporator and the white solid obtained was recrystallized from dichloromethane/hexane at -15 °C to give a white solid.

Yields, IR and analytical data are as follows:

R¹ = (R)-2-Octyl, R² = C₆H₁₃ (1). Yield: 0.13 g, 52 %. ¹H NMR (CDCl₃, 500 MHz): δ₁ 8.12 (d, 2H, O(O)C-Ar, AA' part of AA'XX' spin system, $N = J_{AX} + J_{AX'} = 8.93$ Hz, $J_{AA'} \approx J_{XX'}$), δ₂ 7.63 (d, 2H, CN-Ar, AA' part of AA'XX' spin system, $N = J_{AX} + J_{AX'} = 8.83$ Hz, $J_{AA'} \approx J_{XX'}$), δ₃ 7.40 (d, 2H, CN-Ar, XX' part of AA'XX' spin system, $N = J_{AX} + J_{AX'} = 8.83$ Hz, $J_{AA'} \approx J_{XX'}$), δ₄ 6.99 (d, 2H, O(O)C-Ar, XX' part of AA'XX' spin system, $N = J_{AX} + J_{AX'} = 8.93$ Hz, $J_{AA'} \approx J_{XX'}$), δ₅ 4.30 (m, 1H, CH), δ₆ 4.06 (t, 2H, O-CH₂, $J = 6.60$ Hz), δ₇ 1.80-1.27 (m, 18H, CH₂), δ₈ 1.28 (d, 3H, CH-CH₃, $J = 6.11$ Hz), δ₉ 0.92 (t, 3H, CH₃, $J = 7.02$ Hz), δ₁₀ 0.89 (t, 3H, CH₃, $J = 6.71$ Hz). ¹⁹F NMR (CDCl₃, 470 MHz): δ₁ -117.85 (m, F_{ortho}), δ₂ -155.94 (m, F_{meta}). ¹³C {¹H} NMR (CDCl₃, 126 MHz): 164.07 (C=O), 163.96 (O-C_{Ar}), 158.26 (C≡N), 153.16 (C_{Ar}-O-C(O)), 149.90 (dm, F_{ortho}-C_{Ar}, $^1J_{C-F} = 228$ Hz), 141.36 (dm, F_{meta}-C_{Ar}, $^1J_{C-F} = 248$ Hz), 134.71 (m, O-C_{Ar}), 132.47, 128.07 (C_{Ar}-H), 127.69 (m, C_{Ar}-Au), 123.79 (C_{Ar}-H), 121.51 (CN-C_{Ar}), 120.23 (OC(O)-C_{Ar}), 114.50 (C_{Ar}-H), 81.27 (Ar-O-CH), 68.43 (CH₂-O-Ar), 36.76 (CH-CH₂), 31.76, 31.50, 29.24, 28.99, 25.61, 25.24, 22.57, 22.55 (CH₂) 20.01 (CH-CH₃), 14.05, 13.99 (CH₂-CH₃). IR (cm⁻¹): ν(C≡N): 2216; ν(C=O): 1726. Anal. calcd (%) for C₃₄H₃₈AuF₄NO₄: C, 51.20; H, 4.80; N, 1.76. Found: C, 51.21; H, 4.56; N, 1.88.

MALDI-TOF MS: m/z 798.2441 $[M+H]^+$ (calcd 798.2475 for $C_{34}H_{39}AuF_4NO_4$). $[\alpha]_{546}^{25}$ ($CHCl_3$): 13.8 deg $cm^2 g^{-1}$.

R¹ = (R)-2-Octyl, R² = C₈H₁₇ (2). Yield: 0.15 g, 58 %. ¹H NMR ($CDCl_3$, 500 MHz): δ_1 8.12 (d, 2H, O(O)C-Ar, AA' part of AA'XX' spin system, $N = J_{AX} + J_{AX'} = 8.93$ Hz, $J_{AA'} \approx J_{XX'}$), δ_2 7.63 (d, 2H, CN-Ar, AA' part of AA'XX' spin system, $N = J_{AX} + J_{AX'} = 8.98$ Hz, $J_{AA'} \approx J_{XX'}$), δ_3 7.40 (d, 2H, CN-Ar, XX' part of AA'XX' spin system, $N = J_{AX} + J_{AX'} = 8.98$ Hz, $J_{AA'} \approx J_{XX'}$), δ_4 6.99 (d, 2H, O(O)C-Ar, XX' part of AA'XX' spin system, $N = J_{AX} + J_{AX'} = 8.93$ Hz, $J_{AA'} \approx J_{XX'}$), δ_5 4.31 (m, 1H, CH), δ_6 4.05 (t, 2H, O-CH₂, $J = 6.51$ Hz), δ_7 1.80-1.20 (m, 22H, CH₂), δ_8 1.28 (d, 3H, CH-CH₃, $J = 6.11$ Hz), δ_9 0.88 (t, 6H, CH₃, $J = 6.90$ Hz). ¹⁹F NMR ($CDCl_3$, 470 MHz): δ_1 -117.83 (m, *Fortho*), δ_2 -155.94 (m, *Fmeta*). ¹³C {¹H} NMR ($CDCl_3$, 126 MHz): 164.07 (C=O), 163.95 (O-C_{Ar}), 158.28 (C≡N), 153.16 (C_{Ar}-O-C(O)), 149.40 (dm, *Fortho*-C_{Ar}, $^1J_{C-F} = 228$ Hz), 141.38 (dm, *Fmeta*-C_{Ar}, $^1J_{C-F} = 248$ Hz), 134.71 (m, O-C_{Ar}), 132.47, 128.07 (C_{Ar}-H), 127.69 (m, C_{Ar}-Au), 123.79 (C_{Ar}-H), 121.51 (CN-C_{Ar}), 120.23 (O(O)C-C_{Ar}), 114.50 (C_{Ar}-H), 81.27 (Ar-O-CH), 68.43 (CH₂-O-Ar), 36.76 (CH-CH₂), 31.77, 29.29, 29.24, 29.18, 29.03, 25.94, 25.25, 22.62, 22.57 (CH₂), 20.01 (CH-CH₃), 14.07, 14.05 (CH₂-CH₃). IR (cm^{-1}): $\nu(C\equiv N)$: 2214; $\nu(C=O)$: 1726. Anal. calcd (%) for $C_{36}H_{42}AuF_4NO_4$: C, 52.37; H, 5.13; N, 1.70. Found: C, 52.46; H, 5.08; N, 1.82. MALDI-TOF MS: m/z 826.2760 $[M+H]^+$ (calcd 826.2788 for $C_{36}H_{43}AuF_4NO_4$). $[\alpha]_{546}^{25}$ ($CHCl_3$): 7.5 deg $cm^2 g^{-1}$.

R¹ = (R)-2-Octyl, R² = C₁₀H₂₁ (3). Yield: 0.15 g, 55 %. ¹H NMR ($CDCl_3$, 500 MHz): δ_1 8.12 (d, 2H, O(O)C-Ar, AA' part of AA'XX' spin system, $N = J_{AX} + J_{AX'} = 8.92$ Hz, $J_{AA'} \approx J_{XX'}$), δ_2 7.63 (d, 2H, CN-Ar, AA' part of AA'XX' spin system, $N = J_{AX} + J_{AX'} = 8.89$ Hz, $J_{AA'} \approx J_{XX'}$), δ_3 7.39 (d, 2H, CN-Ar, XX' part of AA'XX' spin system, $N = J_{AX} + J_{AX'} = 8.89$ Hz, $J_{AA'} \approx J_{XX'}$), δ_4 6.99 (d, 2H, O(O)C-Ar, XX' part of AA'XX' spin system, $N = J_{AX} + J_{AX'} = 8.92$ Hz, $J_{AA'} \approx J_{XX'}$), δ_5 4.30 (m, 1H, CH), δ_6 4.05 (t, 2H, O-CH₂, $J = 6.51$ Hz), δ_7 1.80-1.20 (m, 26H, CH₂), δ_8 1.28 (d, 3H, CH-CH₃, $J = 6.15$ Hz), δ_9 0.88 (t, 6H, CH₃, $J = 6.66$ Hz). ¹⁹F NMR ($CDCl_3$, 470 MHz): δ_1 -117.83 (m, *Fortho*), δ_2 -155.95 (m, *Fmeta*). ¹³C {¹H} NMR ($CDCl_3$, 126 MHz): 164.07 (C=O), 163.95 (O-C_{Ar}), 158.26 (C≡N), 153.16 (C_{Ar}-O-C(O)), 149.91 (dm, *Fortho*-C_{Ar}, $^1J_{C-F} = 229$ Hz), 141.38 (dm, *Fmeta*-C_{Ar}, $^1J_{C-F} = 248$ Hz), 134.71 (m, O-C_{Ar}), 132.47, 128.07 (C_{Ar}-H), 127.70 (m, C_{Ar}-Au), 123.79 (C_{Ar}-H), 121.51 (CN-C_{Ar}), 120.23 (O(O)C-C_{Ar}), 114.50 (C_{Ar}-H), 81.27 (Ar-O-CH), 68.43 (CH₂-O-Ar), 36.76

(CH-CH₂), 31.86, 31.77, 29.52, 29.51, 29.32, 29.28, 29.24, 29.03, 25.94, 25.24, 22.65, 22.57 (CH₂), 20.01 (CH-CH₃), 14.08, 14.05 (CH₂-CH₃). IR (cm⁻¹): ν(C≡N): 2212; ν(C=O): 1728. . Anal. calcd (%) for C₃₈H₄₆AuF₄NO₄: C, 53.46; H, 5.43; N, 1.64. Found: C, 53.22; H, 5.01; N, 1.74. MALDI-TOF MS: *m/z* 854.3090 [M+H]⁺ (calcd 854.3101 for C₃₈H₄₇AuF₄NO₄). [α]₅₄₆²⁵ (CHCl₃): 14.4 deg cm² g⁻¹.

R¹ = C₆H₁₃, R² = (R)-2-Octyl (4). Yield: 0.14 g, 55 %. ¹H NMR (CDCl₃, 500 MHz): δ₁ 8.11 (d, 2H, O(O)C-Ar, AA' part of AA'XX' spin system, $N = J_{AX} + J_{AX'} = 9.02$ Hz, $J_{AA'} \approx J_{XX'}$), δ₂ 7.62 (d, 2H, CN-Ar, AA' part of AA'XX' spin system, $N = J_{AX} + J_{AX'} = 8.91$ Hz, $J_{AA'} \approx J_{XX'}$), δ₃ 7.39 (d, 2H, CN-Ar, XX' part of AA'XX' spin system, $N = J_{AX} + J_{AX'} = 8.91$ Hz, $J_{AA'} \approx J_{XX'}$), δ₄ 6.96 (d, 2H, O(O)C-Ar, XX' part of AA'XX' spin system, $N = J_{AX} + J_{AX'} = 9.02$ Hz, $J_{AA'} \approx J_{XX'}$), δ₅ 4.48 (m, 1H, CH), δ₆ 4.14 (t, 2H, O-CH₂, $J = 6.65$ Hz), δ₇ 1.80-1.20 (m, 18H, CH₂), δ₈ 1.35 (d, 3H, CH-CH₃, $J = 6.06$ Hz), δ₉ 0.87 (t, 6H, CH₃, $J = 7.37$ Hz). ¹⁹F NMR (CDCl₃, 470 MHz): δ₁ -117.68 (m, F_{ortho}), δ₂ -156.99 (m, F_{meta}). ¹³C {¹H} NMR (CDCl₃, 126 MHz): 163.94 (C=O), 163.32 (O-C_{Ar}), 158.21 (C≡N), 153.18 (C_{Ar}-O-C(O)), 149.89 (dm, F_{ortho}-C_{Ar}, ¹J_{C-F} = 229 Hz), 140.90 (dm, F_{meta}-C_{Ar}, ¹J_{C-F} = 248 Hz), 135.73 (m, O-C_{Ar}), 132.53, 128.07 (C_{Ar}-H), 127.50 (m, C_{Ar}-Au), 123.78 (C_{Ar}-H), 121.49 (CN-C_{Ar}), 119.91 (O(O)C-C_{Ar}), 115.35 (C_{Ar}-H), 75.03 (CH₂-O-Ar), 74.29 (Ar-O-CH), 36.25 (CH-CH₂), 31.73, 31.47, 29.84, 29.18, 25.38, 25.25, 22.55, 22.54 (CH₂), 19.54 (CH-CH₃), 14.09, 13.99 (CH₂-CH₃). IR (cm⁻¹): ν(C≡N): 2215; ν(C=O): 1729. Anal. calcd (%) for C₃₄H₃₈AuF₄NO₄: C, 51.20; H, 4.80; N, 1.76. Found: C, 51.29; H, 5.02; N, 1.86. MALDI-TOF MS: *m/z* 798.2502 [M+H]⁺ (calcd 798.2475 for C₃₄H₃₉AuF₄NO₄). [α]₅₄₆²⁵ (CHCl₃): 4.5 deg cm² g⁻¹.

R¹ = C₈H₁₇, R² = (R)-2-Octyl (5). Yield: 0.14 g, 55 %. ¹H NMR (CDCl₃, 500 MHz): δ₁ 8.11 (d, 2H, O(O)C-Ar, AA' part of AA'XX' spin system, $N = J_{AX} + J_{AX'} = 8.98$ Hz, $J_{AA'} \approx J_{XX'}$), δ₂ 7.62 (d, 2H, CN-Ar, AA' part of AA'XX' spin system, $N = J_{AX} + J_{AX'} = 8.97$ Hz, $J_{AA'} \approx J_{XX'}$), δ₃ 7.39 (d, 2H, CN-Ar, XX' part of AA'XX' spin system, $N = J_{AX} + J_{AX'} = 8.97$ Hz, $J_{AA'} \approx J_{XX'}$), δ₄ 6.96 (d, 2H, O(O)C-Ar, XX' part of AA'XX' spin system, $N = J_{AX} + J_{AX'} = 8.98$ Hz, $J_{AA'} \approx J_{XX'}$), δ₅ 4.50 (m, 1H, CH), δ₆ 4.14 (t, 2H, O-CH₂, $J = 6.70$ Hz), δ₇ 1.80-1.20 (m, 22H, CH₂), δ₈ 1.35 (d, 3H, CH-CH₃, $J = 6.52$ Hz), δ₉ 0.87 (t, 6H, CH₃, $J = 6.79$ Hz). ¹⁹F NMR (CDCl₃, 470 MHz): δ₁ -117.70 (m, F_{ortho}), δ₂ -156.99 (m, F_{meta}). ¹³C {¹H} NMR (CDCl₃, 126 MHz): 163.94 (C=O), 163.32 (O-C_{Ar}),

158.21 (C≡N), 153.18 (C_{Ar}-O-C(O)), 149.90 (dm, F_{ortho}-C_{Ar}, ¹J_{C-F} = 228 Hz), 140.90 (dm, F_{meta}-C_{Ar}, ¹J_{C-F} = 250 Hz), 135.73 (m, O-C_{Ar}), 132.53, 128.06 (C_{Ar}-H), 127.49 (m, C_{Ar}-Au), 123.79 (C_{Ar}-H), 121.49 (CN-C_{Ar}), 119.91 (O(O)C-C_{Ar}), 115.35 (C_{Ar}-H), 75.03 (CH₂-O-Ar), 74.29 (Ar-O-CH), 36.25 (CH-CH₂), 31.76, 31.73, 29.88, 29.24, 29.18, 29.18, 25.58, 25.38, 22.62, 22.55 (CH₂), 19.54 (CH-CH₃), 14.07, 14.04 (CH₂-CH₃). IR (cm⁻¹): ν(C≡N): 2215; ν(C=O): 1729. Anal. calcd (%) for C₃₆H₄₂AuF₄NO₄: C, 52.37; H, 5.13; N, 1.70. Found: C, 52.45; H, 4.92; N, 1.53. MALDI-TOF MS: *m/z* 826.2797 [M+H]⁺ (calcd 826.2788 for C₃₆H₄₃AuF₄NO₄). [α]₅₄₆²⁵ (CHCl₃): 5.0 deg cm² g⁻¹.

R¹ = C₁₀H₂₁, R² = (R)-2-Octyl (6). Yield: 0.15 g, 58 %. ¹H NMR (CDCl₃, 500 MHz): δ₁ 8.11 (d, 2H, O(O)C-Ar, AA' part of AA'XX' spin system, *N* = *J*_{AX} + *J*_{AX'} = 8.93 Hz, *J*_{AA'} ≈ *J*_{XX'}), δ₂ 7.62 (d, 2H, CN-Ar, AA' part of AA'XX' spin system, *N* = *J*_{AX} + *J*_{AX'} = 8.92 Hz, *J*_{AA'} ≈ *J*_{XX'}), δ₃ 7.39 (d, 2H, CN-Ar, XX' part of AA'XX' spin system, *N* = *J*_{AX} + *J*_{AX'} = 8.92 Hz, *J*_{AA'} ≈ *J*_{XX'}), δ₄ 6.96 (d, 2H, O(O)C-Ar, XX' part of AA'XX' spin system, *N* = *J*_{AX} + *J*_{AX'} = 8.93 Hz, *J*_{AA'} ≈ *J*_{XX'}), δ₅ 4.50 (m, 1H, CH), δ₆ 4.14 (t, 2H, O-CH₂, *J* = 6.67 Hz), δ₇ 1.80-1.20 (m, 26H, CH₂), δ₈ 1.35 (d, 3H, CH-CH₃, *J* = 6.06 Hz), δ₉ 0.88 (t, 6H, CH₃, *J* = 6.89 Hz). ¹⁹F NMR (CDCl₃, 470 MHz): δ₁ -117.70 (m, F_{ortho}), δ₂ -158.00 (m, F_{meta}). ¹³C {¹H} NMR (CDCl₃, 126 MHz): 163.94 (C=O), 163.32 (C_{Ar}-O), 158.22 (C≡N), 153.18 (C_{Ar}-O-C(O)), 148.89 (dm, F_{ortho}-C_{Ar}, ¹J_{C-F} = 228 Hz), 140.88 (dm, F_{meta}-C_{Ar}, ¹J_{C-F} = 250 Hz), 135.74 (m, O-C_{Ar}), 132.53, 128.07 (C_{Ar}-H), 127.48 (m, C_{Ar}-Au), 123.79 (C_{Ar}-H), 121.49 (C≡N-C_{Ar}), 119.91 (O(O)C-C_{Ar}), 115.35 (C_{Ar}-H), 75.03 (CH₂-O-Ar), 74.29 (Ar-O-CH), 36.25 (CH-CH₂), 31.87, 31.73, 29.88, 29.52, 29.51, 29.28, 29.18, 25.58, 25.38, 22.66, 22.55 (CH₂), 19.54 (CH-CH₃), 14.09, 14.04 (CH₂-CH₃). IR (cm⁻¹): ν(C≡N): 2214; ν(C=O): 1729. Anal. calcd (%) for C₃₈H₄₆AuF₄NO₄: C, 53.46; H, 5.43; N, 1.64. Found: C, 53.53; H, 5.18; N, 1.72. MALDI-TOF MS: *m/z* 854.3105 [M+H]⁺ (calcd 854.3101 for C₃₈H₄₇AuF₄NO₄). [α]₅₄₆²⁵ (CHCl₃): 4.0 deg cm² g⁻¹.

R¹ = (R)-2-Octyl, R² = (R)-2-Octyl (7). Yield: 0.13 g, 51 %. ¹H NMR (CDCl₃, 500 MHz): δ₁ 8.11 (d, 2H, O(O)C-Ar, AA' part of AA'XX' spin system, *N* = *J*_{AX} + *J*_{AX'} = 9.01 Hz, *J*_{AA'} ≈ *J*_{XX'}), δ₂ 7.62 (d, 2H, CN-Ar, AA' part of AA'XX' spin system, *N* = *J*_{AX} + *J*_{AX'} = 8.95 Hz, *J*_{AA'} ≈ *J*_{XX'}), δ₃ 7.39 (d, 2H, CN-Ar, XX' part of AA'XX' spin system, *N* = *J*_{AX} + *J*_{AX'} = 8.95 Hz, *J*_{AA'} ≈ *J*_{XX'}), δ₄ 6.96 (d, 2H, O(O)C-Ar, XX' part of AA'XX' spin system, *N* = *J*_{AX} + *J*_{AX'} = 8.93 Hz, *J*_{AA'} ≈ *J*_{XX'}),

δ_5 4.49 (m, 1H, CH), δ_6 4.30 (m, 1H, CH), δ_7 1.80-1.20 (m, 20H, CH₂), δ_8 1.35 (d, 3H, CH-CH₃, $J = 6.09$ Hz), δ_9 1.27 (d, 3H, CH-CH₃, $J = 6.08$ Hz), δ_{10} 0.89 (t, 6H, CH₃, $J = 6.85$ Hz). ¹⁹F NMR (CDCl₃, 470 MHz): δ_1 -117.83 (m, F_{ortho}), δ_2 -155.94 (m, F_{meta}). ¹³C {¹H} NMR (CDCl₃, 126 MHz): 163.94 (C=O), 163.32 (O-C_{Ar}), 158.28 (C≡N), 153.18 (C_{Ar}-O-C(O)), 149.91 (dm, F_{ortho}-C_{Ar}, ¹J_{C-F} = 228 Hz), 141.38 (dm, F_{meta}-C_{Ar}, ¹J_{C-F} = 248 Hz), 134.72 (m, O-C_{Ar}), 132.53 (C_{Ar}-H), 128.16 (m, C_{Ar}-Au) 128.07 (C_{Ar}-H), 123.80 (C_{Ar}-H), 121.50 (CN-C_{Ar}), 119.91 (O(O)C-C_{Ar}), 115.35 (C_{Ar}-H), 81.27, 74.29 (Ar-O-CH), 36.76, 36.24 (CH-CH₂), 31.76, 31.73, 29.24, 29.17, 25.38, 25.24, 22.57, 22.55 (CH₂), 20.01, 19.54 (CH-CH₃), 14.05, 14.03 (CH₂-CH₃). IR (cm⁻¹): ν (C≡N): 2213; ν (C=O): 1727. Anal. calcd (%) for C₃₆H₄₂AuF₄NO₄: C, 52.37; H, 5.13; N, 1.70. Found: C, 53.31; H, 5.00; N, 1.88. MALDI-TOF MS: m/z 826.2750 [M+H]⁺ (calcd 826.2788 for C₃₆H₄₃AuF₄NO₄). [α]₅₄₆²⁵ (CHCl₃): 4.2 deg cm² g⁻¹.

¹H RMN spectra [Varian 500 (499.72 MHz)].

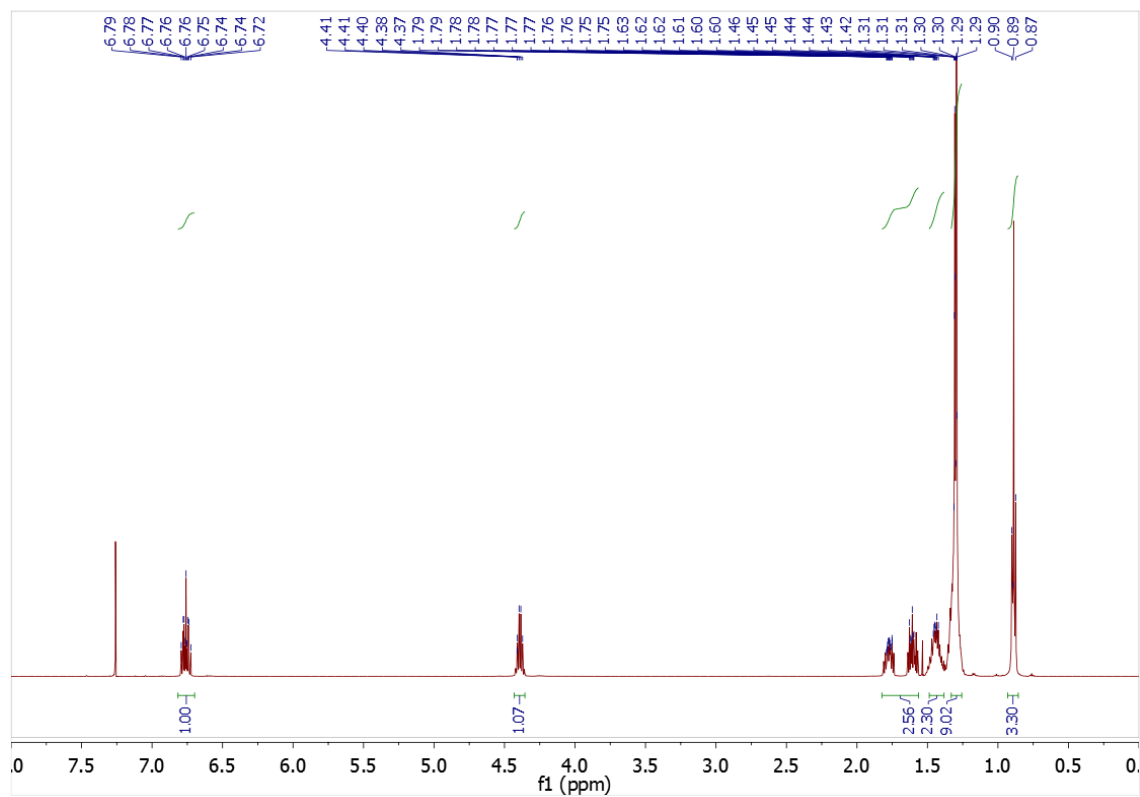


Figure S1: ¹H NMR (CDCl₃) spectrum of HC₆F₄O-(R)-2-Octyl.

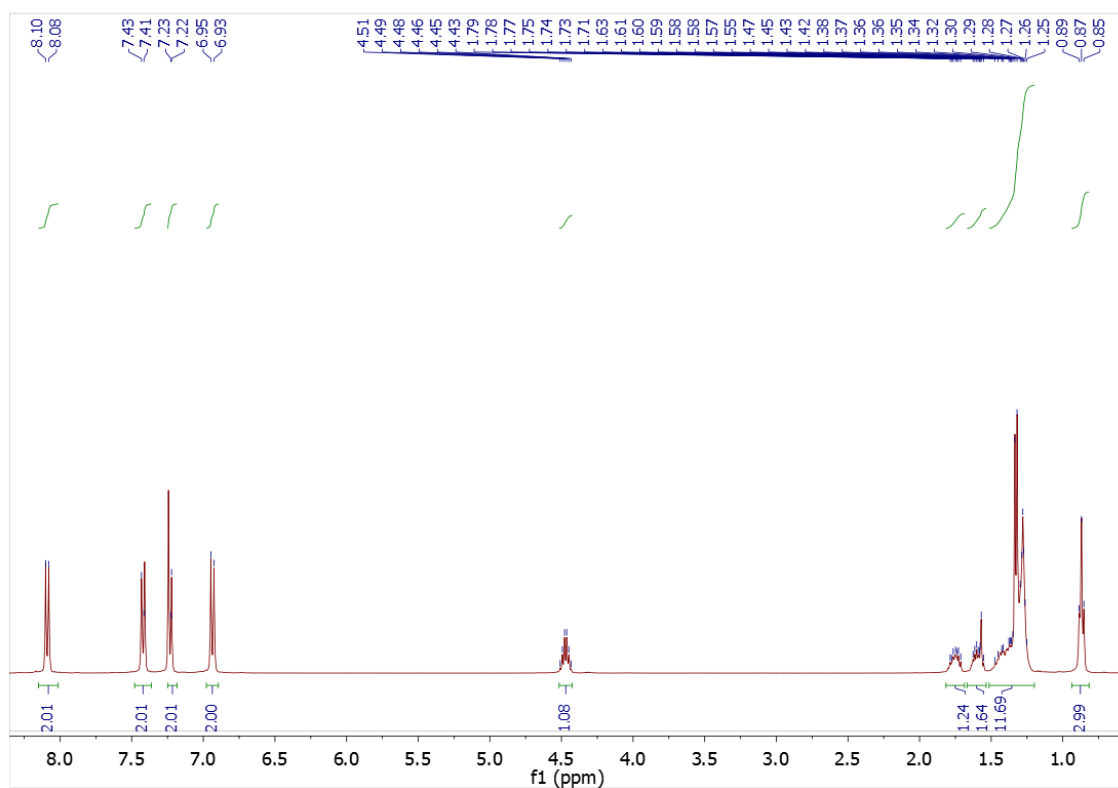


Figure S2: ^1H NMR (CDCl_3) spectrum of CNC8*.

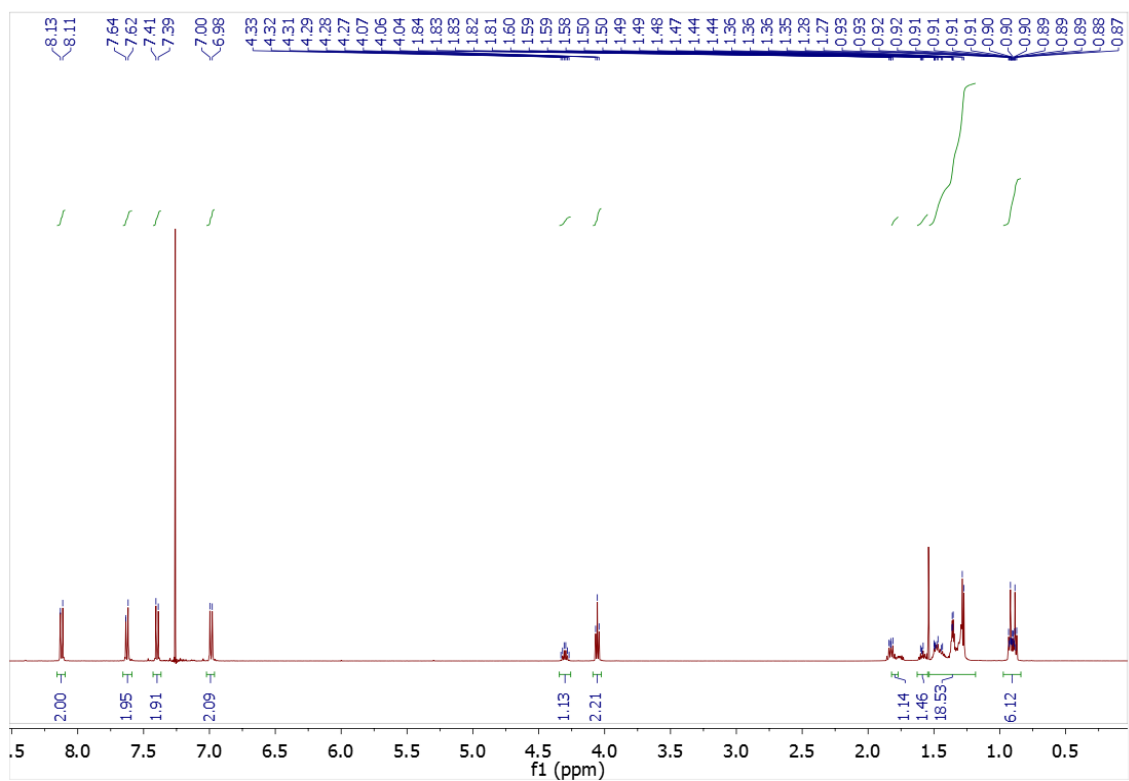


Figure S3: ^1H NMR (CDCl_3) spectrum of **1**.

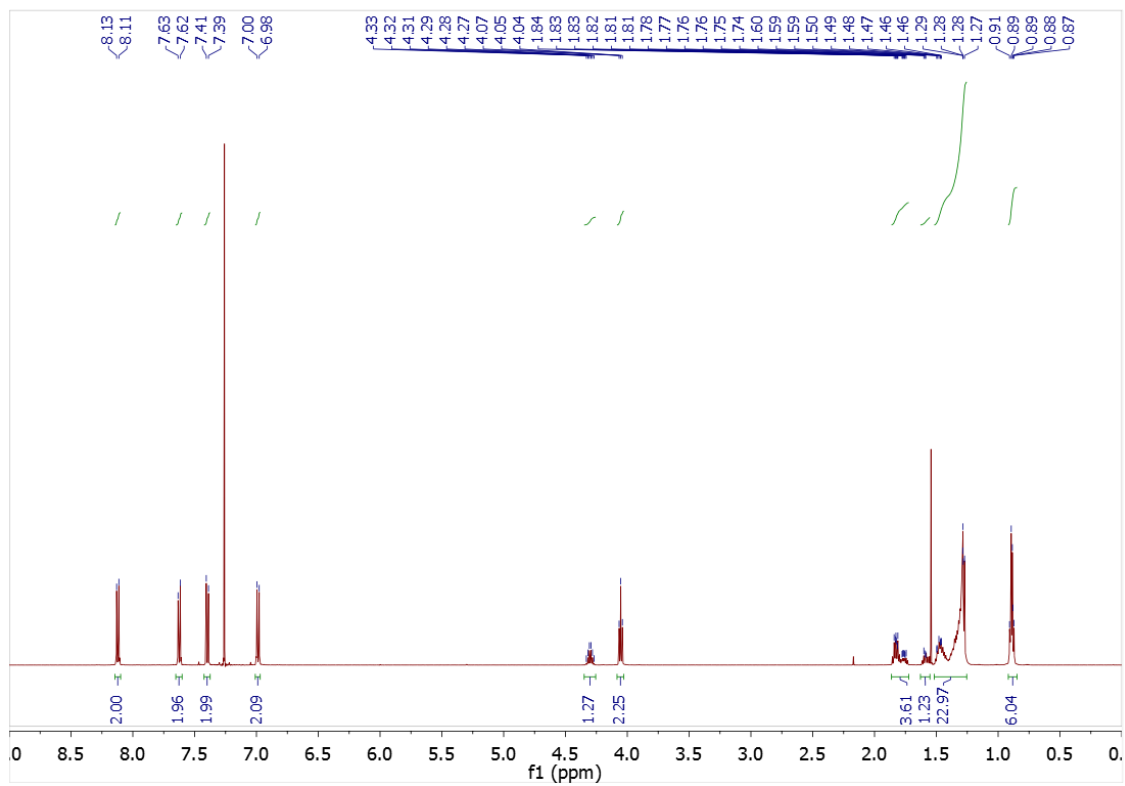


Figure S4: ^1H NMR (CDCl_3) spectrum of **2**.

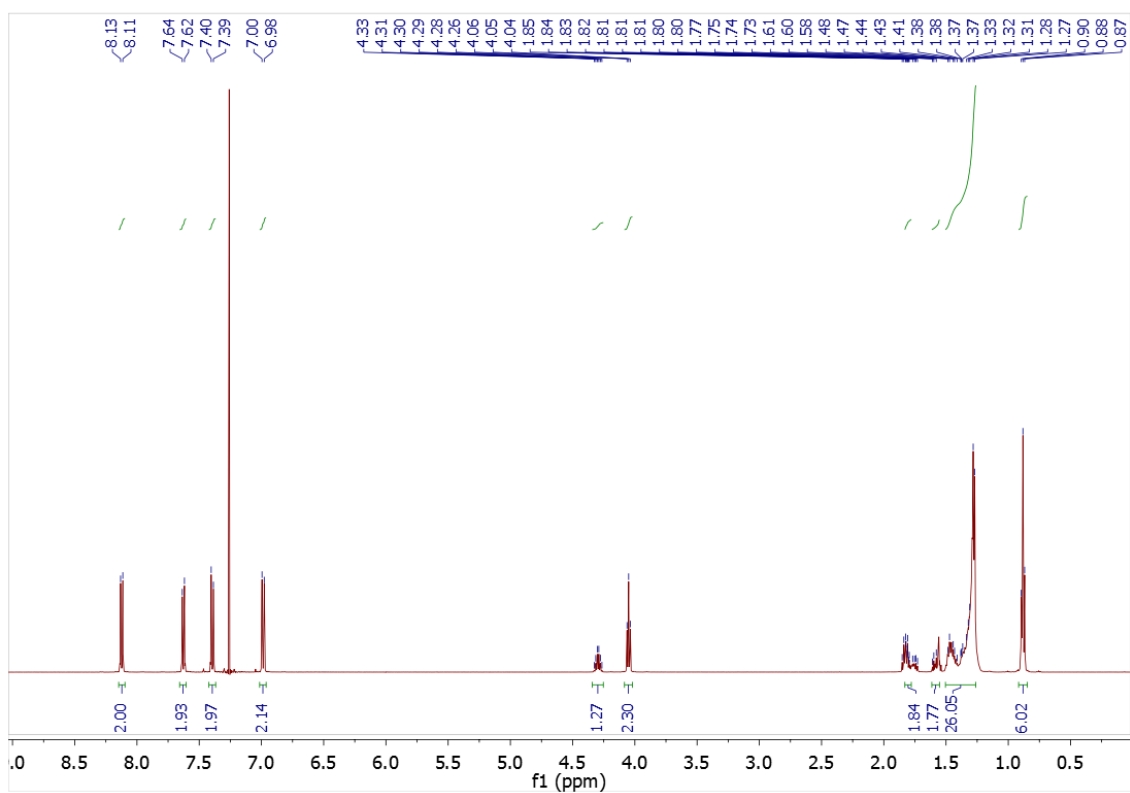


Figure S5: ^1H NMR (CDCl_3) spectrum of **3**.

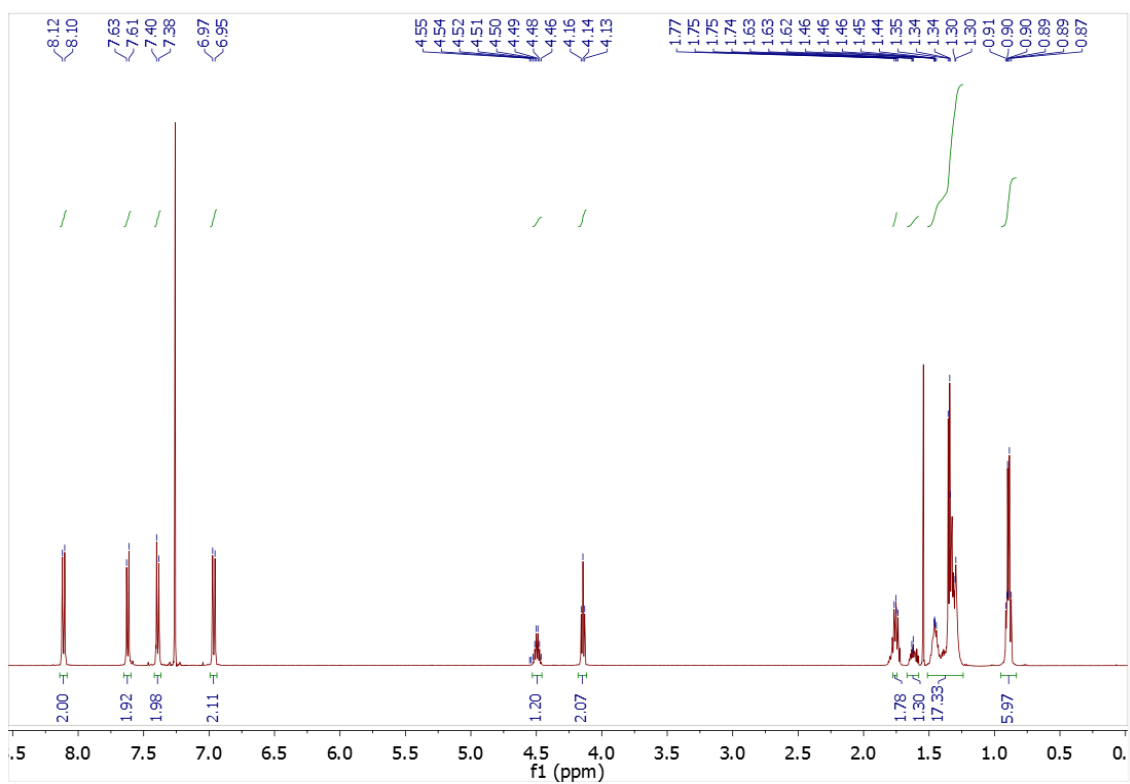


Figure S6: ^1H NMR (CDCl_3) spectrum of **4**.

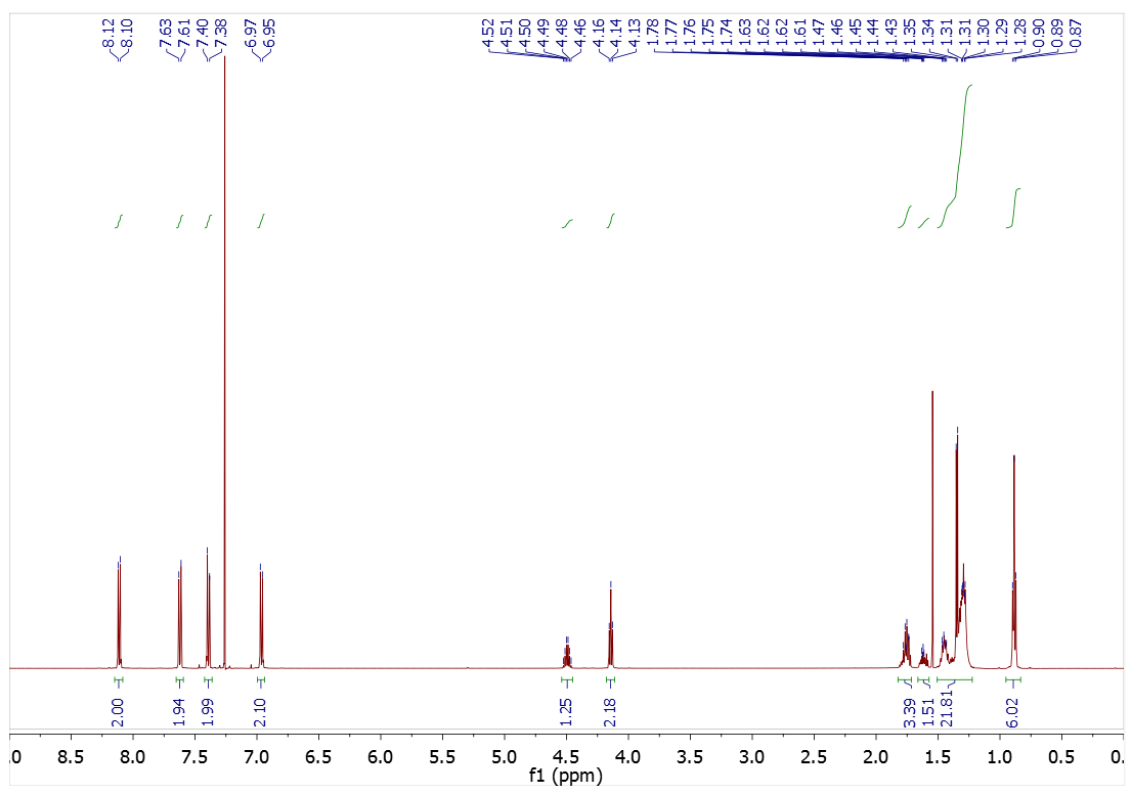


Figure S7: ^1H NMR (CDCl_3) spectrum of **5**.

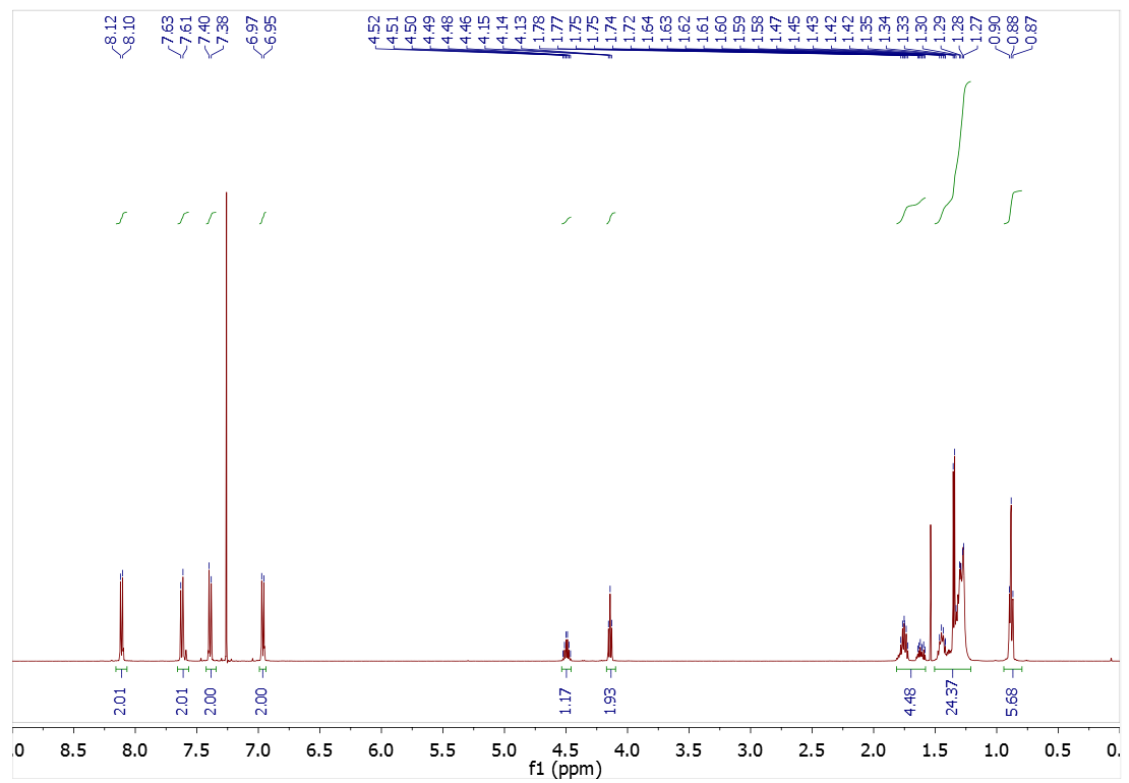


Figure S8: ^1H NMR (CDCl_3) spectrum of **6**.

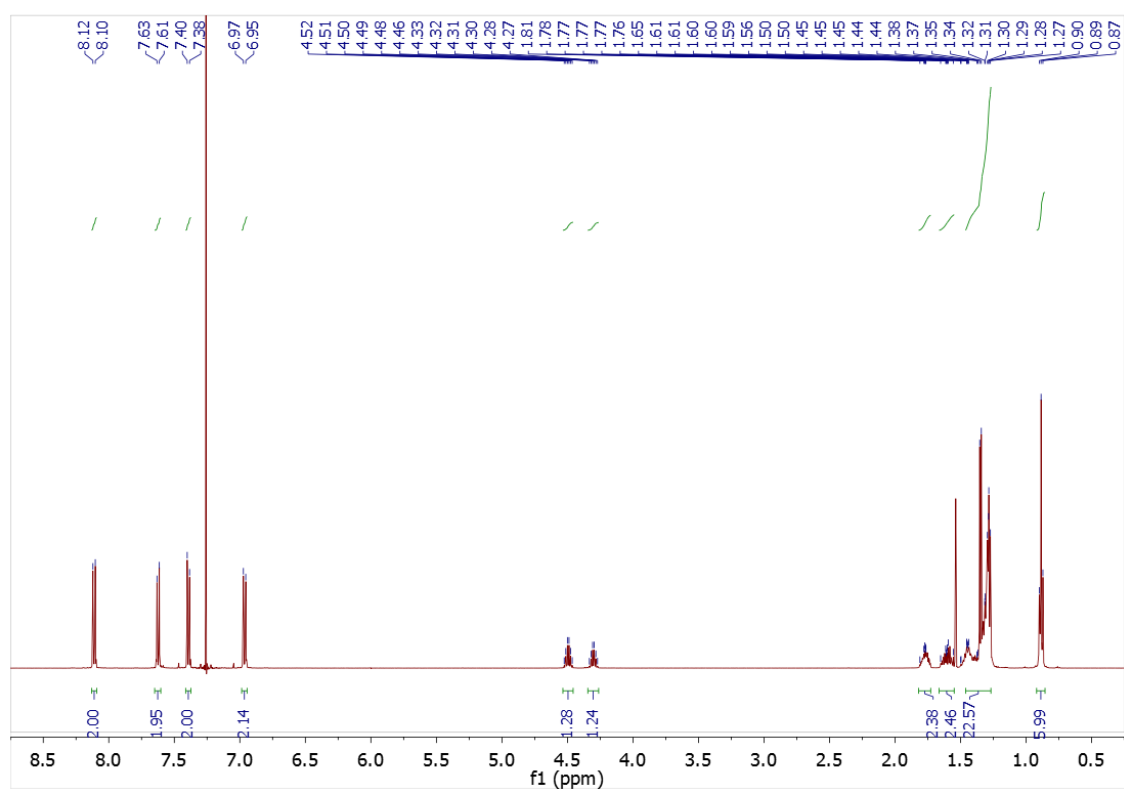


Figure S9: ^1H NMR (CDCl_3) spectrum of 7.

$^{13}\text{C}\{^1\text{H}\}$ NMR spectra [Varian 500 (125.67 MHz)].

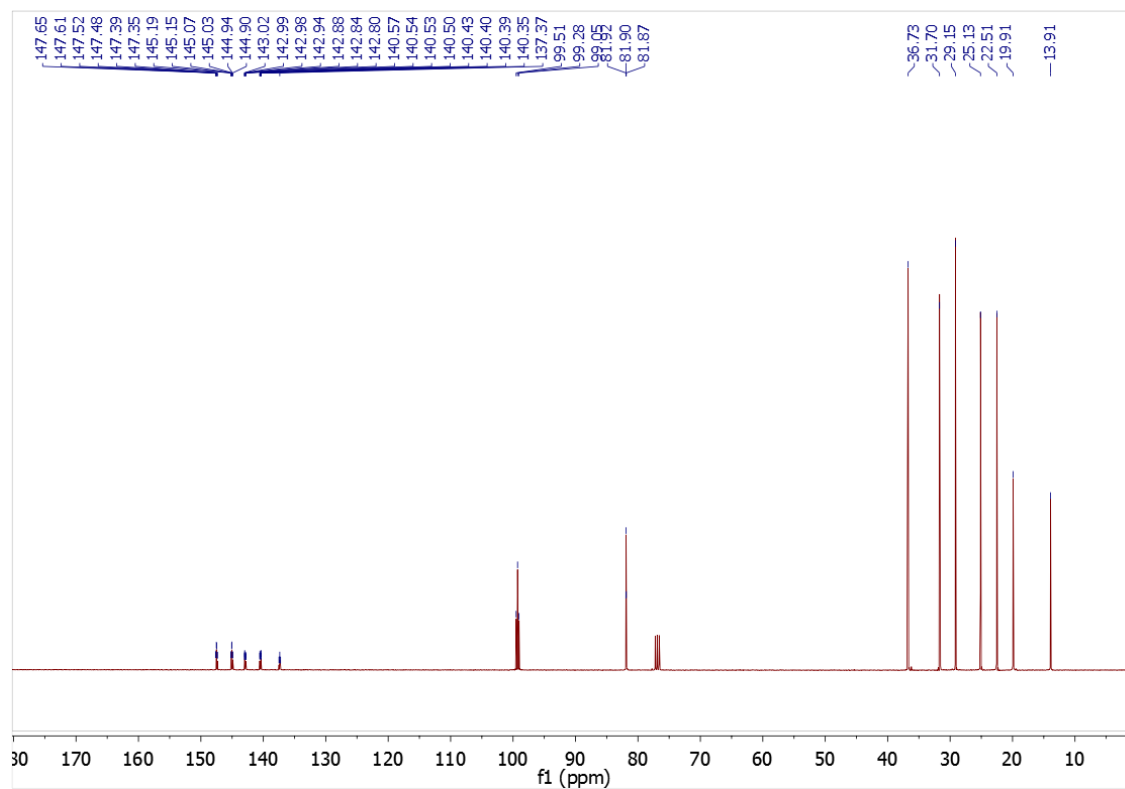


Figure S10: $^{13}\text{C}\{^1\text{H}\}$ NMR (CDCl_3) spectrum of $\text{HC}_6\text{F}_4\text{O}-(\text{R})-2\text{-Octyl}$.

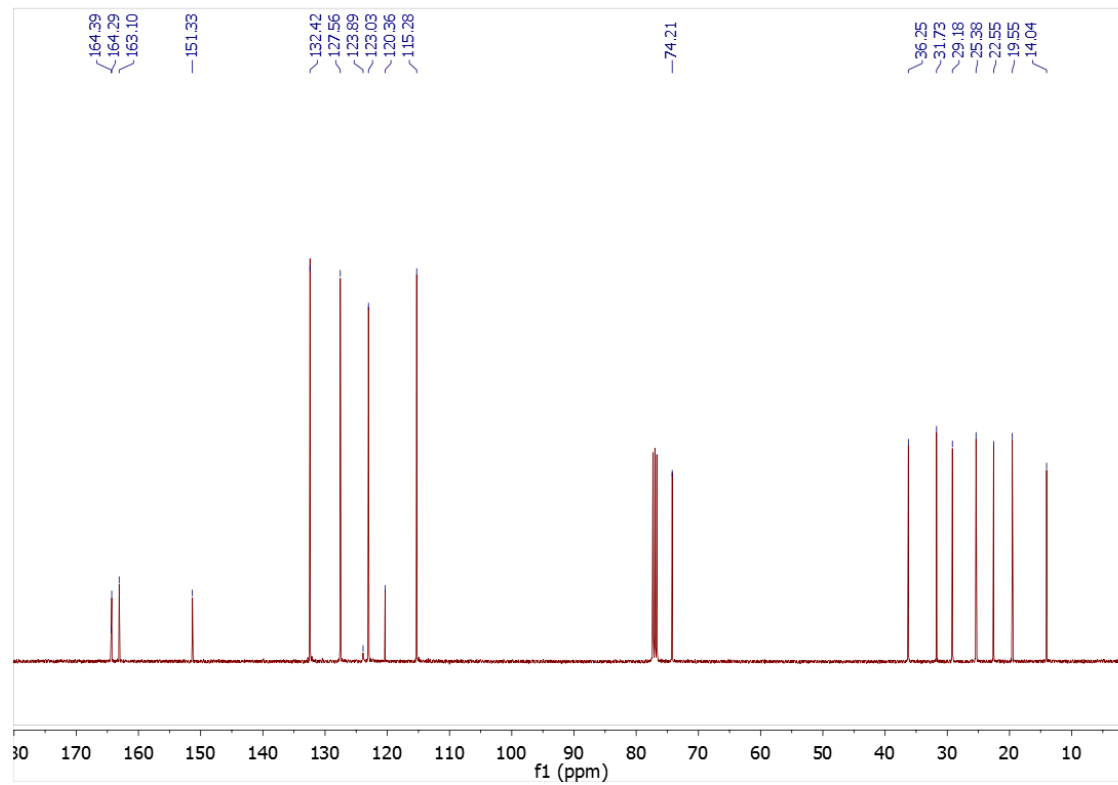


Figure S11: $^{13}\text{C}\{^1\text{H}\}$ NMR (CDCl_3) spectrum of CN8^* .

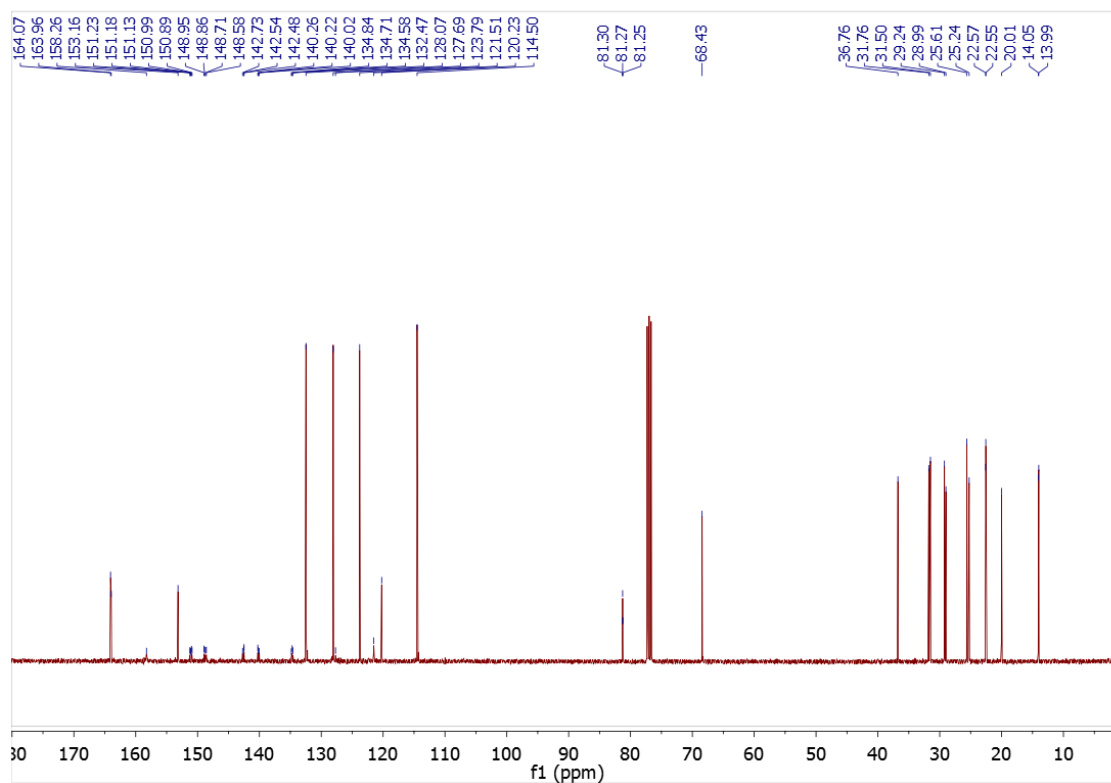


Figure S12: $^{13}\text{C}\{^1\text{H}\}$ NMR (CDCl_3) spectrum of **1**.

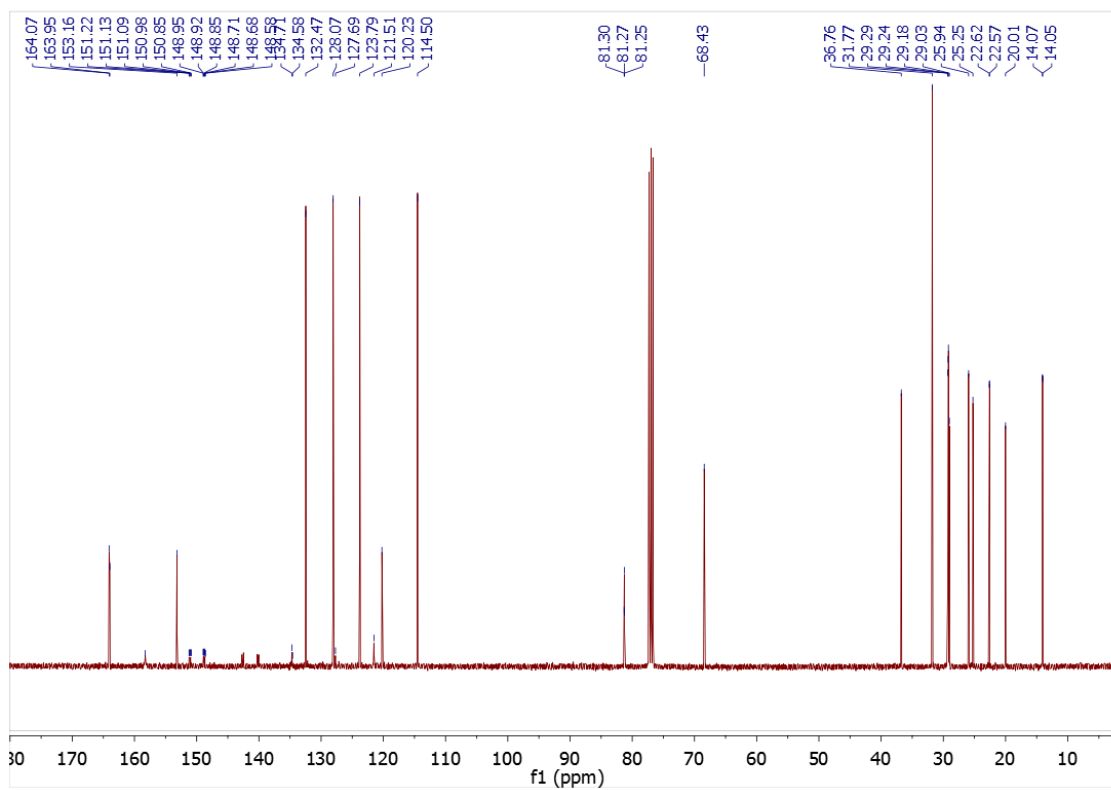


Figure S13: $^{13}\text{C}\{^1\text{H}\}$ NMR (CDCl_3) spectrum of **2**.

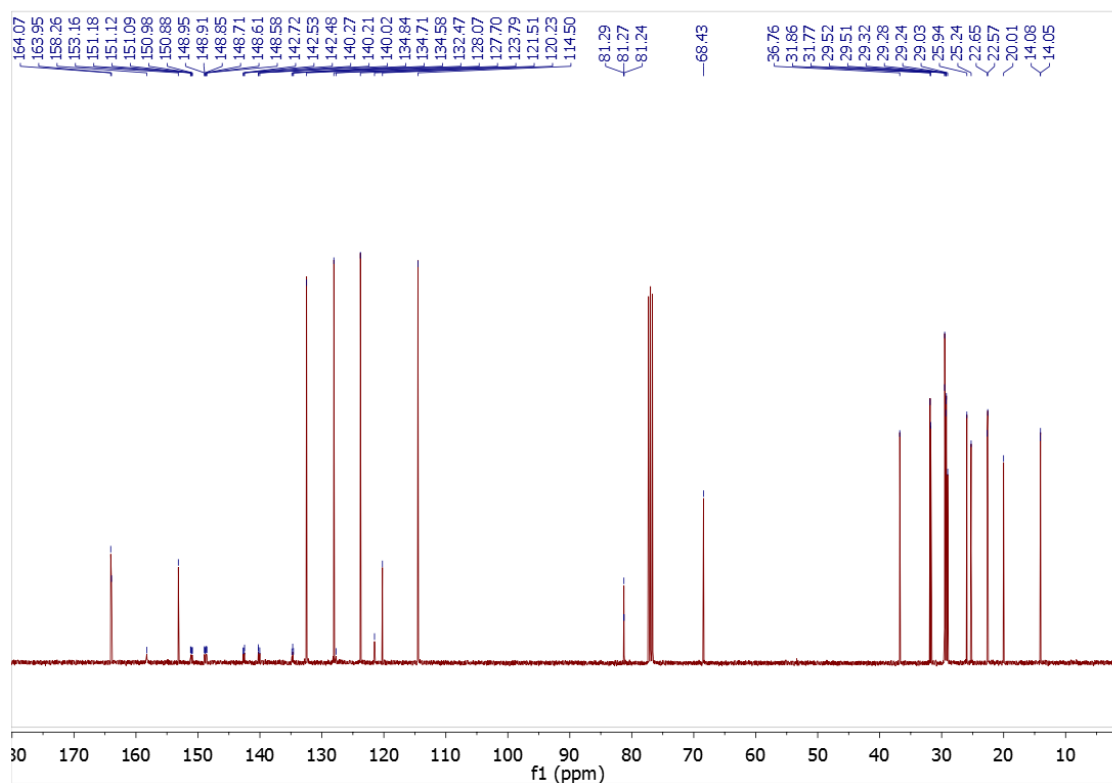


Figure S14: $^{13}\text{C}\{^1\text{H}\}$ NMR (CDCl_3) spectrum of **3**.

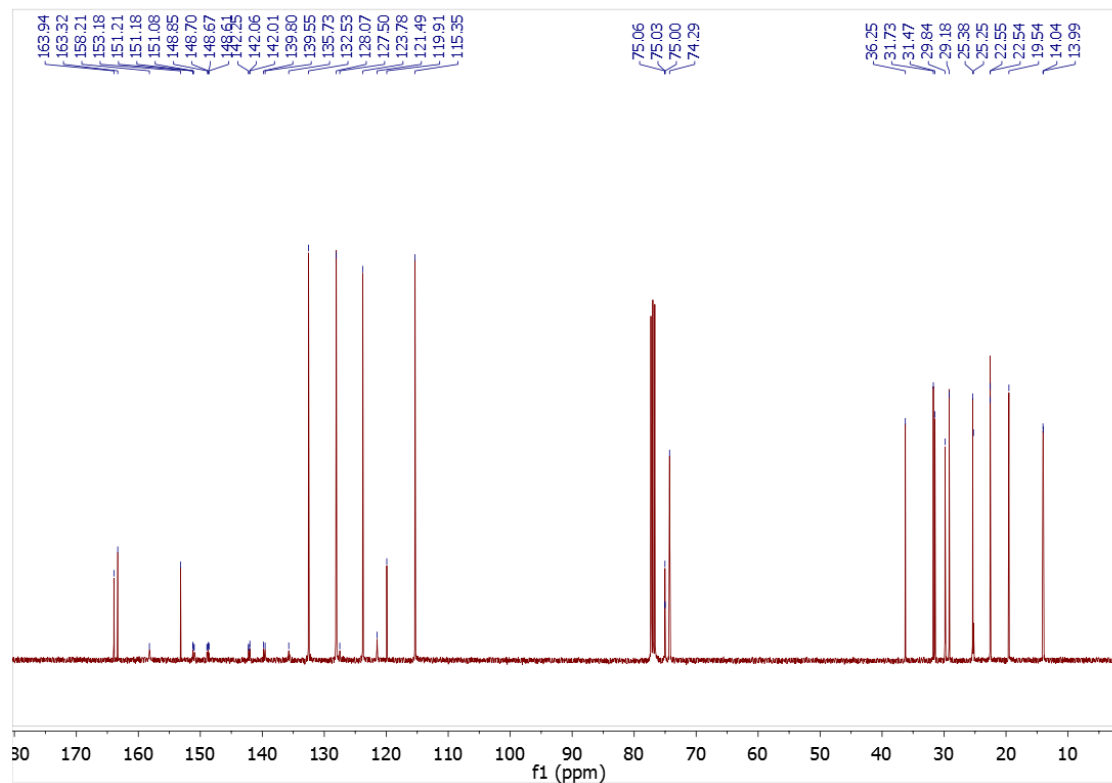


Figure S15: $^{13}\text{C}\{^1\text{H}\}$ NMR (CDCl_3) spectrum of **4**.

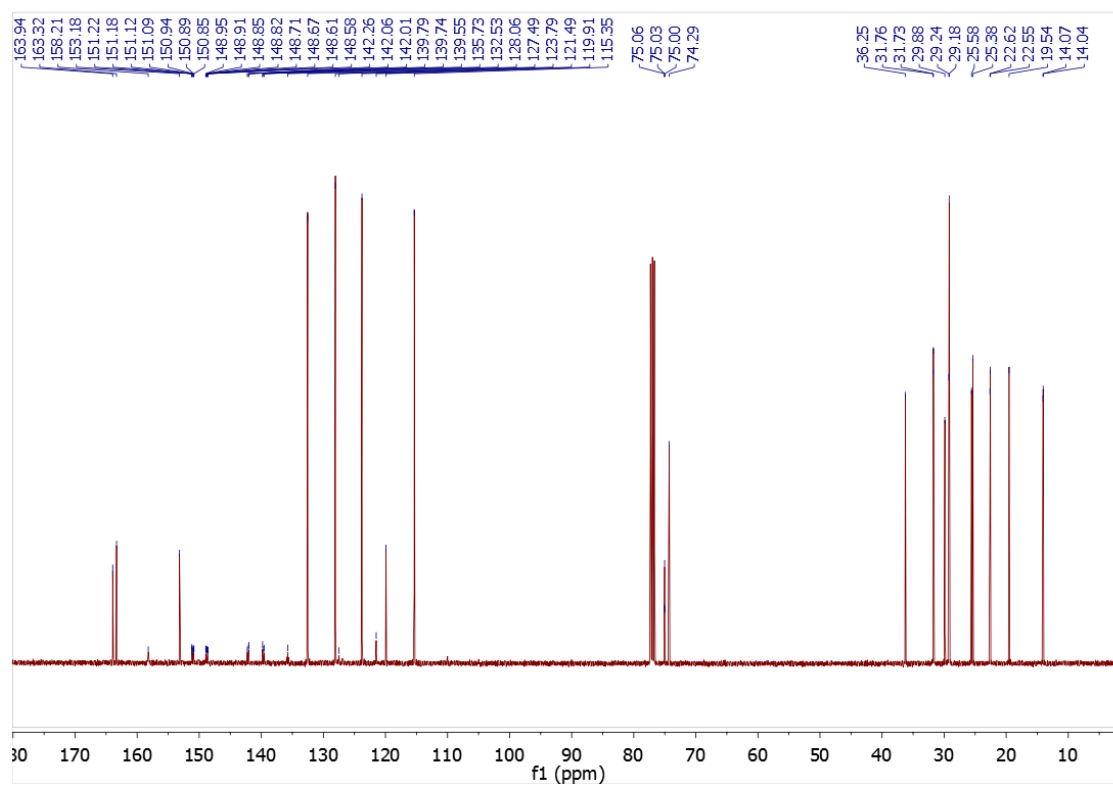


Figure S16: $^{13}\text{C}\{^1\text{H}\}$ NMR (CDCl_3) spectrum of **5**.

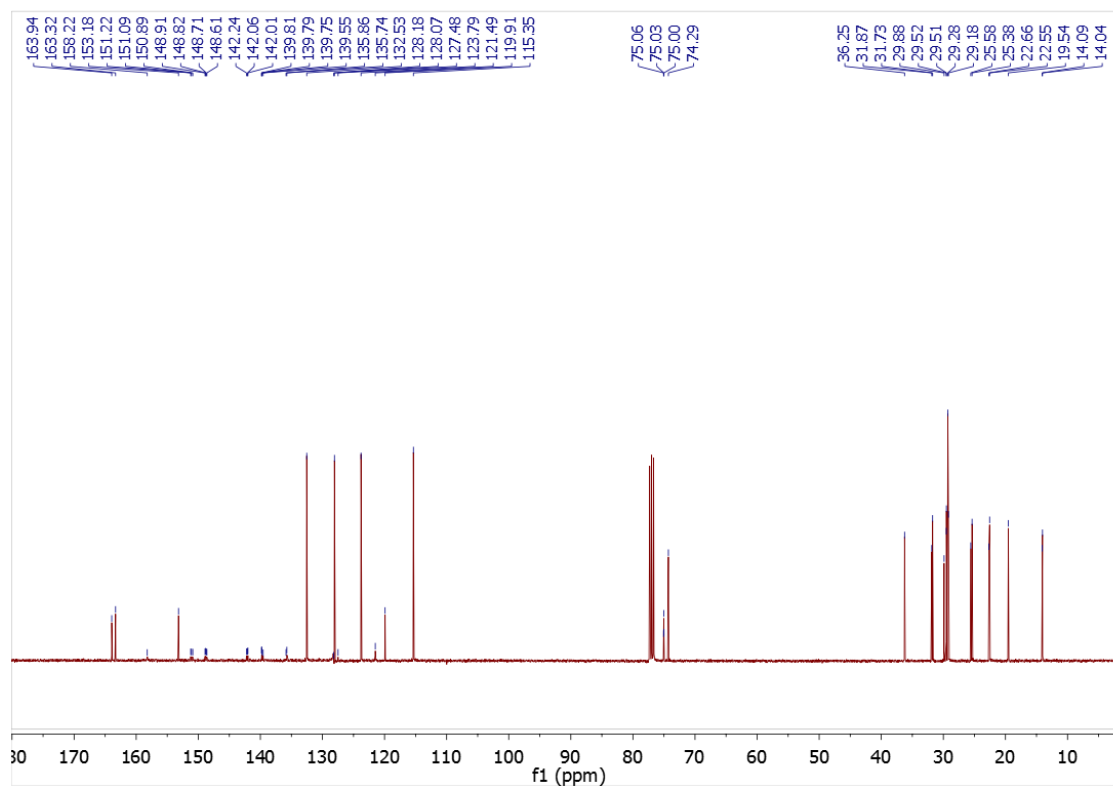


Figure S17: $^{13}\text{C}\{^1\text{H}\}$ NMR (CDCl_3) spectrum of **6**.

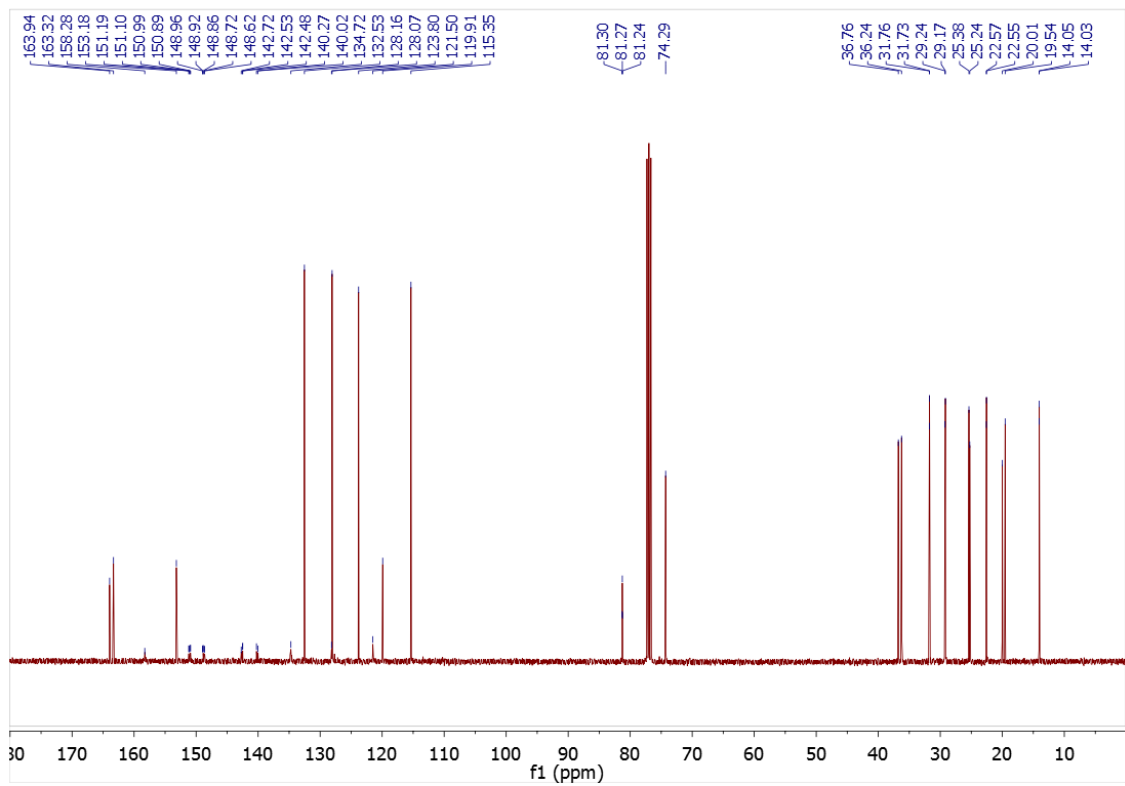


Figure S18: $^{13}\text{C}\{^1\text{H}\}$ NMR (CDCl_3) spectrum of 7.

^{19}F NMR spectra [Varian 500 (470.14 MHz)].

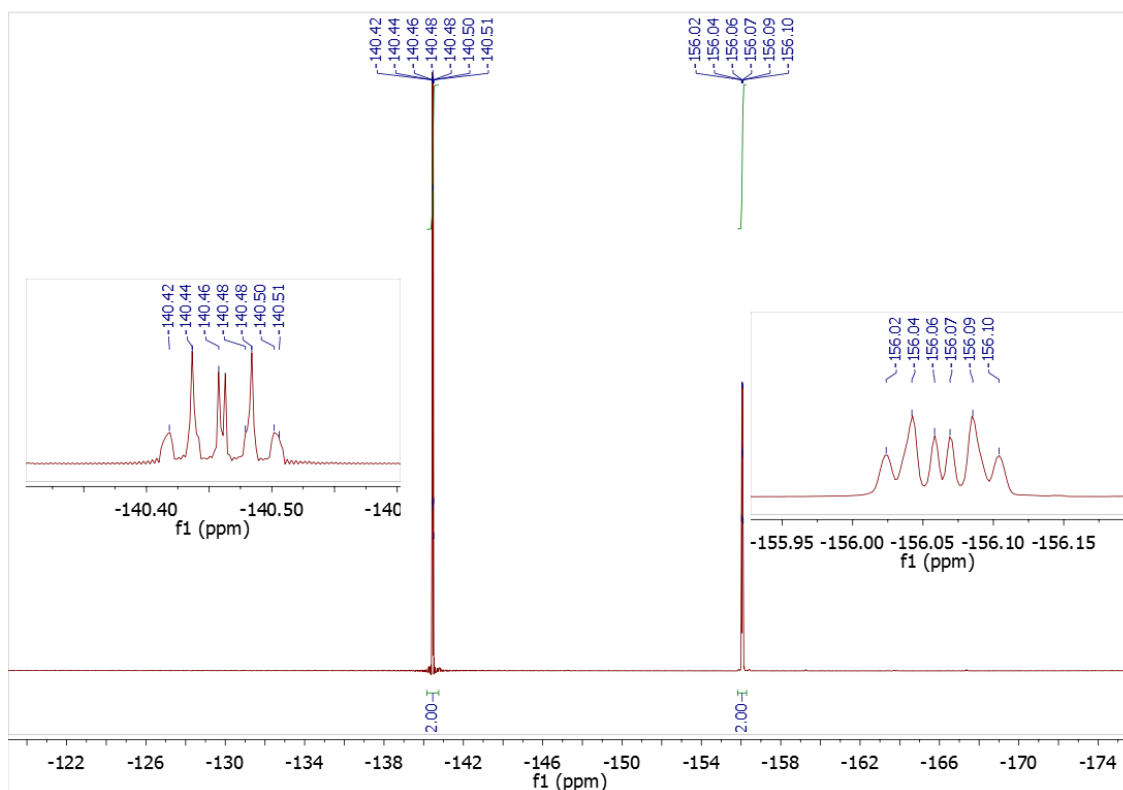


Figure S19: ^{19}F NMR (CDCl_3) spectrum of $\text{HC}_6\text{F}_4\text{O}-(\text{R})-2\text{-Octyl}$.

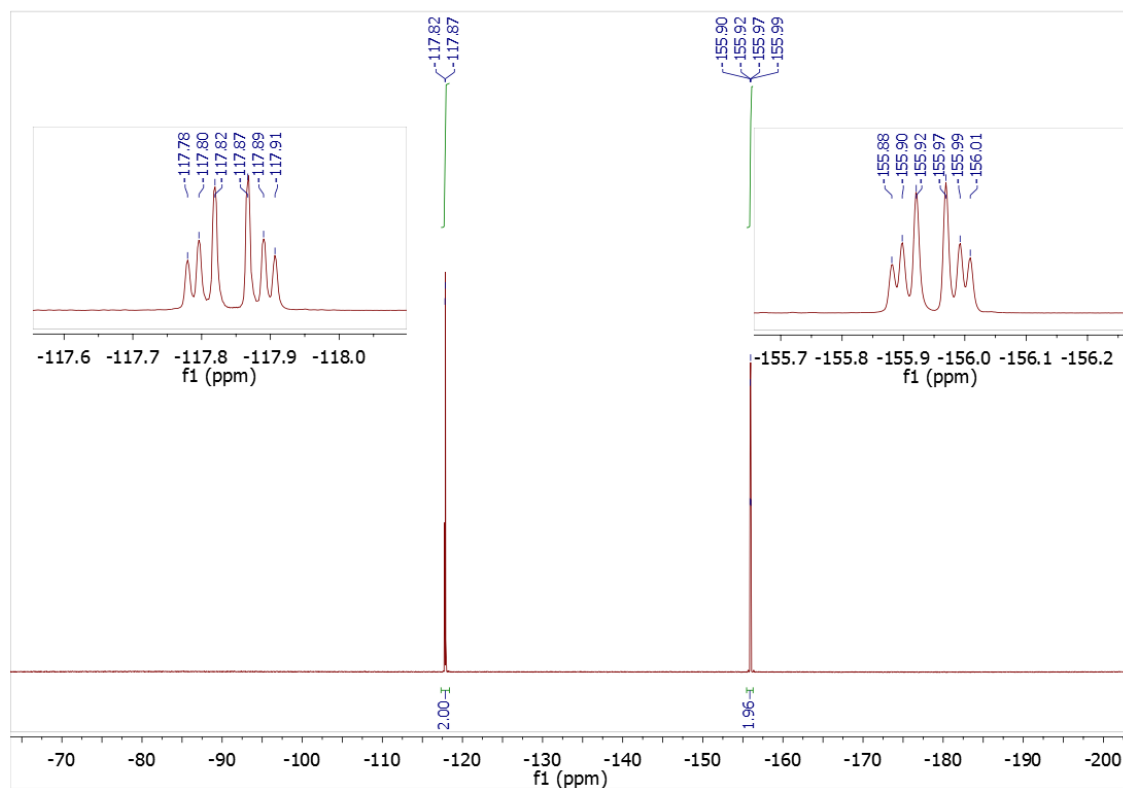


Figure S20: ^{19}F NMR (CDCl_3) spectrum of **1**.

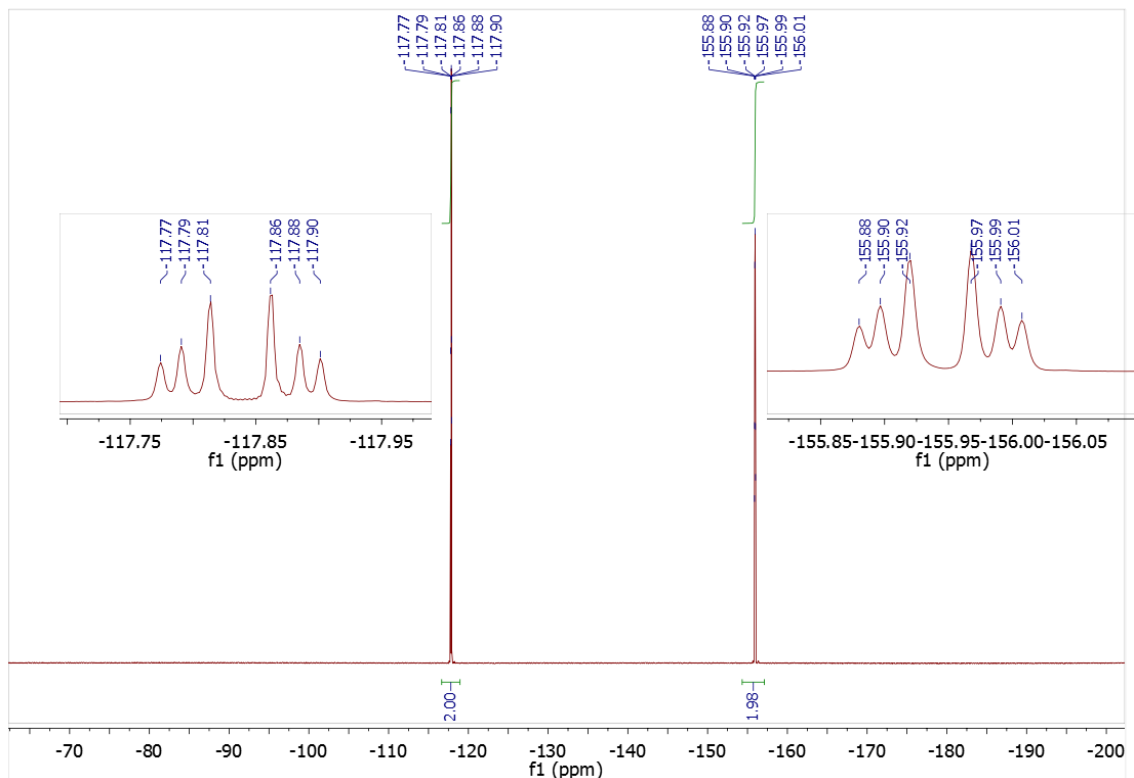


Figure S21: ^{19}F NMR (CDCl_3) spectrum of **2**.

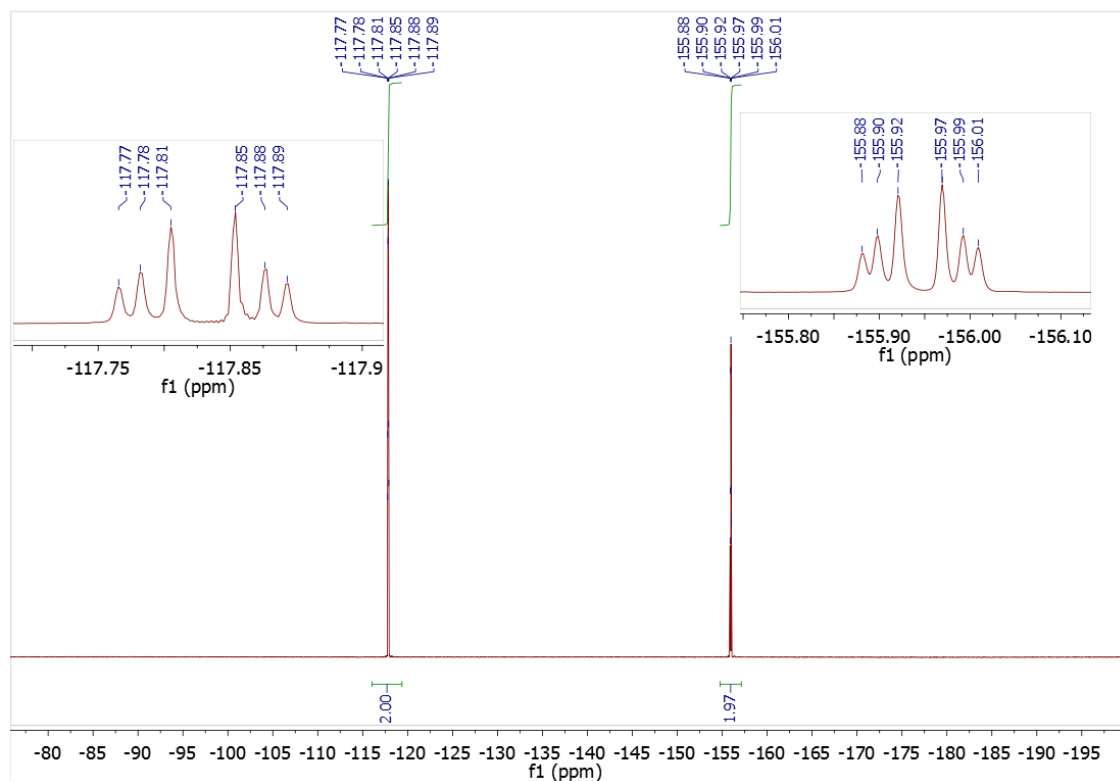


Figure S22: ^{19}F NMR (CDCl_3) spectrum of **3**.

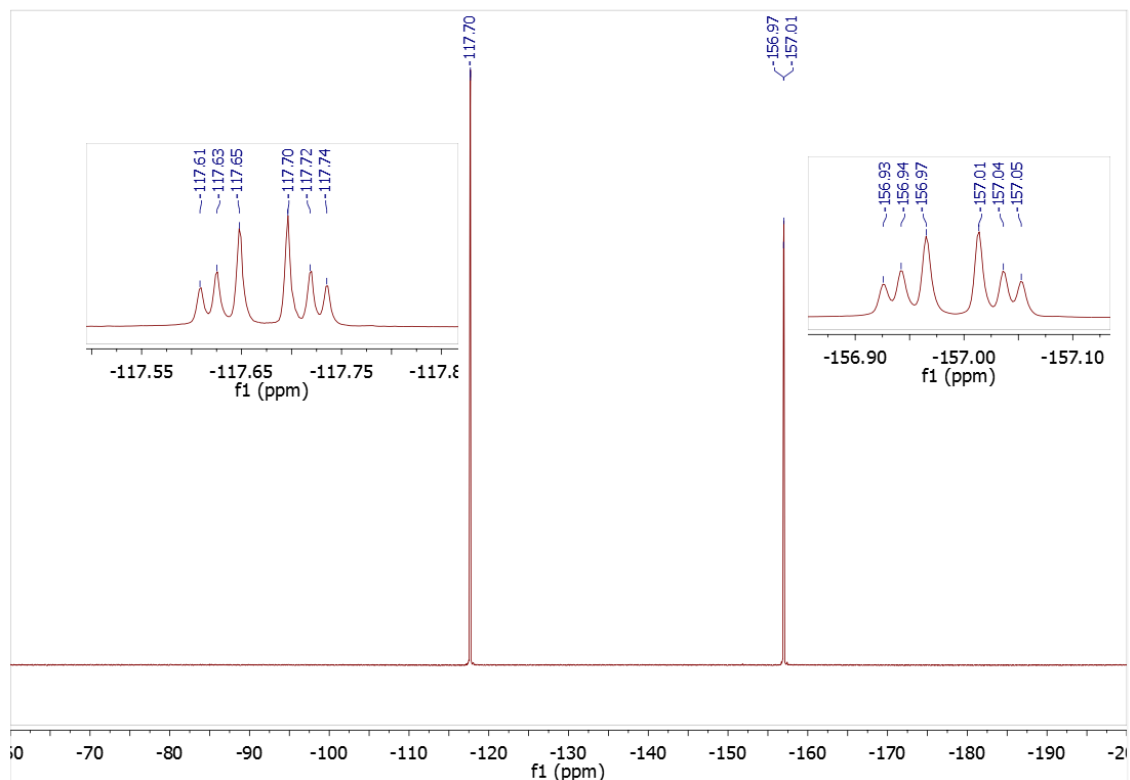


Figure S23: ^{19}F NMR (CDCl_3) spectrum of 4.

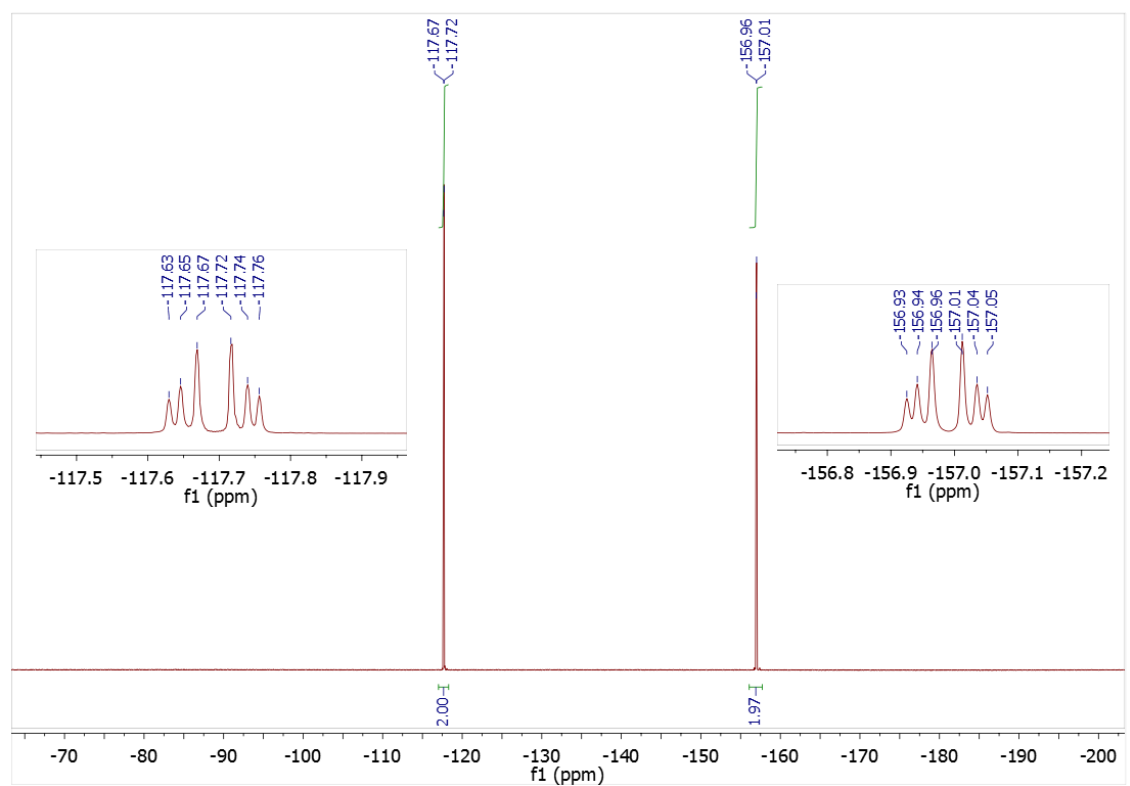


Figure S24: ^{19}F NMR (CDCl_3) spectrum of 5.

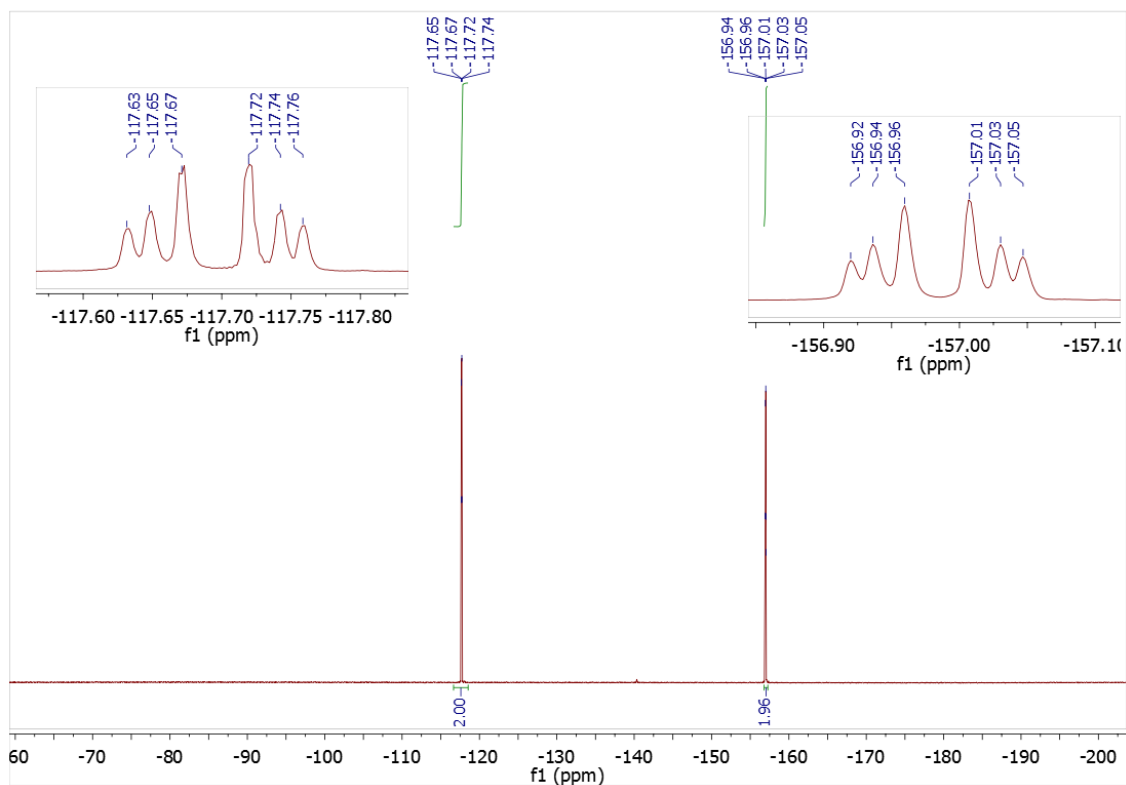


Figure S25: ^{19}F NMR (CDCl_3) spectrum of 6.

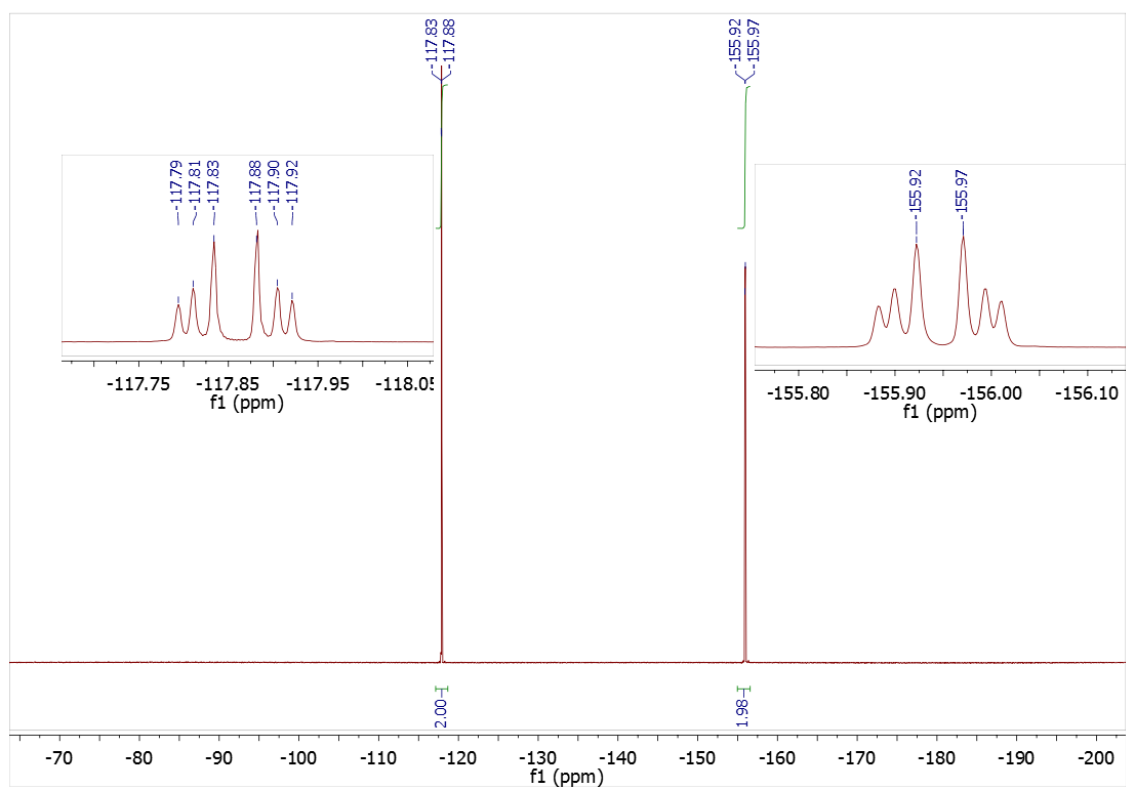


Figure S26: ^{19}F NMR (CDCl_3) spectrum of 7.

MALDI-TOF MS

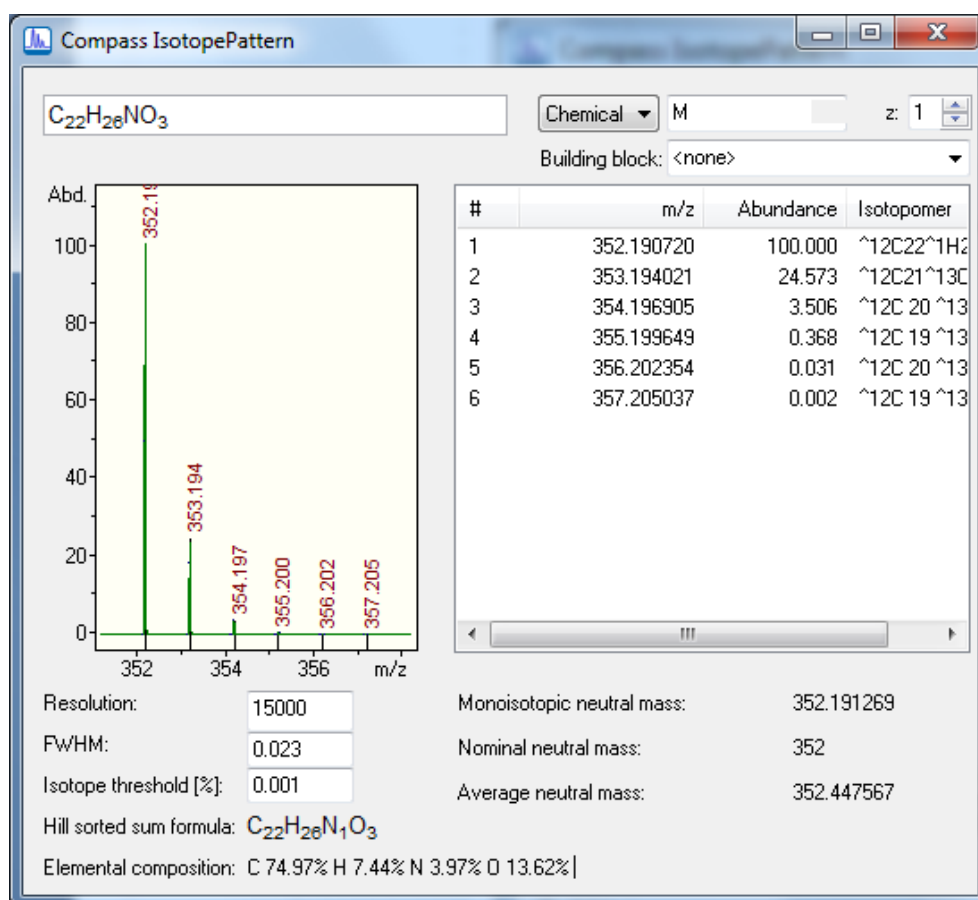
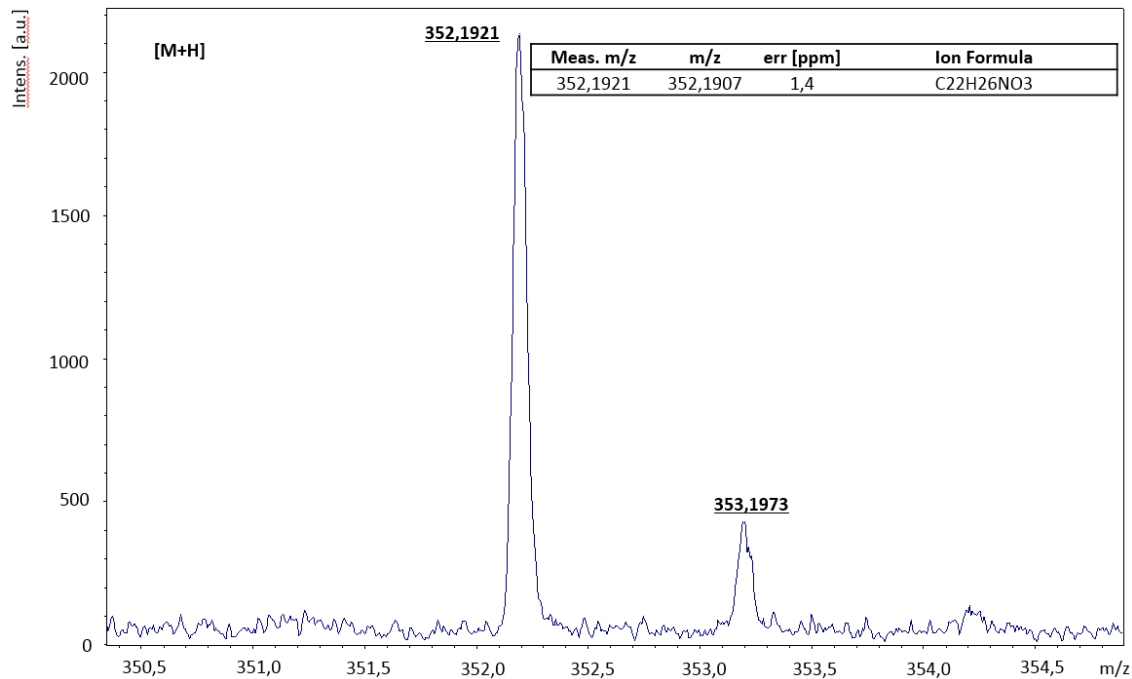


Figure S27: MALDI-TOF mass spectrum and simulated isotopic pattern of CN8*.

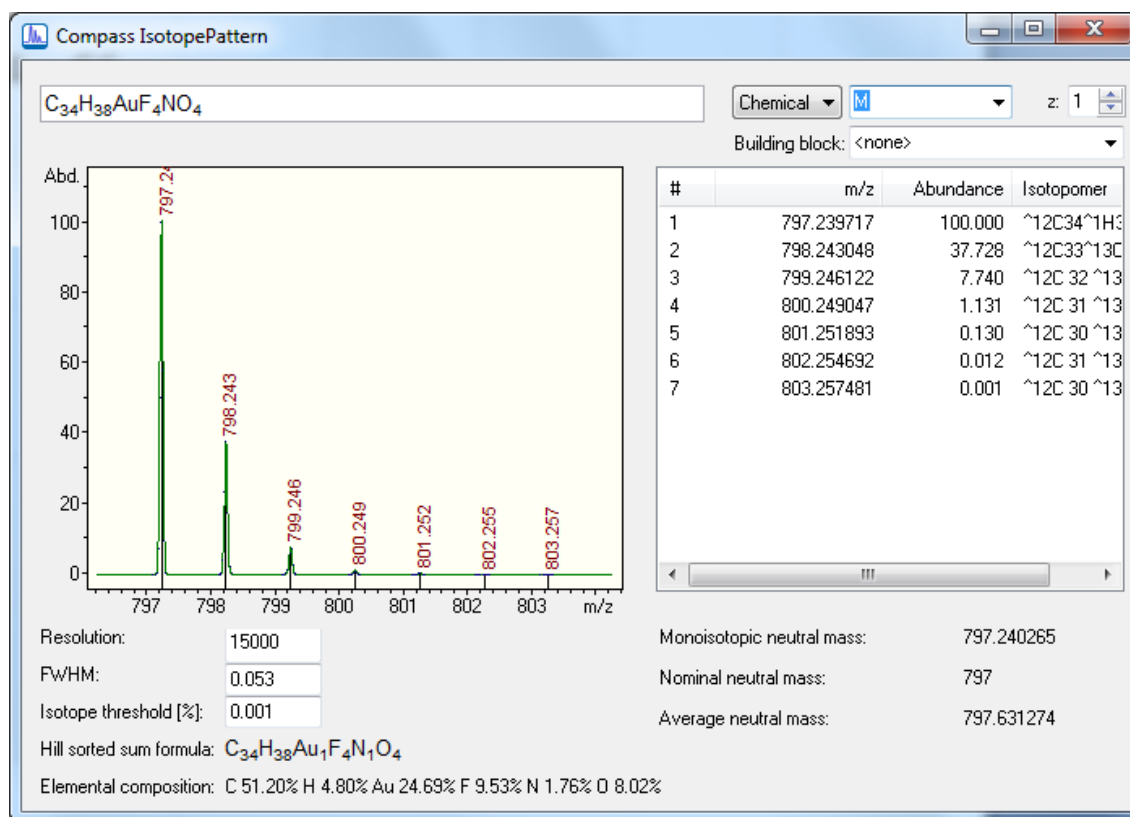
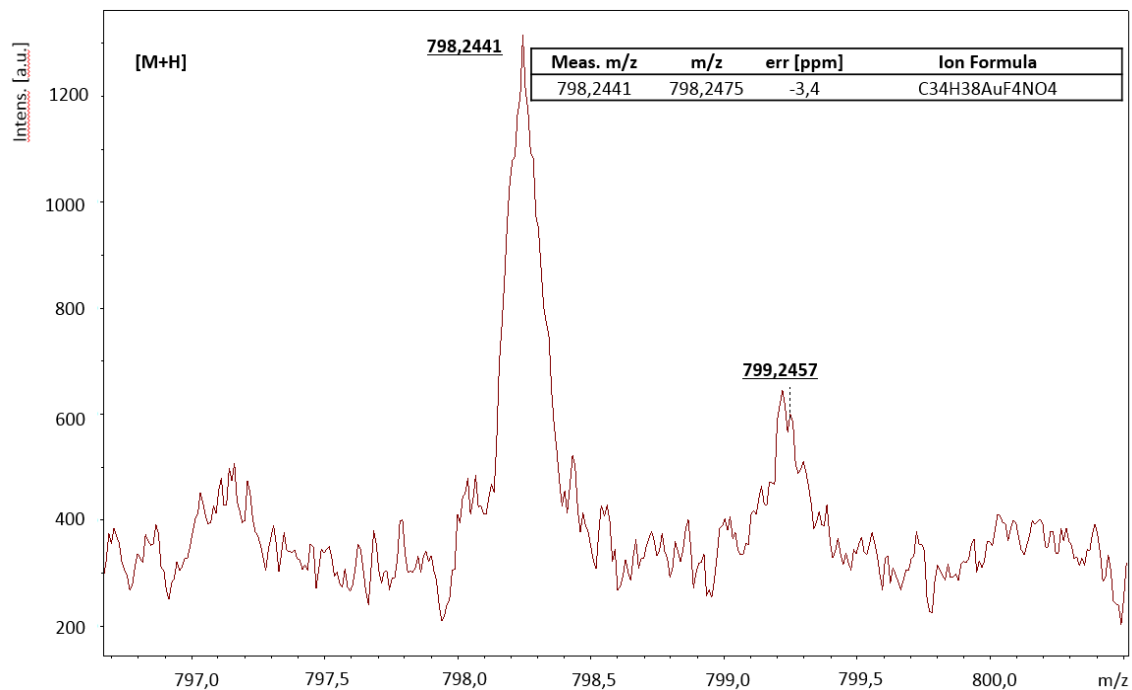


Figure S28: MALDI-TOF mass spectrum and simulated isotopic pattern of **1**.

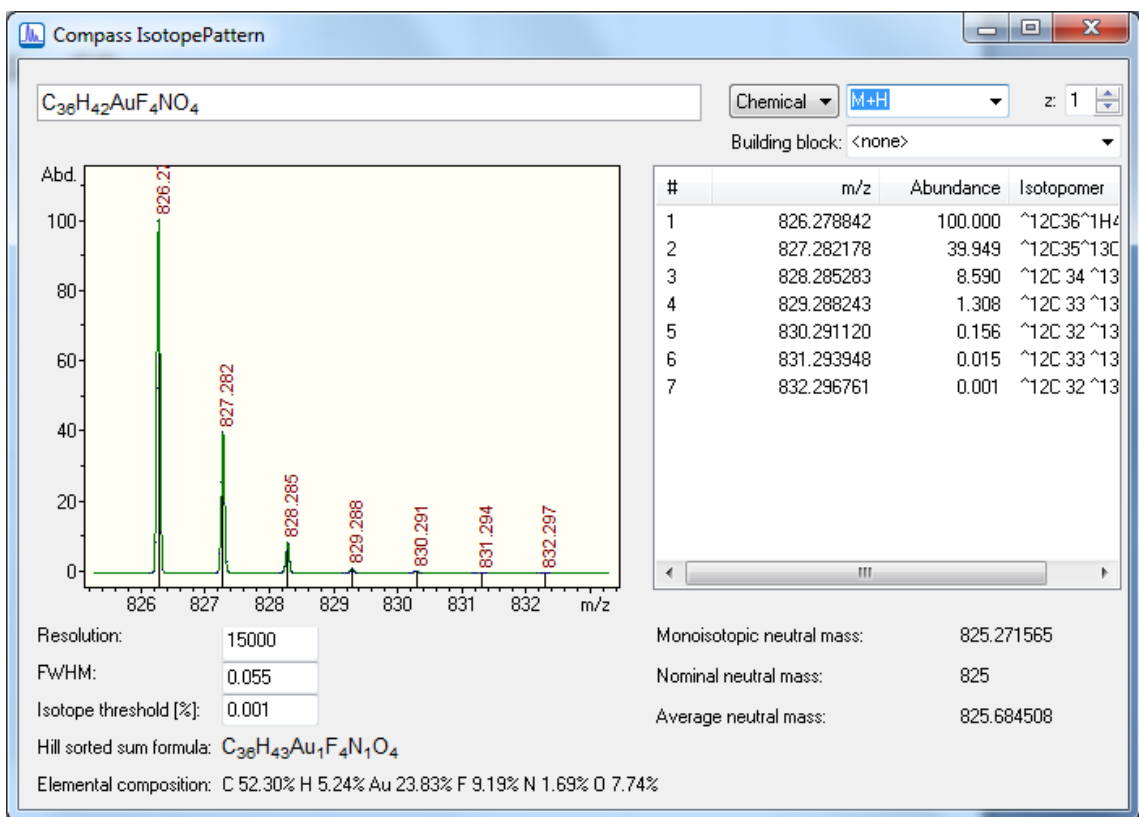
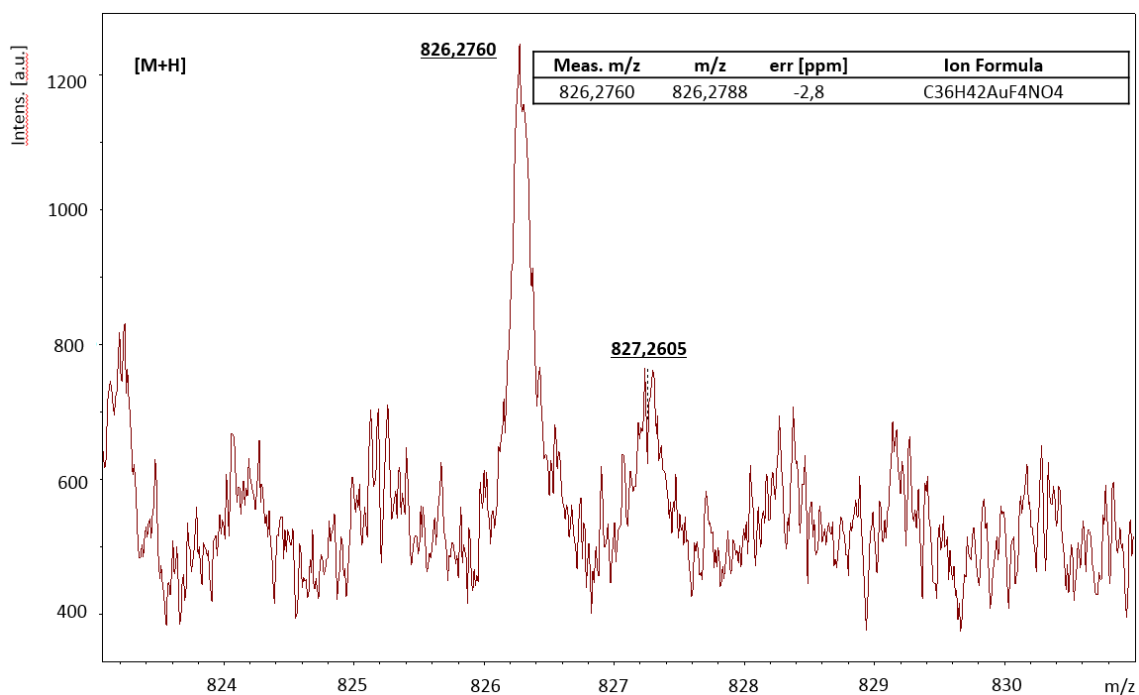


Figure S29: MALDI-TOF mass spectrum and simulated isotopic pattern of **2**.

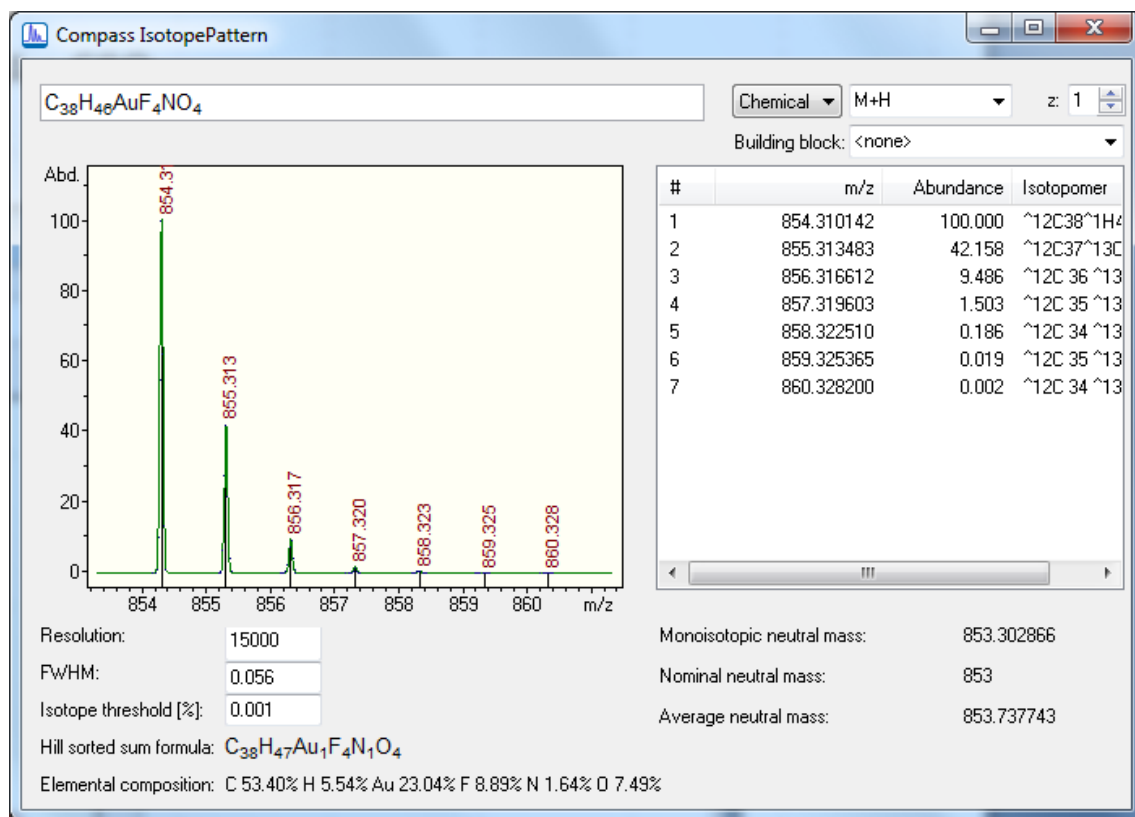
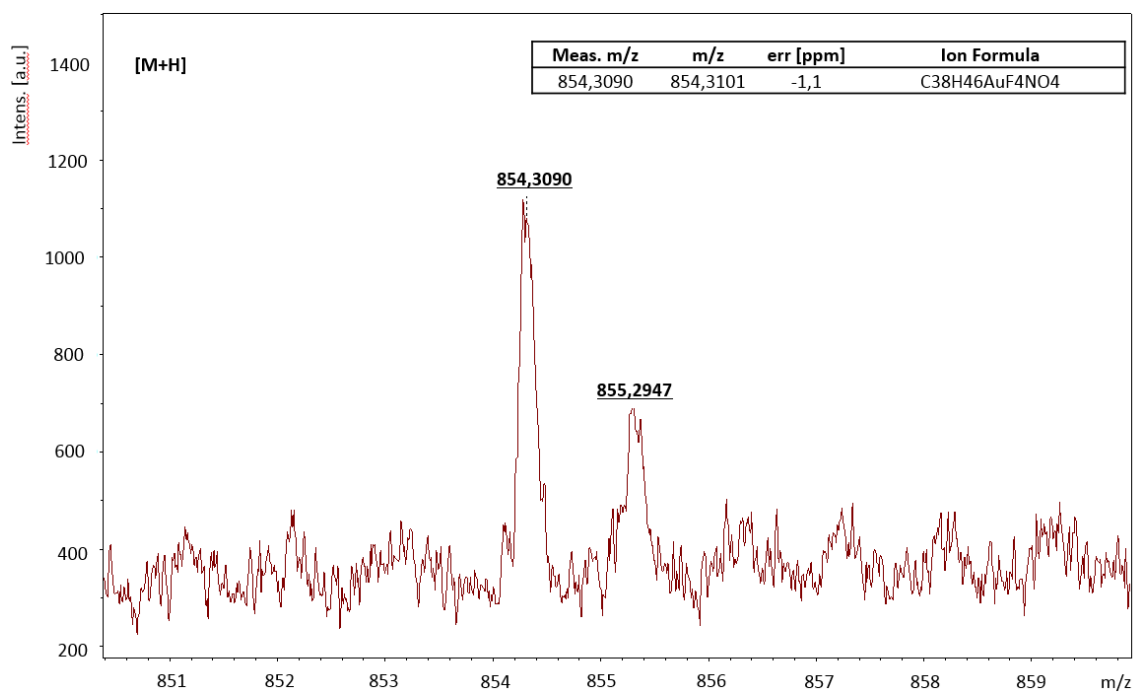


Figure S30: MALDI-TOF mass spectrum and simulated isotopic pattern of **3**.

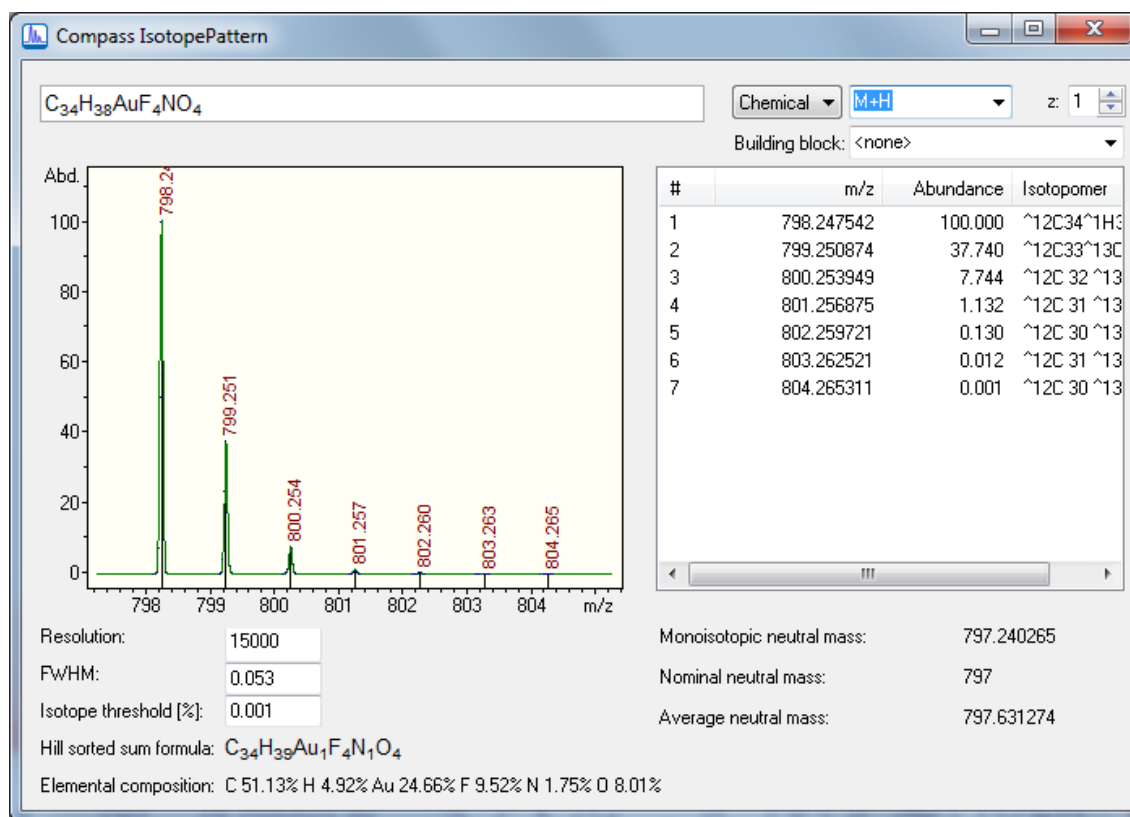
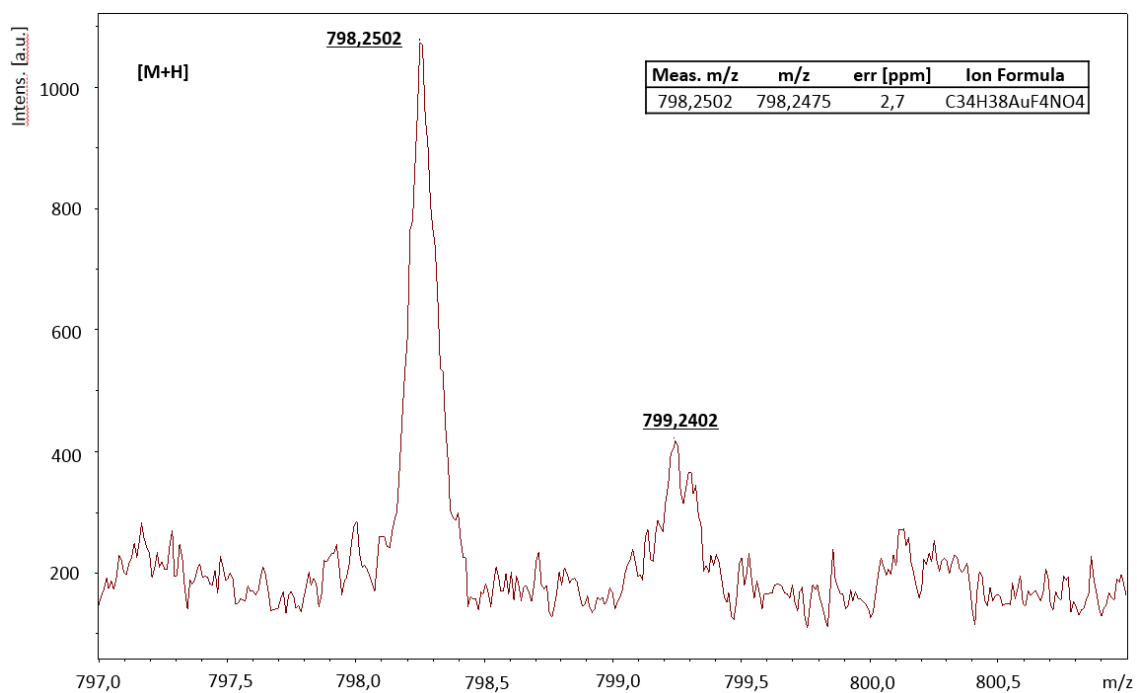


Figure S31: MALDI-TOF mass spectrum and simulated isotopic pattern of **4**.

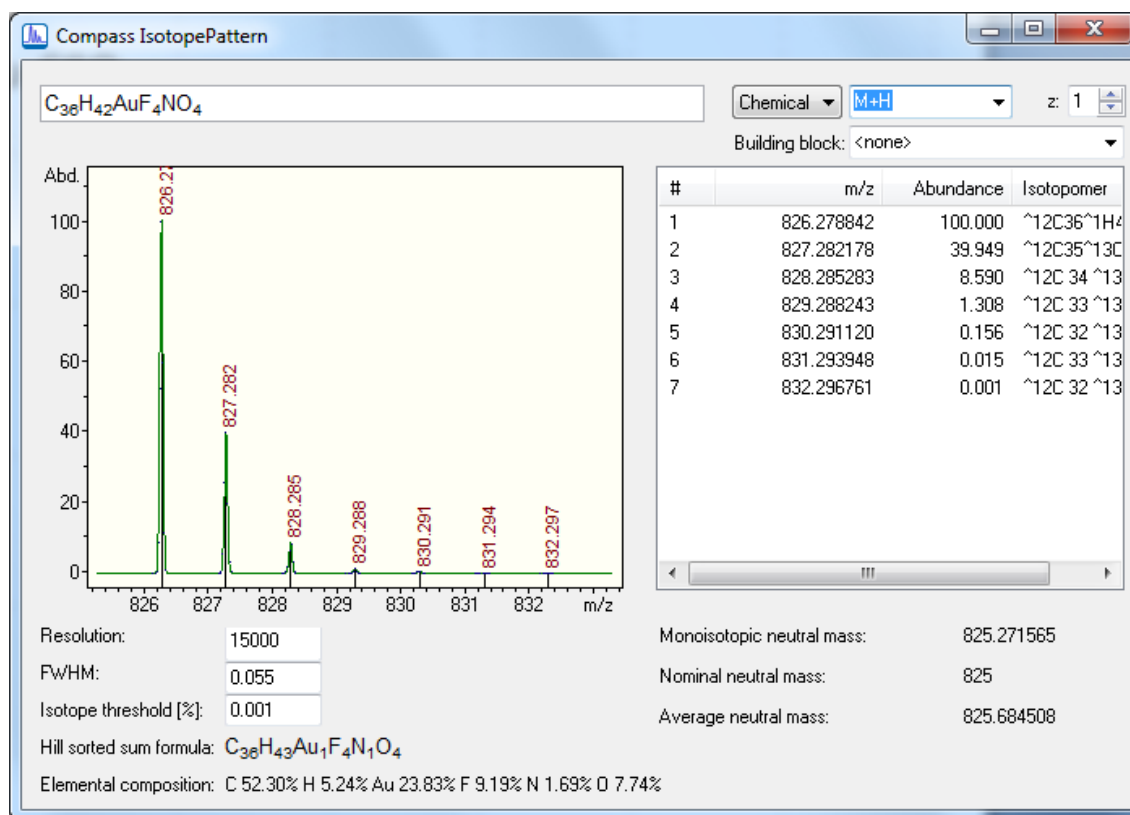
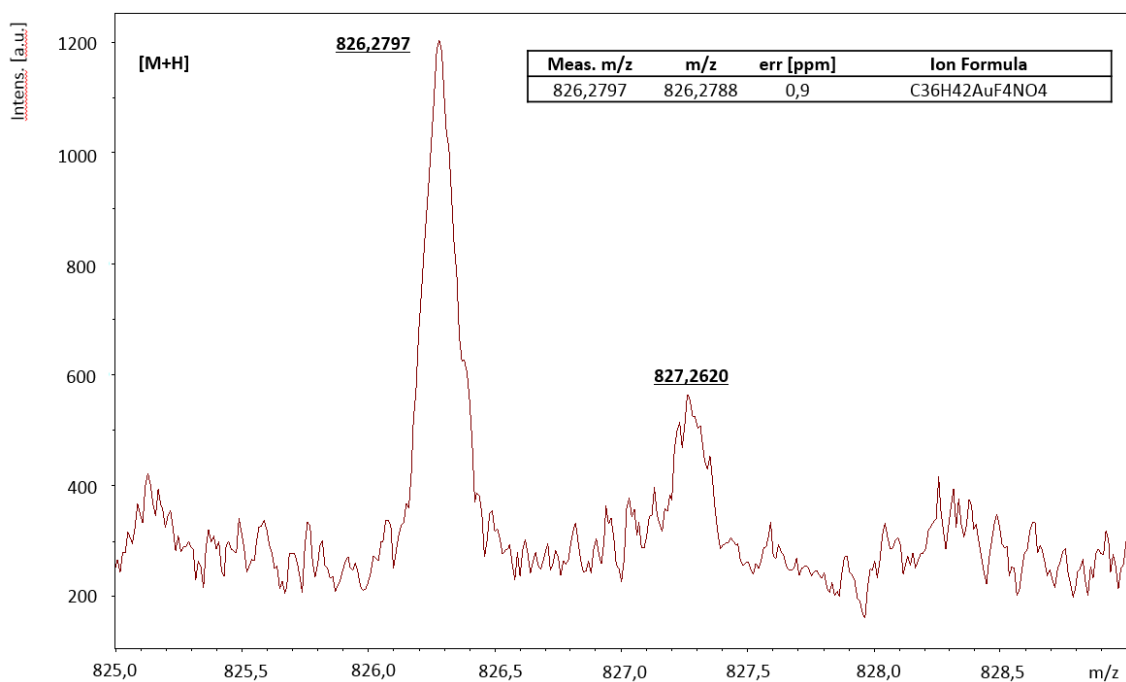


Figure S32: MALDI-TOF mass spectrum and simulated isotopic pattern of 5.

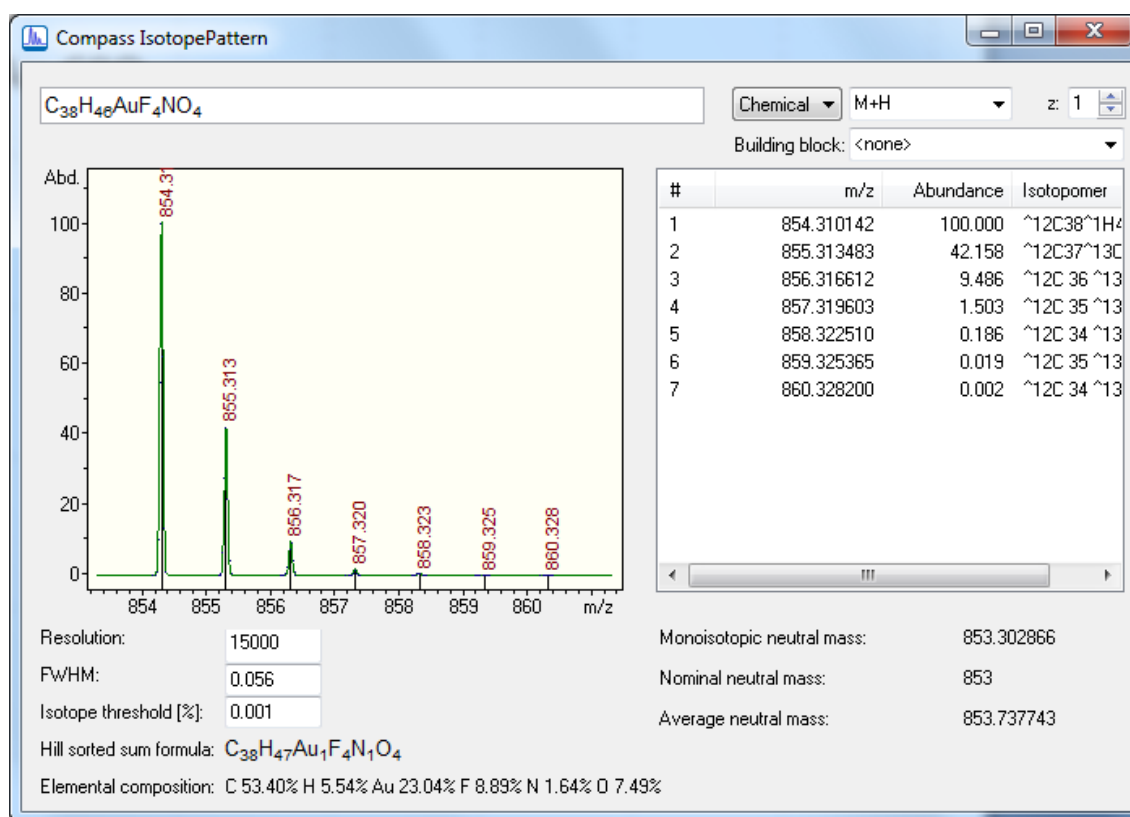
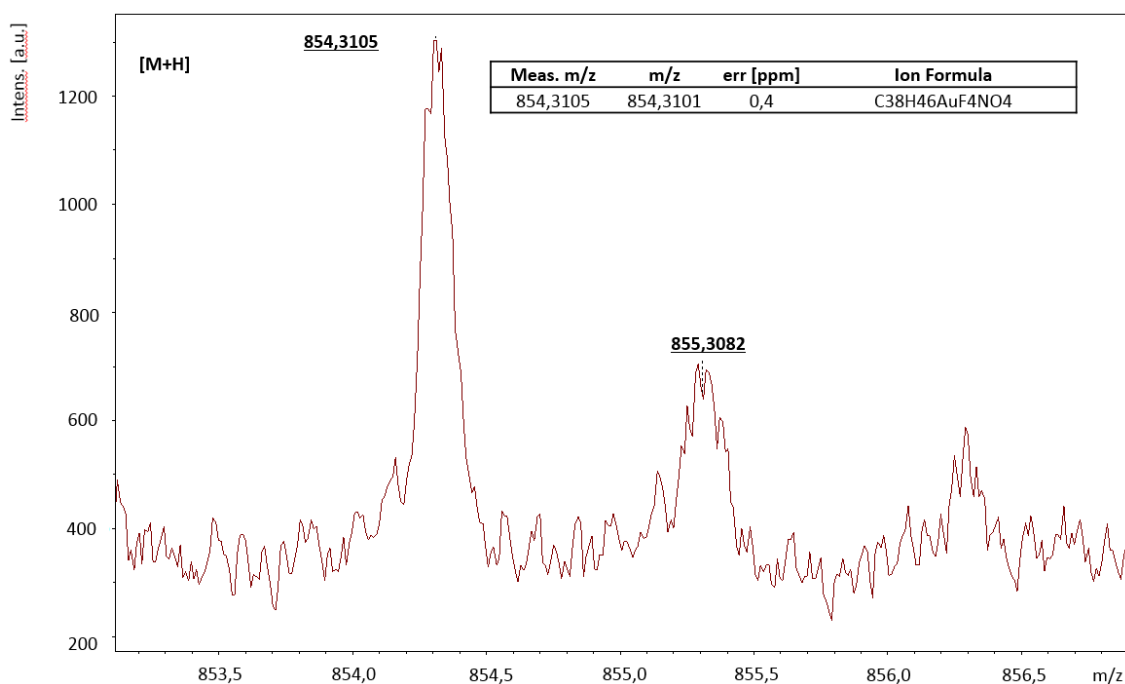


Figure S33: MALDI-TOF mass spectrum and simulated isotopic pattern of **6**.

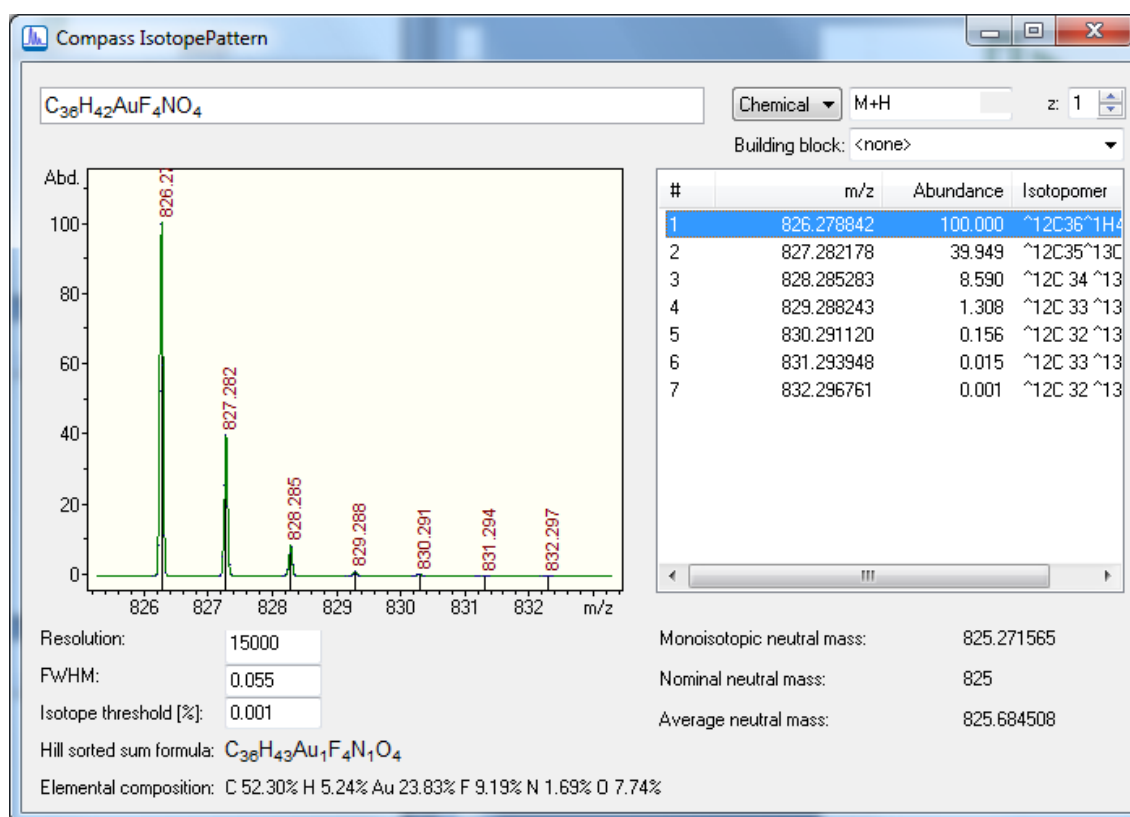
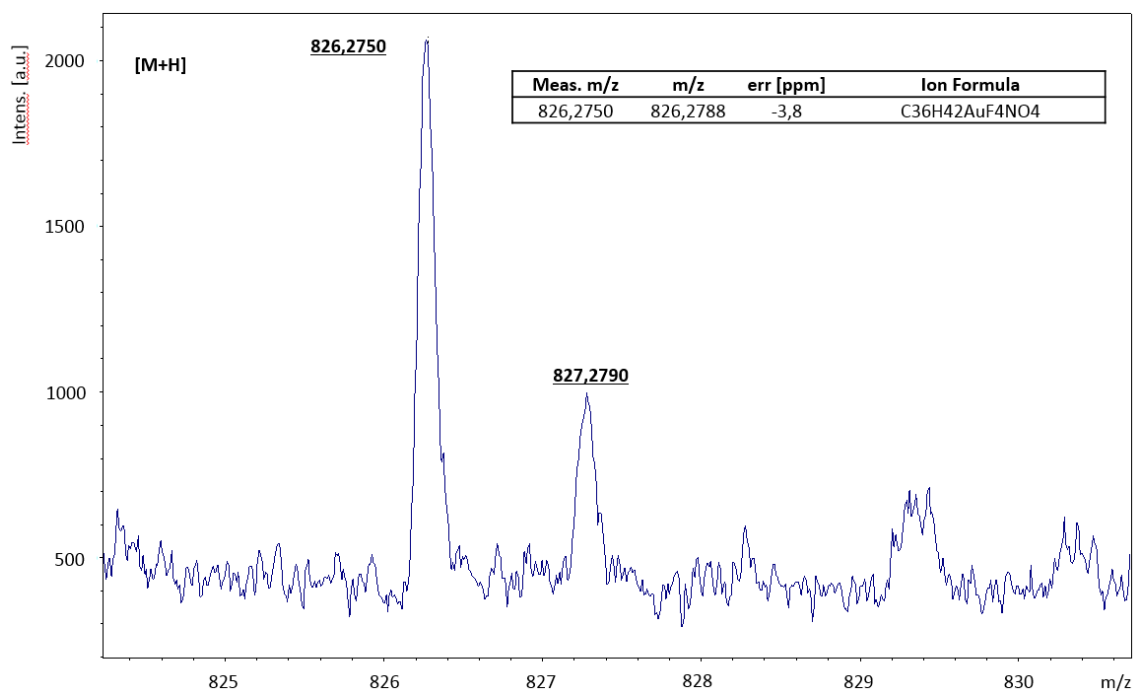


Figure S34: MALDI-TOF mass spectrum and simulated isotopic pattern of 7.

POM textures

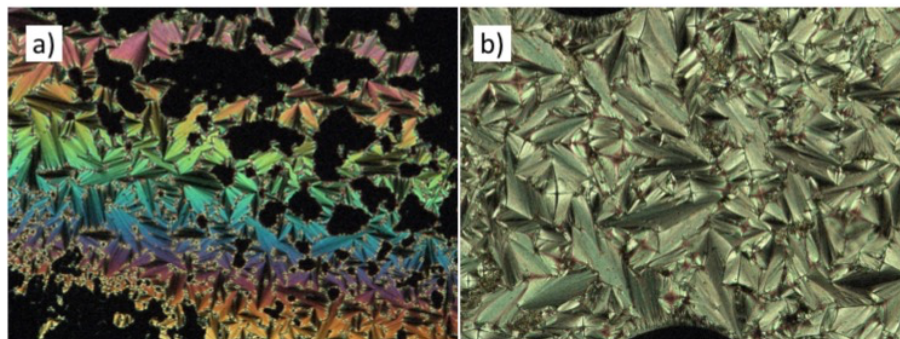


Figure S35. Polarized optical microscopic texture (x100, crossed polarizers) of the SmA phase observed upon cooling from the isotropic liquid of (a) **1** at 150 °C, (b) **5** at 130°C.

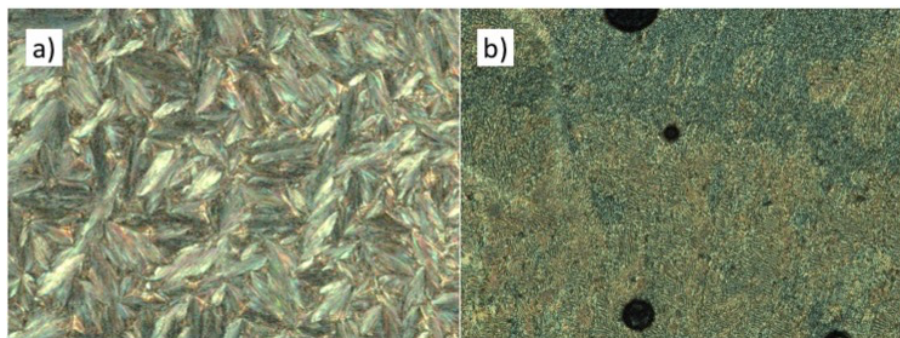


Figure S36. Polarized optical microscopic texture (x100, crossed polarizers) of the SmC* phase observed upon cooling from a SmA mesophase of (a) **2** at 118 °C, (b) **6** at 88°C.

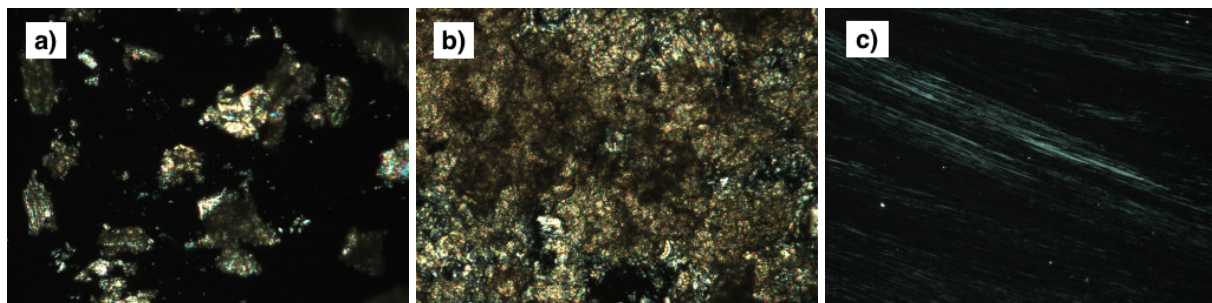


Figure S37. POM textures (x100, crossed polarizers) observed for **2** at 25 °C. a) virgin crystalline sample; b) sandy-like texture obtained by grinding the sample under a cover glass; c) “grayish texture” obtained by shearing the sample without a cover glass.

DSC scans. From top to bottom: first heating, first cooling, second heating.

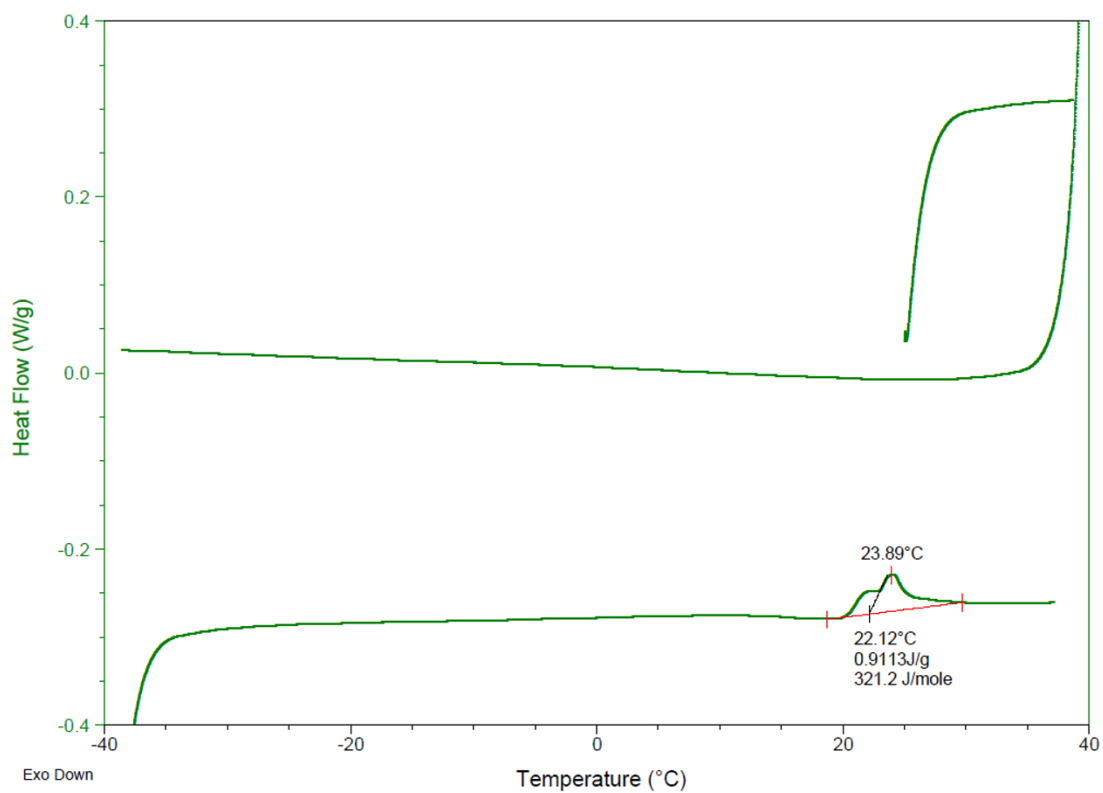


Figure S38: DSC scans of CN8*.

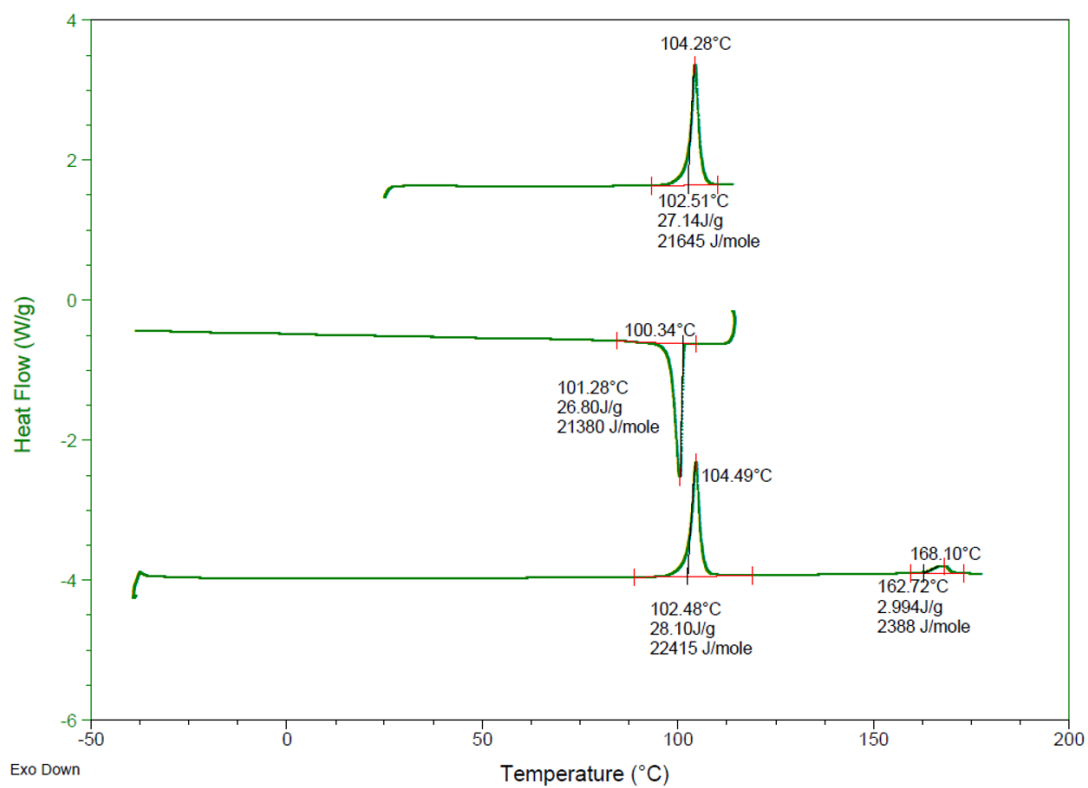


Figure S39: DSC scans of 1.

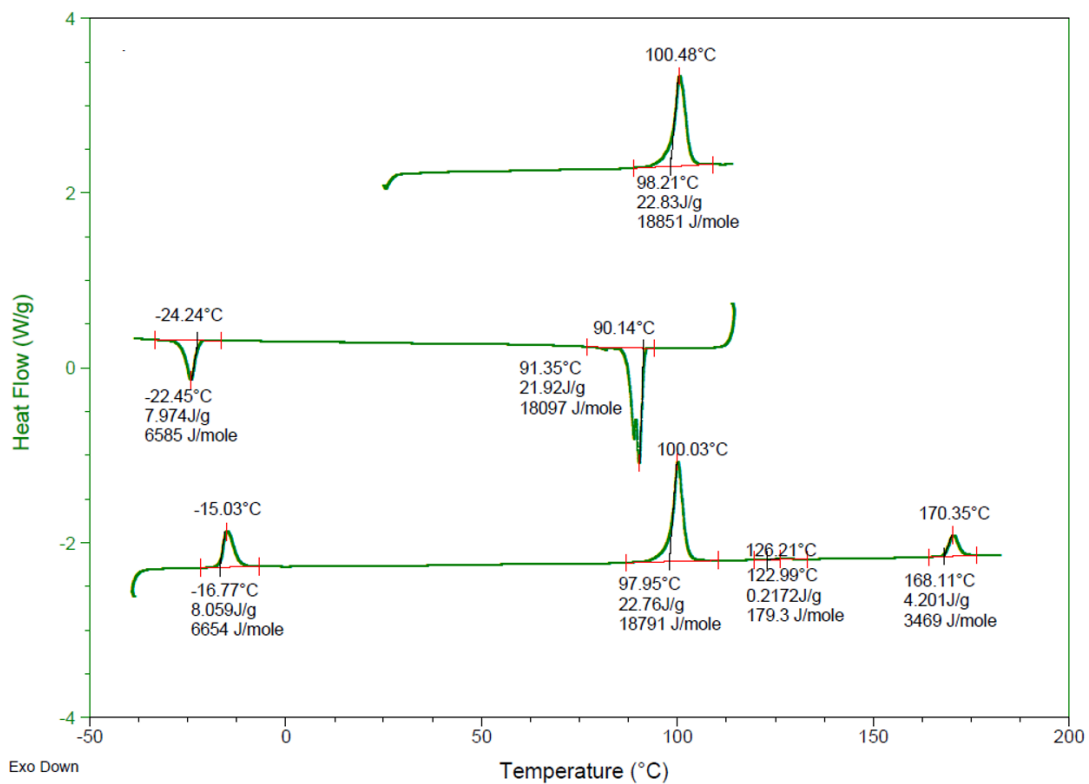


Figure S40: DSC scans of 2.

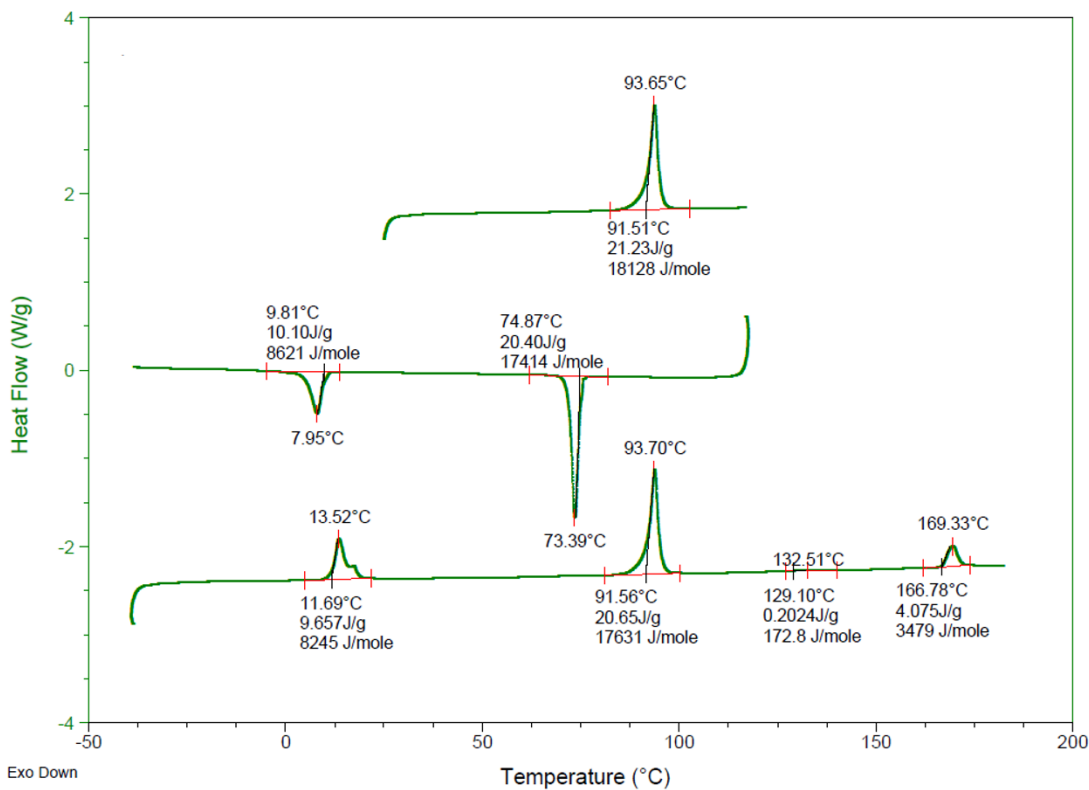


Figure S41: DSC scans of 3.

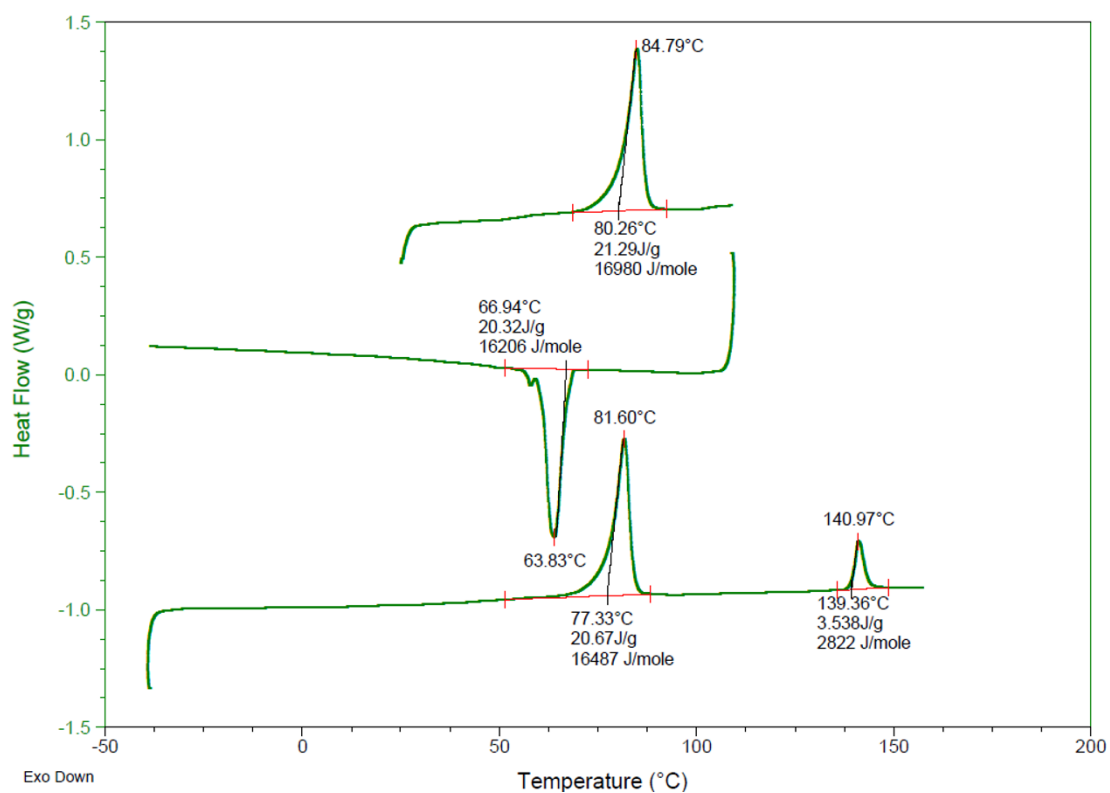


Figure S42: DSC scans of 4.

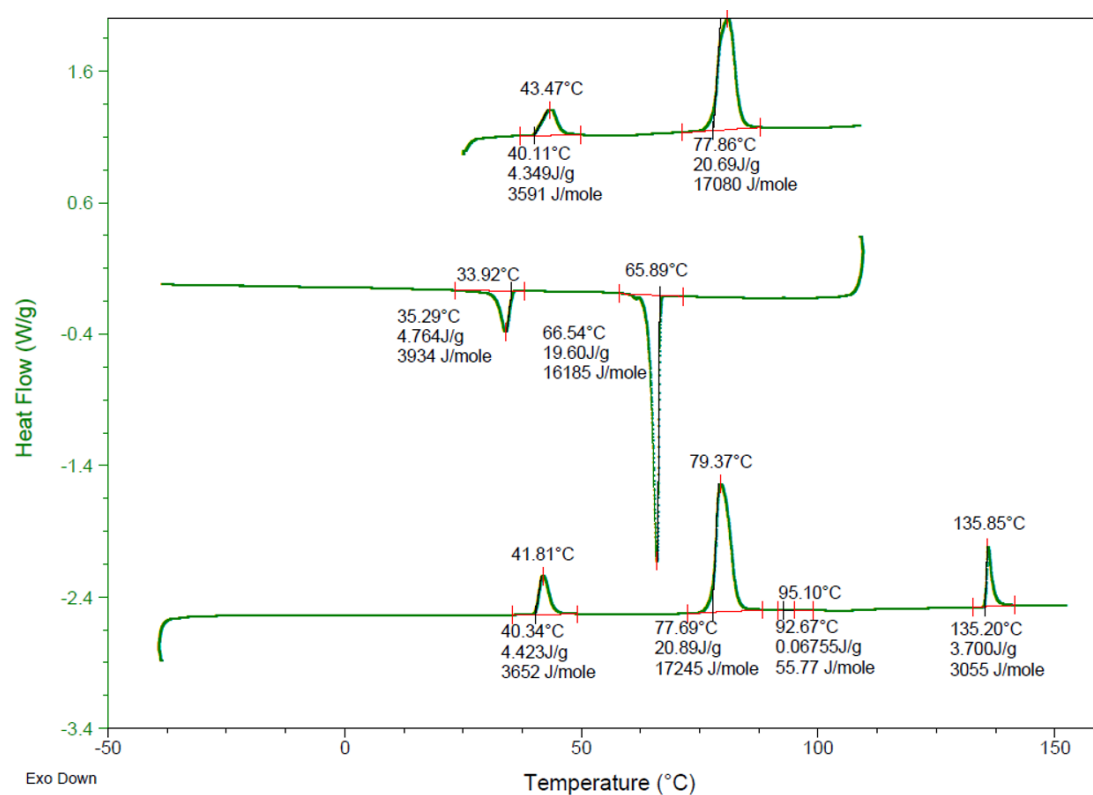


Figure S43: DSC scans of 5.

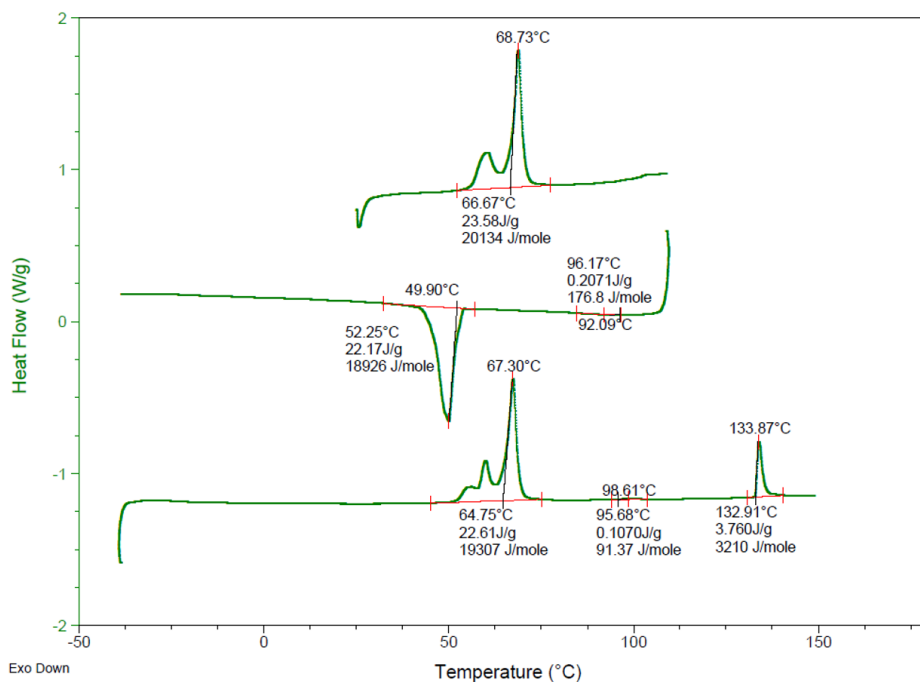


Figure S44: DSC scans of 6.

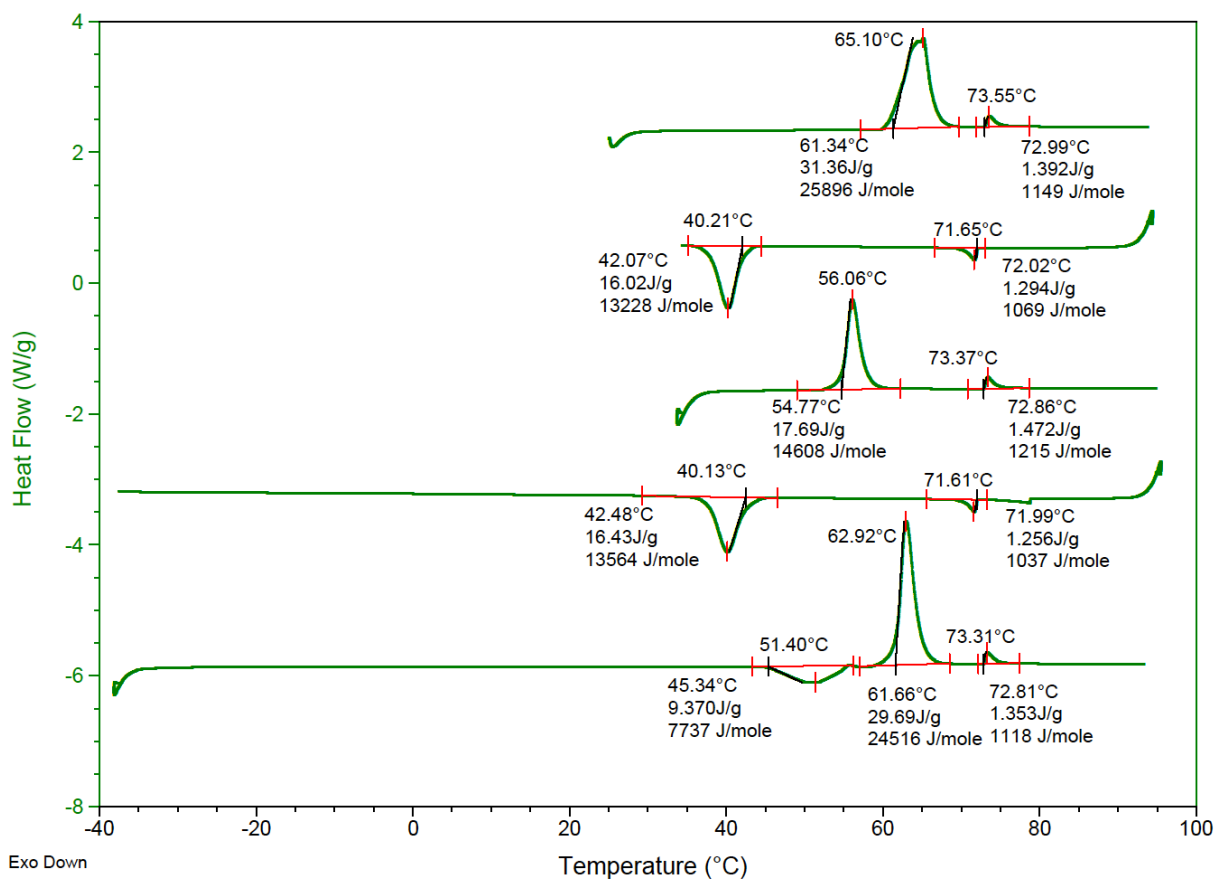


Figure S45: DSC scans of 7.

UV-Visible and luminescence data

Table S1. UV-Visible and luminescence data for the free isocyanides, and for their metal complexes **1-7**, in dichloromethane solution at 298 K (10^{-5} M).

Compound ^a	λ /nm ($\epsilon/ 10^3 \text{ M}^{-1} \text{ cm}^{-1}$)	$\lambda_{\text{max, ex}}$ /nm	$\lambda_{\text{max, em}}$ /nm	τ_{av} ^b /(ns)	τ_n ^c ; A_n ^d
CN6	267 (25.5)	291	374	6.75	$\tau_1 = 1.19$; $A_1 = 31.65$ $\tau_2 = 7.17$; $A_2 = 68.35$
CN8	267 (26.4)	294	373	7.96	$\tau_1 = 1.31$; $A_1 = 37.84$ $\tau_2 = 8.59$; $A_2 = 62.16$
CN10	267 (7.7)	296	377	6.80	$\tau_1 = 1.40$; $A_1 = 31.53$ $\tau_2 = 7.29$; $A_2 = 68.47$
CN8*	269 (24.6)	295	378	6.02	$\tau_1 = 1.07$; $A_1 = 38.73$ $\tau_2 = 6.54$; $A_2 = 61.27$
1	279 (51.1)	304	378	3.92	$\tau_1 = 0.62$; $A_1 = 33.33$ $\tau_2 = 4.17$; $A_2 = 66.67$
2	279 (52.2)	305	379	5.13	$\tau_1 = 0.96$; $A_1 = 42.83$ $\tau_2 = 5.66$; $A_2 = 57.17$
3	279 (53.3)	306	379	4.96	$\tau_1 = 0.92$; $A_1 = 39.43$ $\tau_2 = 5.41$; $A_2 = 60.57$
4	280 (52.8)	305	375	3.22	$\tau_1 = 0.64$; $A_1 = 40.29$ $\tau_2 = 3.53$; $A_2 = 59.71$
5	280 (53.3)	305	377	5.01	$\tau_1 = 1.23$; $A_1 = 32.32$ $\tau_2 = 5.42$; $A_2 = 67.68$
6	280 (53.1)	306	378	4.82	$\tau_1 = 0.84$; $A_1 = 41.35$ $\tau_2 = 5.27$; $A_2 = 58.65$
7	280 (49.0)	307	384	6.88	$\tau_1 = 0.91$; $A_1 = 37.74$ $\tau_2 = 7.29$; $A_2 = 68.26$

^a The isocyanides are labeled as CN followed by the number of carbons of the alkoxy substituent.

^b Average lifetime $\tau_{\text{av}} = (A_1\tau_1^2 + A_2\tau_2^2 + \dots) / (A_1\tau_1 + A_2\tau_2 + \dots)$. ^c τ_n = Natural lifetime. ^d A_n = Intensity coefficients

UV-Visible spectra in dichloromethane solution (10^{-5} M)

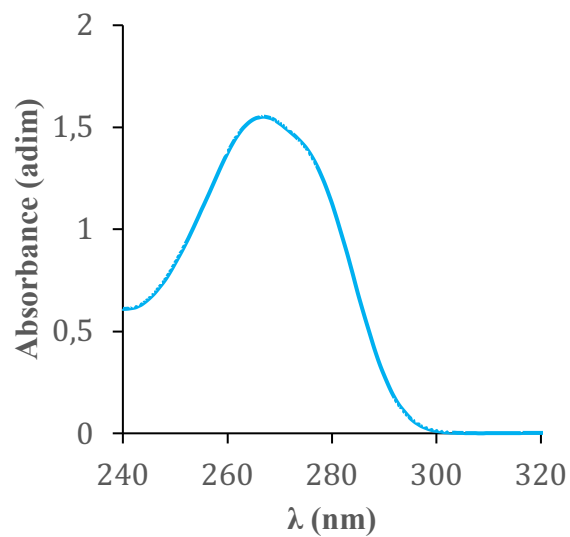


Figure S46. UV-Visible spectra of **CN6**

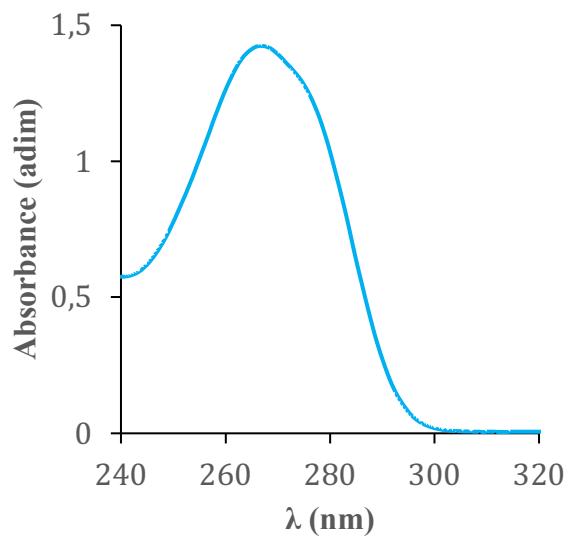


Figure S47. UV-Visible spectra of **CN8**

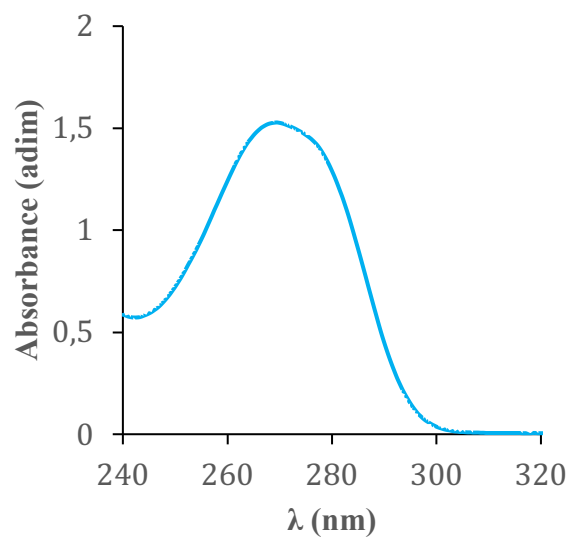


Figure S48. UV-Visible spectra of **CN8***

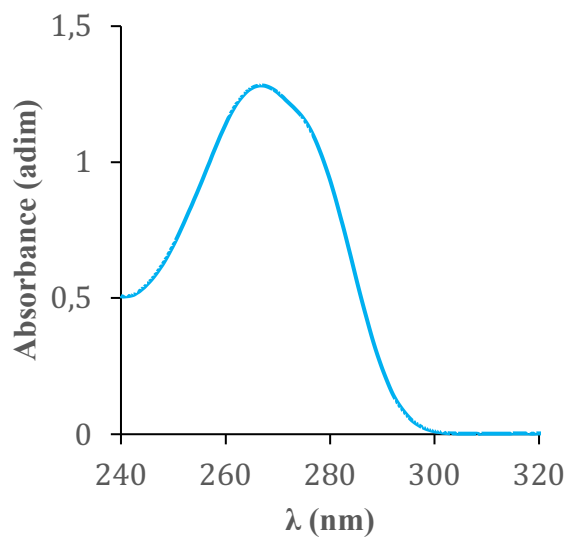


Figure S49. UV-Visible spectra of **CN10**

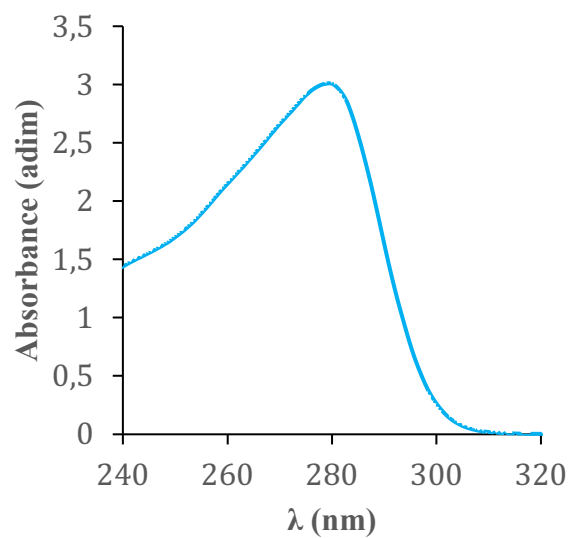


Figure S50. UV-Visible spectra of **1**

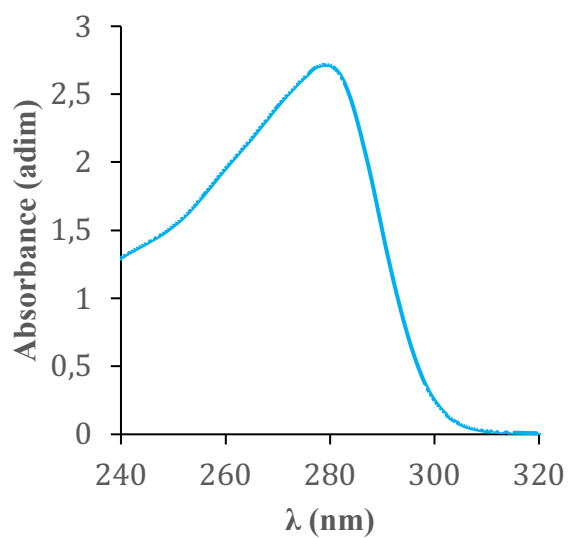


Figure S51. UV-Visible spectra of **2**

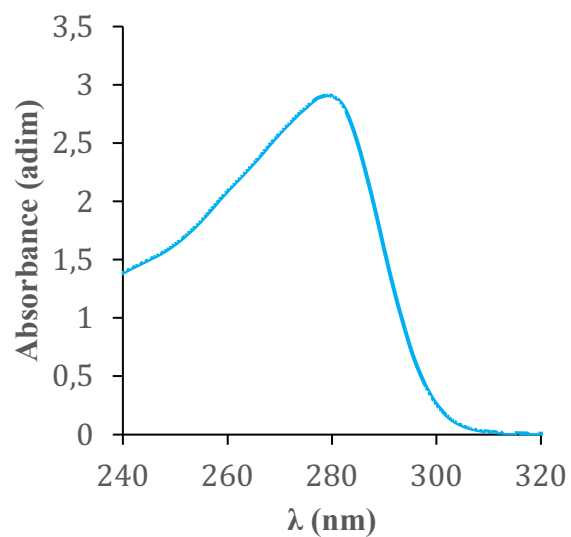


Figure S52. UV-Visible spectra of **3**

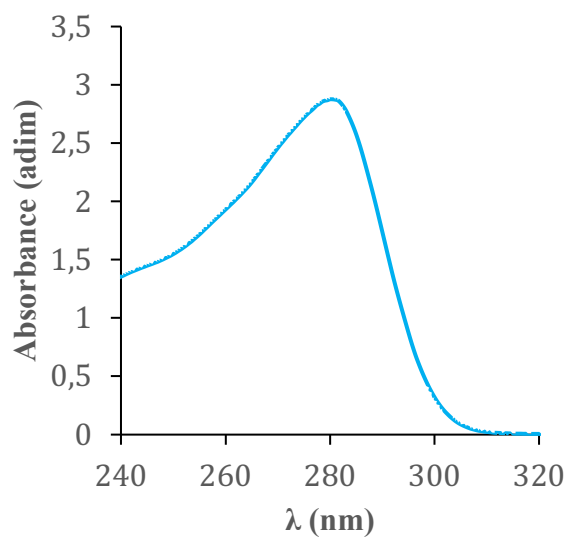


Figure S53. UV-Visible spectra of **4**

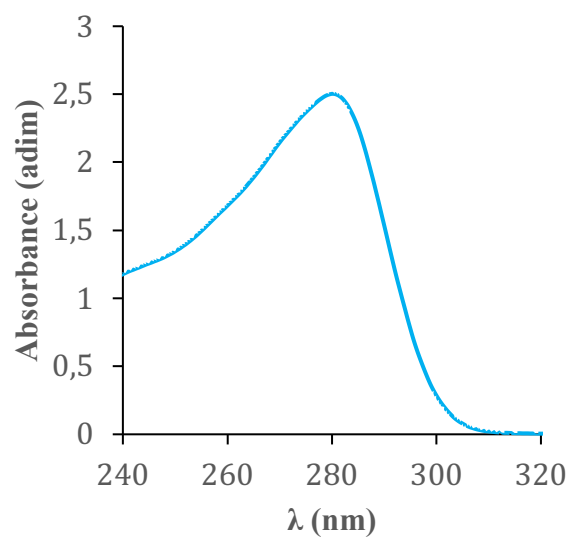


Figure S54. UV-Visible spectra of **5**

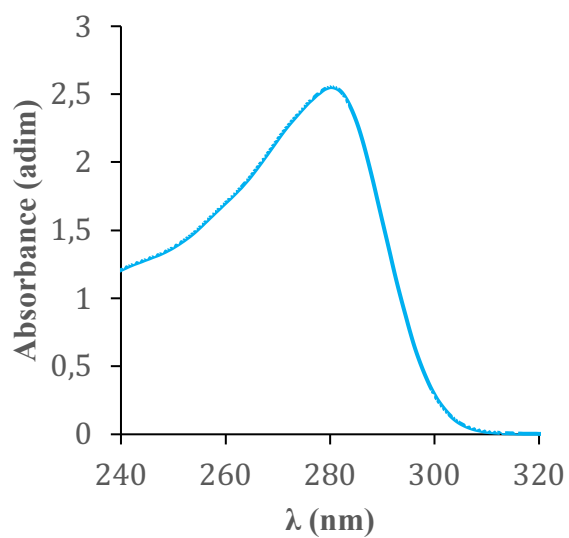


Figure S55. UV-Visible spectra of **6**.

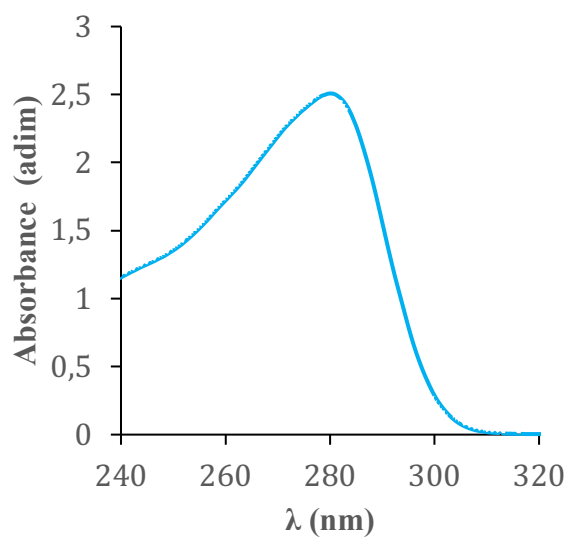


Figure S56. UV-Visible spectra of **7**

Emission Decay Profiles in dichloromethane solution (excitation LED 280 nm).

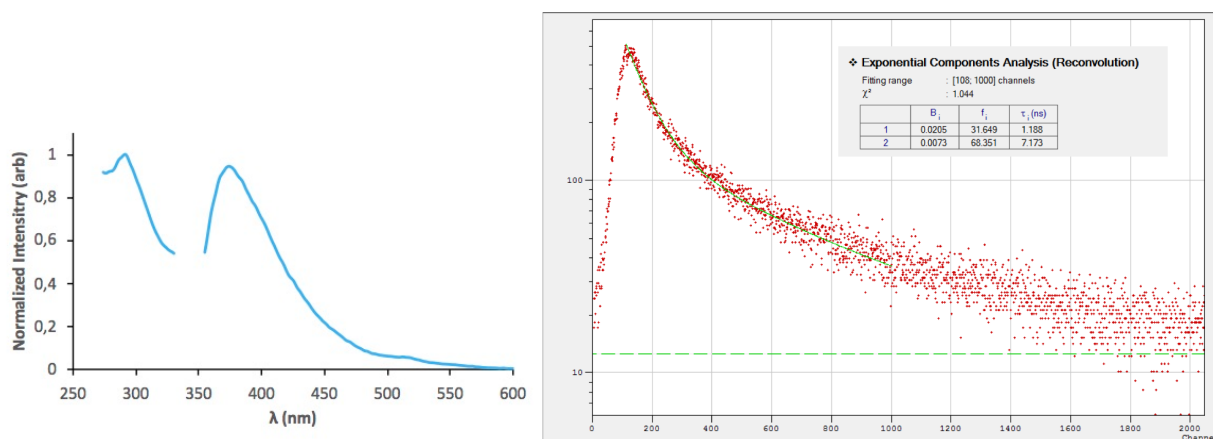


Figure S57. Luminescence spectra and emission decay profile of **CN6** (CH_2Cl_2).

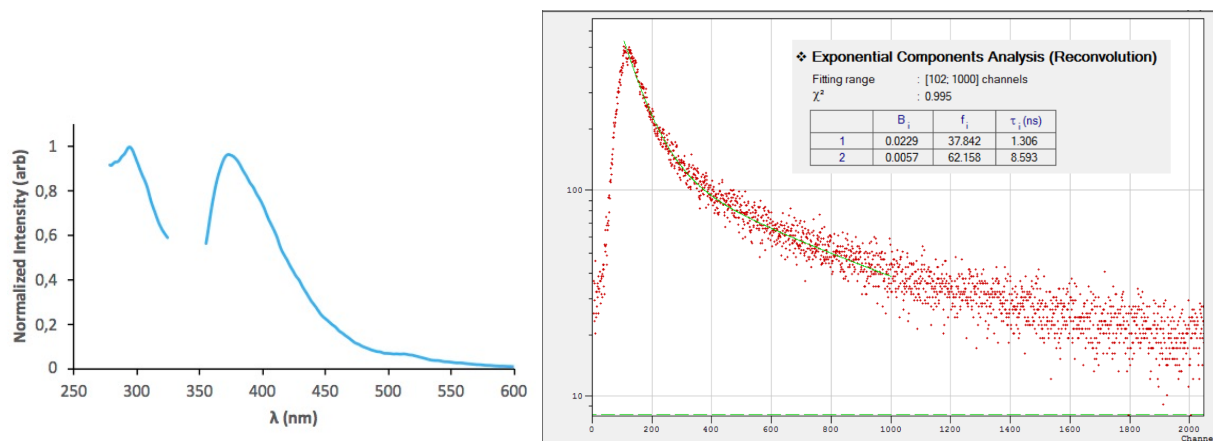


Figure S58. Luminescence spectra and emission decay profile of **CN8** (CH_2Cl_2).

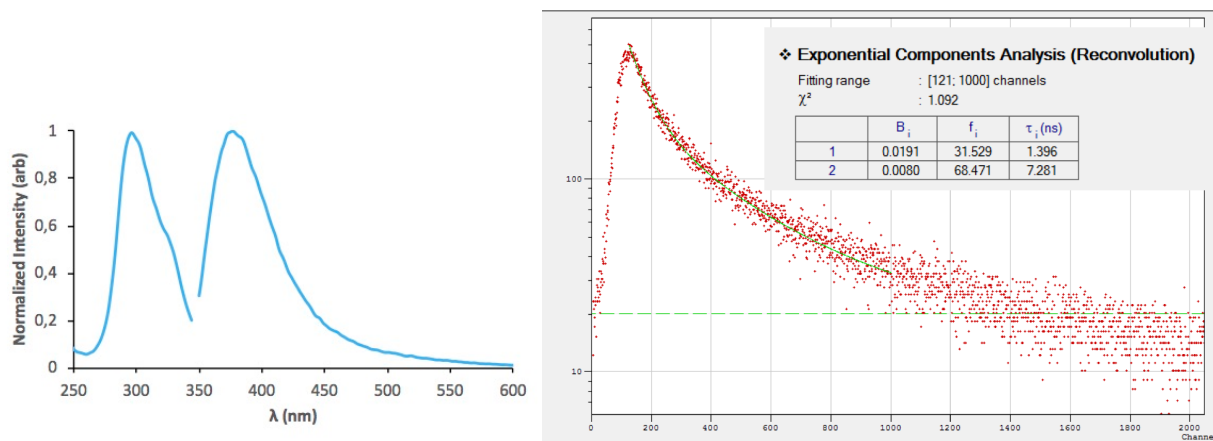


Figure S59. Luminescence spectra and emission decay profile of **CN10** (CH_2Cl_2).

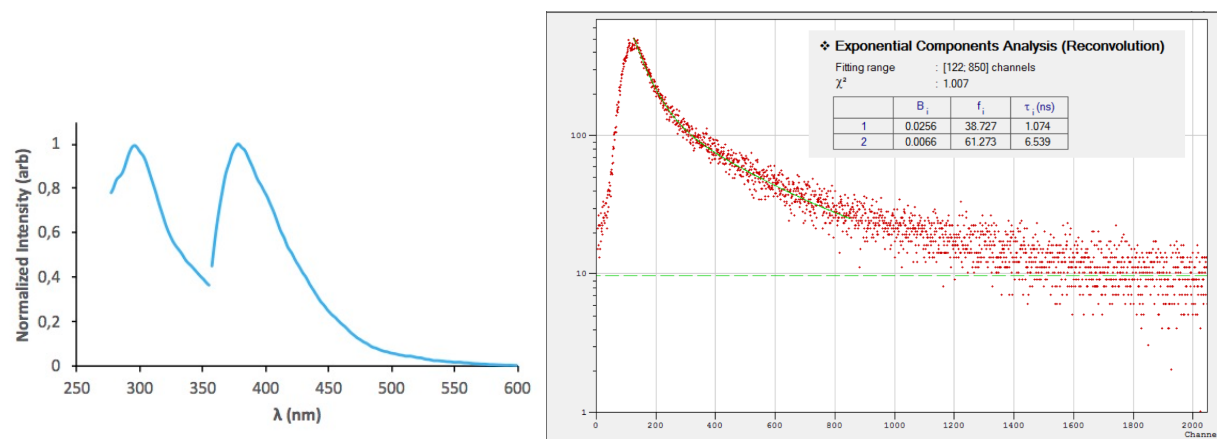


Figure S60. Luminescence spectra and emission decay profile of CN8* (CH₂Cl₂).

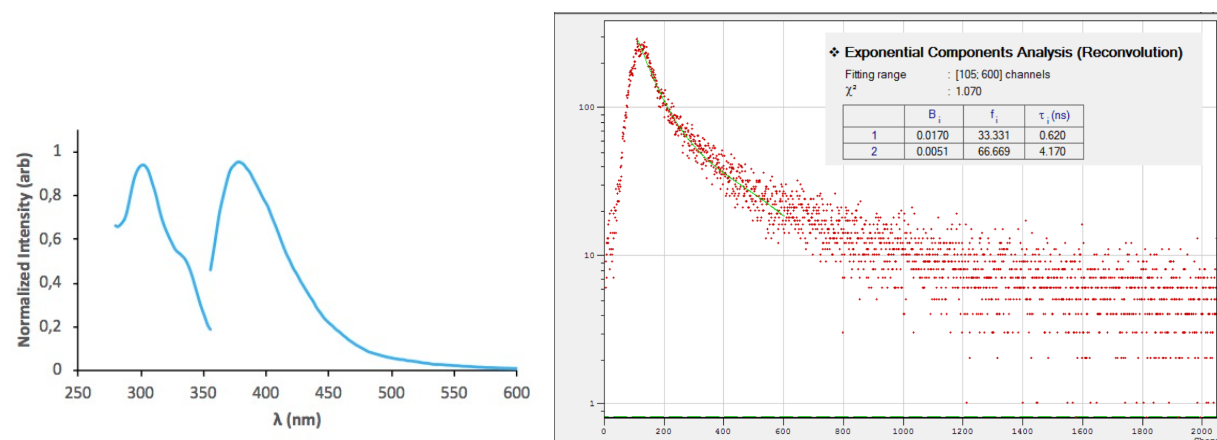


Figure S61. Luminescence spectra and emission decay profile of 1 (CH₂Cl₂).

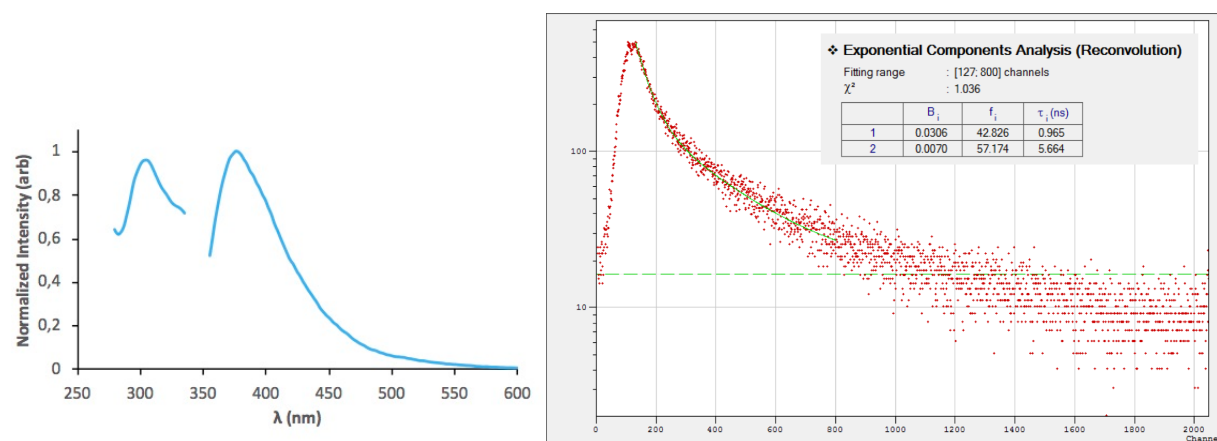


Figure S62. Luminescence spectra and emission decay profile of 2 (CH₂Cl₂).

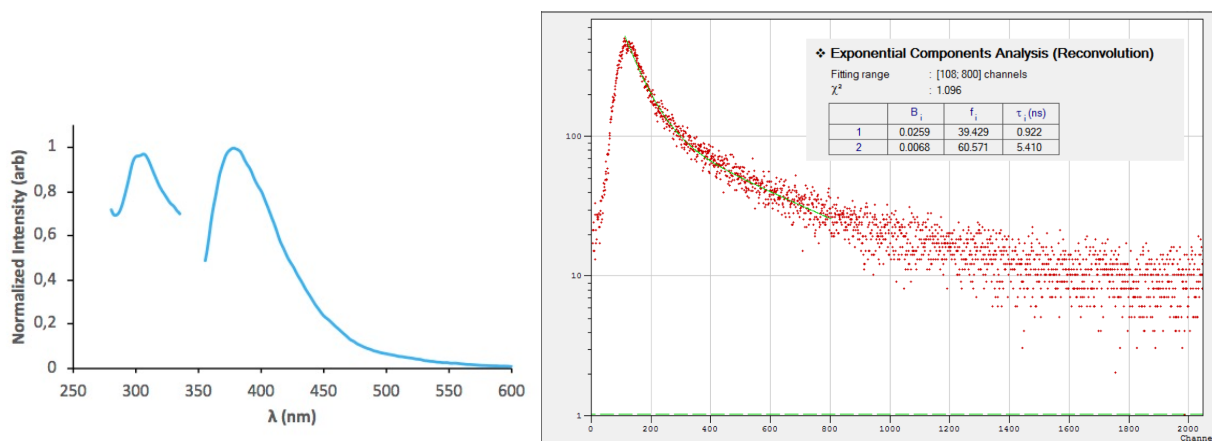


Figure S63. Luminescence spectra and emission decay profile of **3** (CH_2Cl_2).

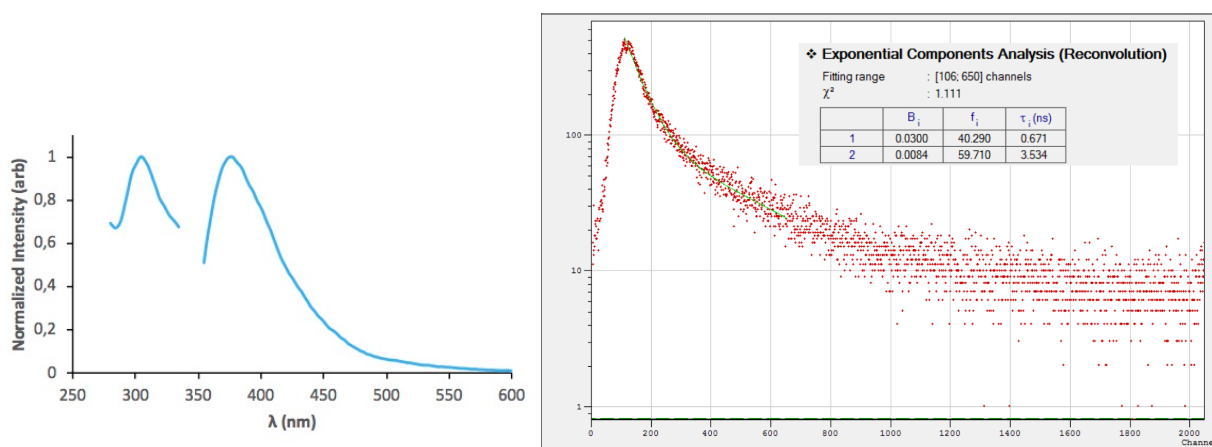


Figure S64. Luminescence spectra and emission decay profile of **4** (CH_2Cl_2).

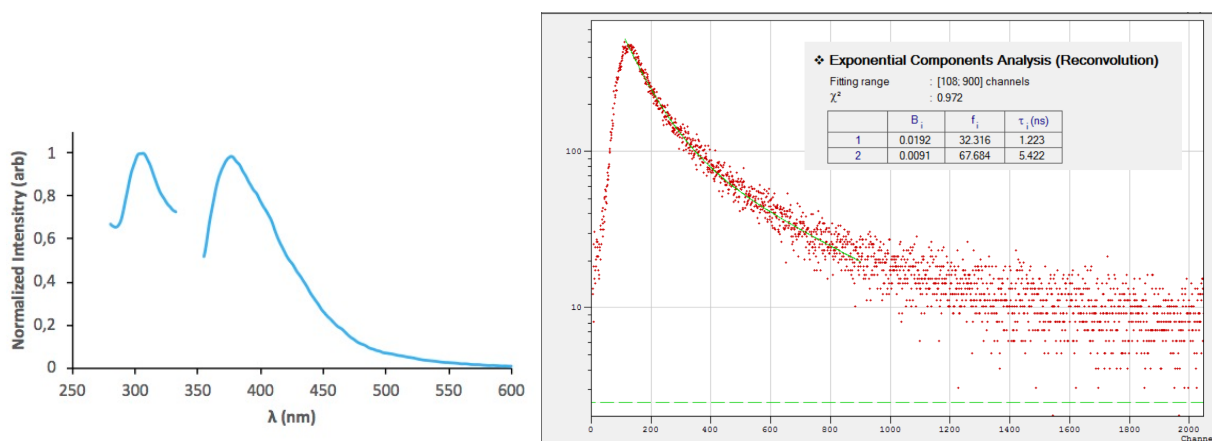


Figure S65. Luminescence spectra and emission decay profile of **5** (CH_2Cl_2).

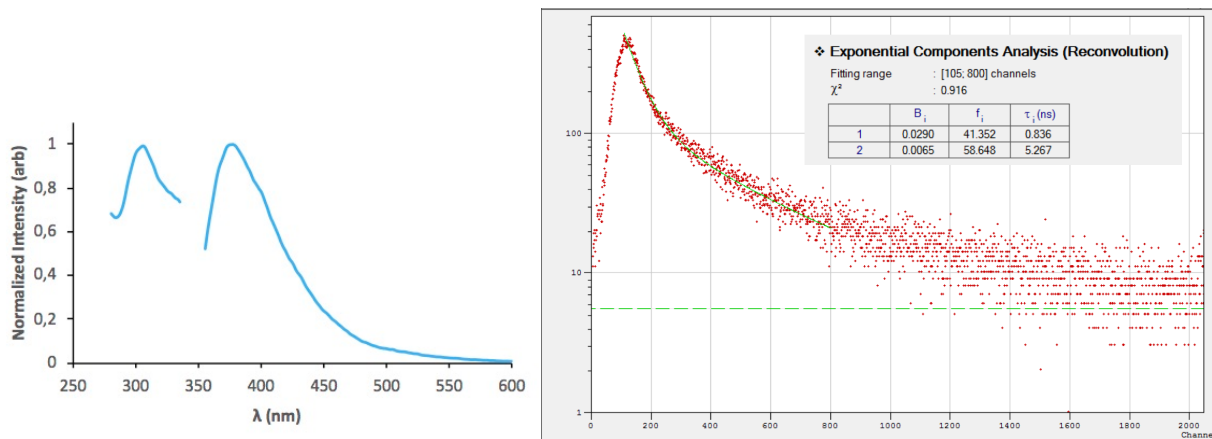


Figure S66. Luminescence spectra and emission decay profile of **6** (CH_2Cl_2).

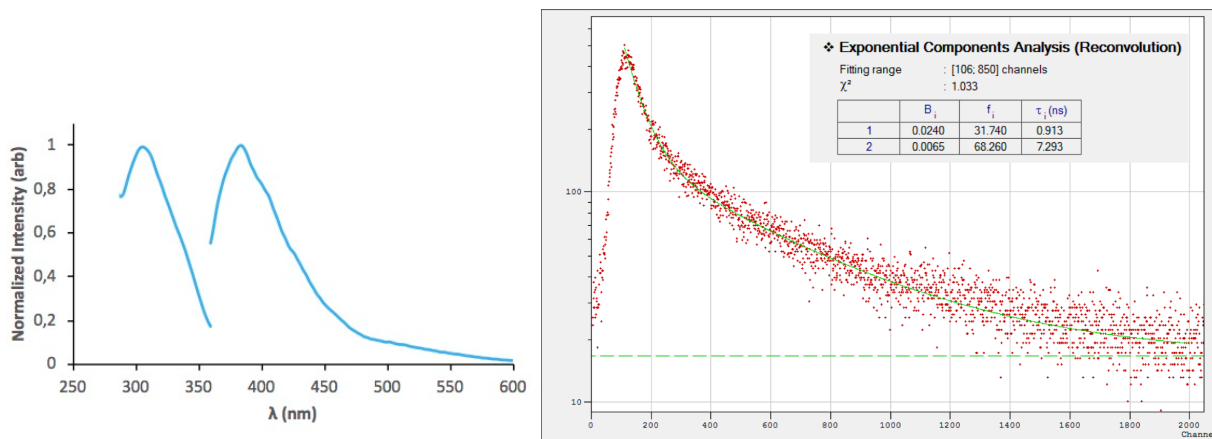


Figure S67. Luminescence spectra and emission decay profile of **7** (CH_2Cl_2).

Excitation and emission data at different temperatures

Table S2. Luminescence data for the gold complexes (4-7) in the mesomorphic states.

Compound ^a	SmC*				SmA			
	$\lambda_{\text{max, ex}}$	$\lambda_{\text{max, em}}$	$\tau/(\mu\text{s})$	$T^a/^\circ\text{C}$	$\lambda_{\text{max, ex}}$	$\lambda_{\text{max, em}}$	$\tau/(\mu\text{s})$	$T^a/^\circ\text{C}$
4	-	-	-		329	536	0.08	95
5	330	536	0.13	85	330	533	0.04	115
6	329	531	0.15	80	322	526	0.05	115
7	-	-	-		330	529	0.26	66

λ : nm.

Excitation and emission spectra at different temperatures

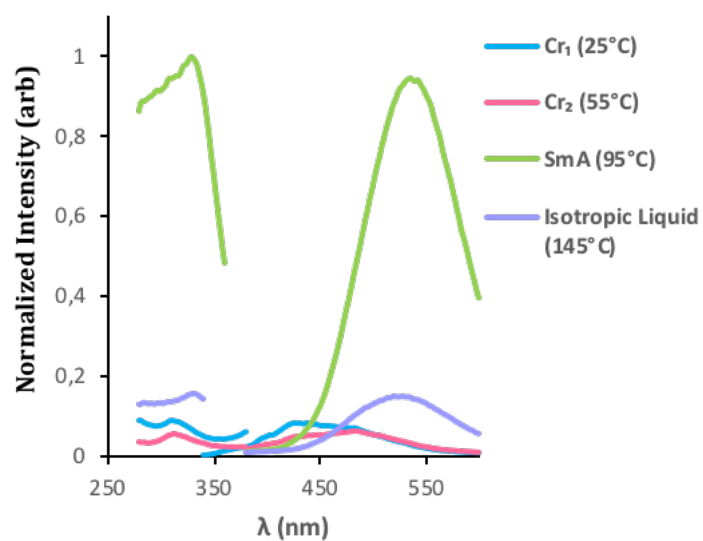


Figure S68. Excitation and emission spectra ($\lambda_{\text{exc}} = 329$ nm) of 4.

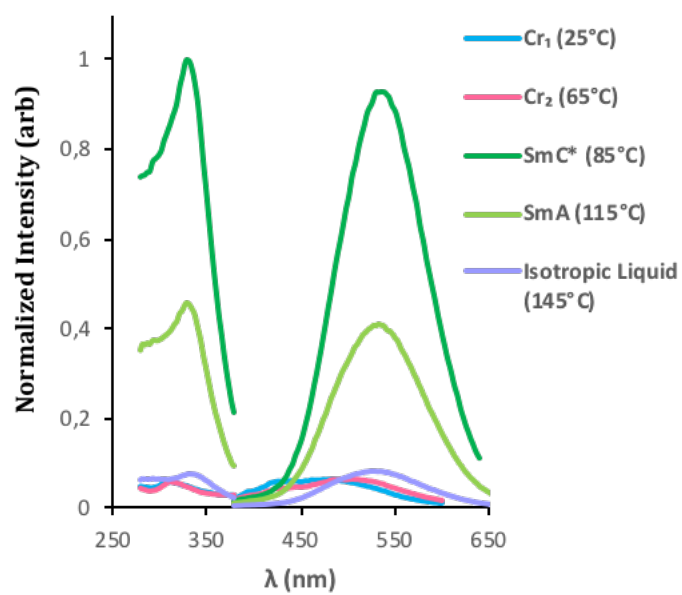


Figure S69. Excitation and emission spectra ($\lambda_{\text{exc}} = 330 \text{ nm}$) of **5**.

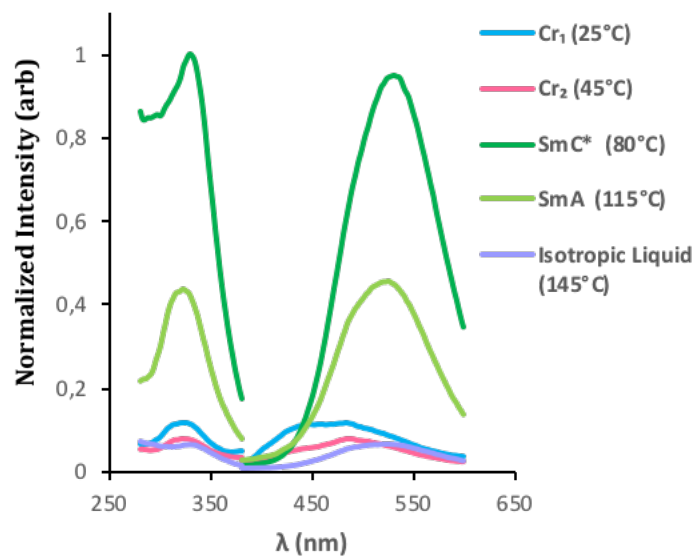


Figure S70. Excitation and emission spectra (SmC*: $\lambda_{\text{exc}} = 329 \text{ nm}$, SmA: $\lambda_{\text{exc}} = 322 \text{ nm}$) of **6**.

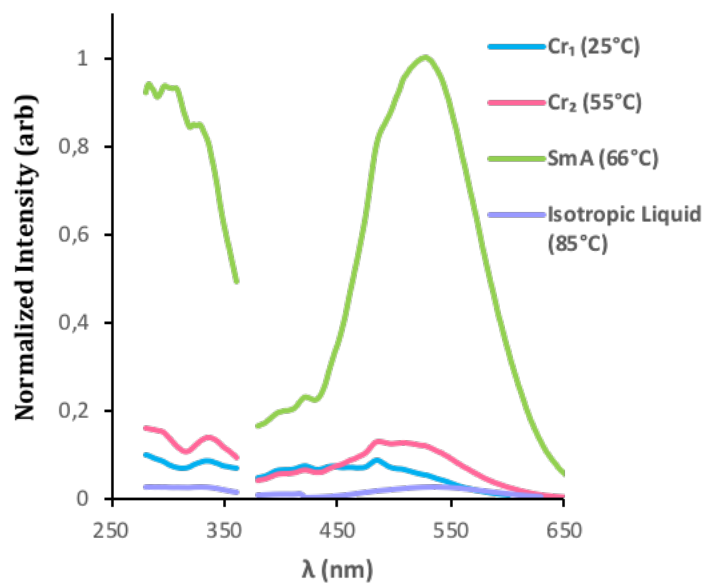


Figure S71. Excitation and emission spectra ($\lambda_{\text{exc}} = 330 \text{ nm}$) of **7**.

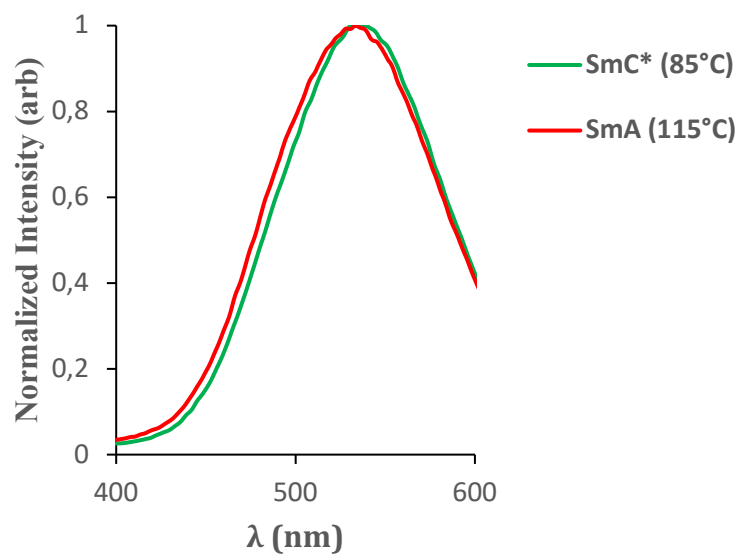


Figure S72. Emission spectra ($\lambda_{\text{exc}} = 330 \text{ nm}$) of **5** among the different mesophases.

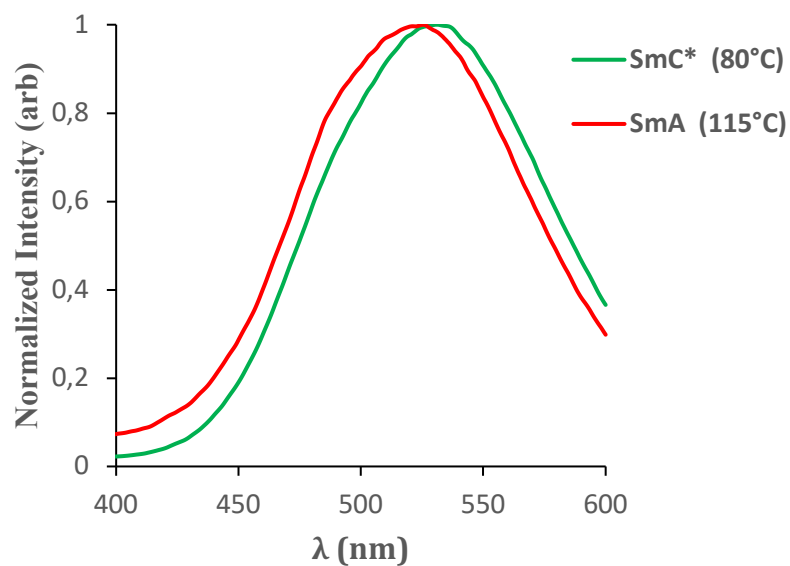


Figure S73. Emission spectra (SmC*: $\lambda_{\text{exc}} = 329$ nm, SmA: $\lambda_{\text{exc}} = 322$ nm) of **6** among the different mesophases.

Emission Decay Profiles in mesophase (excitation LED 375 nm).

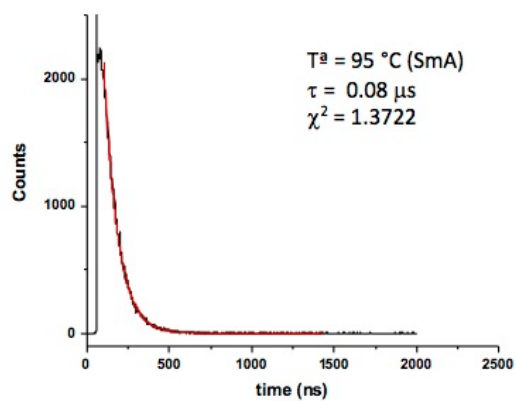


Figure S74. Emission decay profile of **4** in the SmA mesophase at 95 °C.

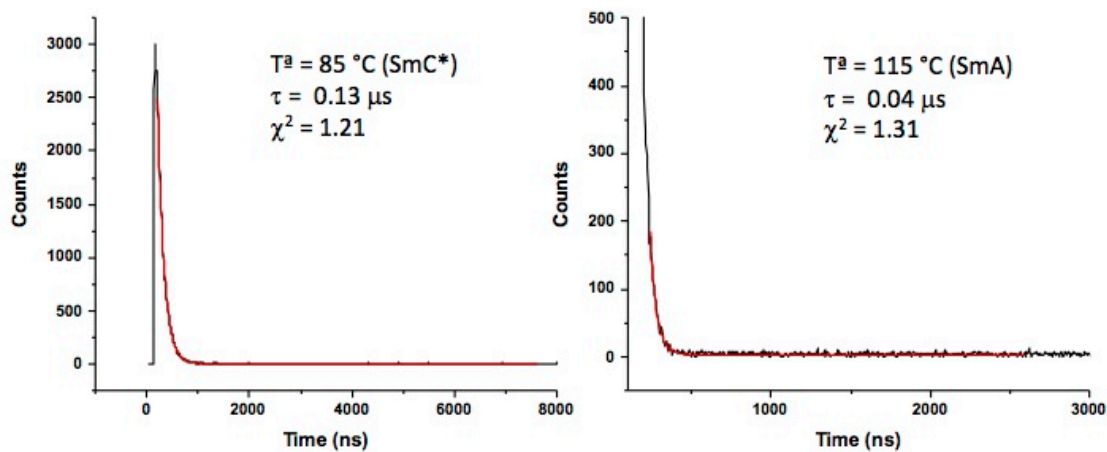


Figure S75. Emission decay profile of **5** in the mesophases: a) SmC* at 85 °C, b) SmA at 115 °C.

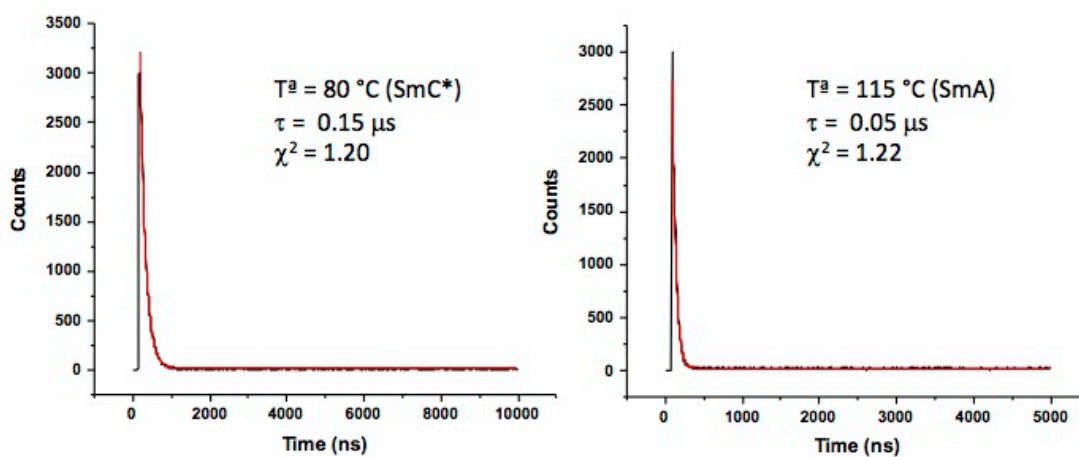


Figure S76. Emission decay profile of **6** in the mesophases: a) SmC* at 80 °C, b) SmA at 115 °C.

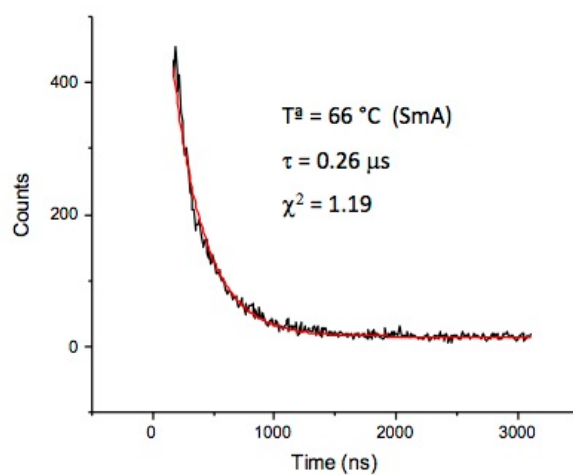


Figure S77. Emission Decay Profile of **7** in the SmA mesophase at 66 °C.

X-ray diffraction diagrams

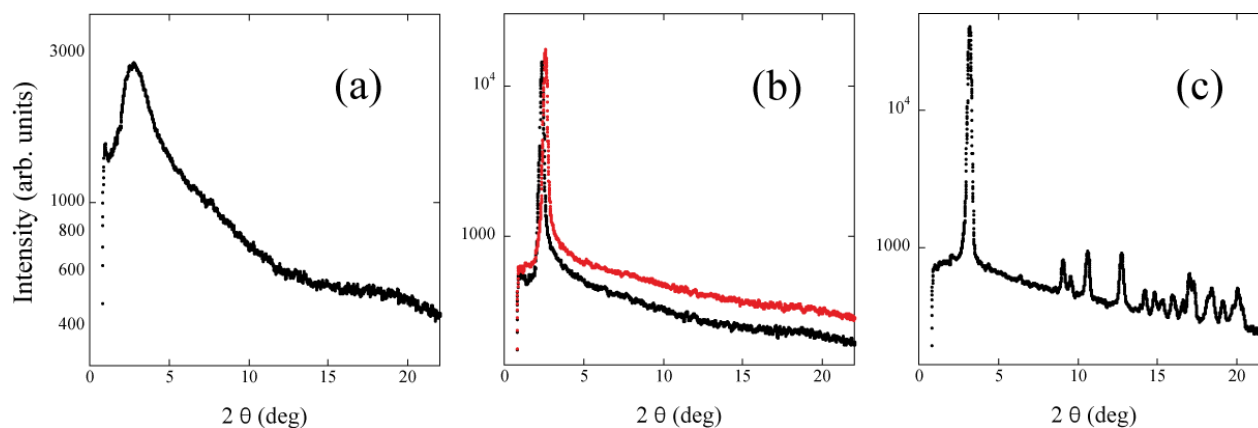


Figure S78. X-ray diffraction patterns of compound 2. (a) Isotropic phase. (b) Interdigitated SmA (black) and SmC* (red). (c) Crystal.

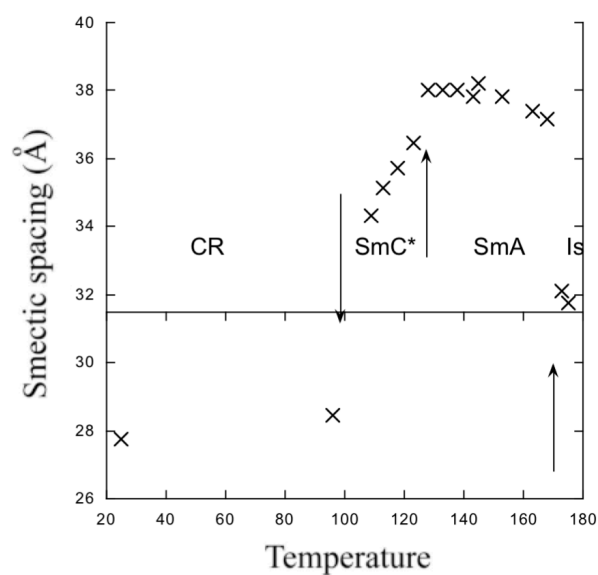


Figure S79. Smectic spacing vs temperature for compound 2. The transitions between the different phases are marked with arrows.

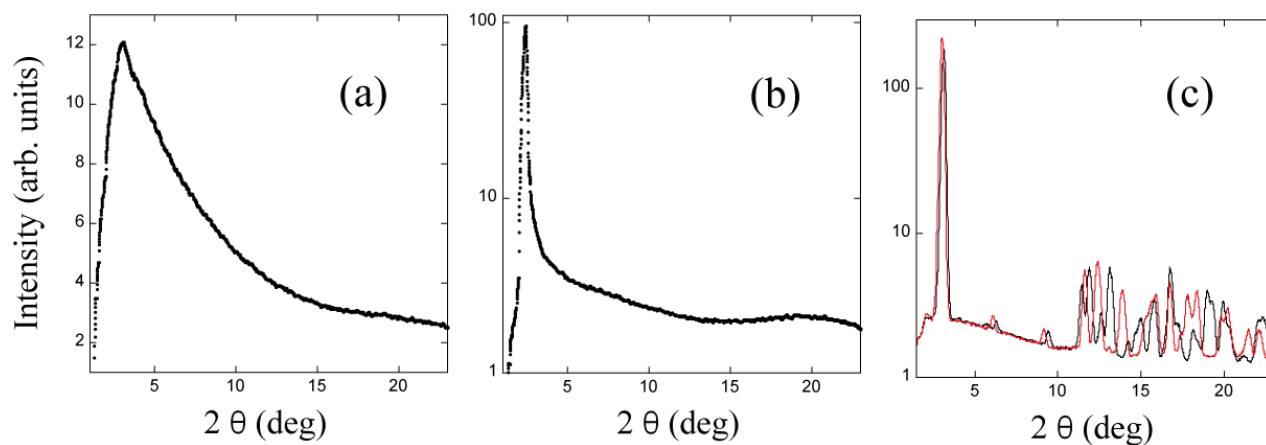


Figure S80. X-ray diffraction patterns of compound **5**. (a) in the isotropic phase. (b) in the interdigitated smectic A phase, where the layer spacing is 35 Å. (c) at 25 °C in the Cr₂ phase, just after cooling (red line), and in the Cr₁ phase after relaxing for a few hours (black line).

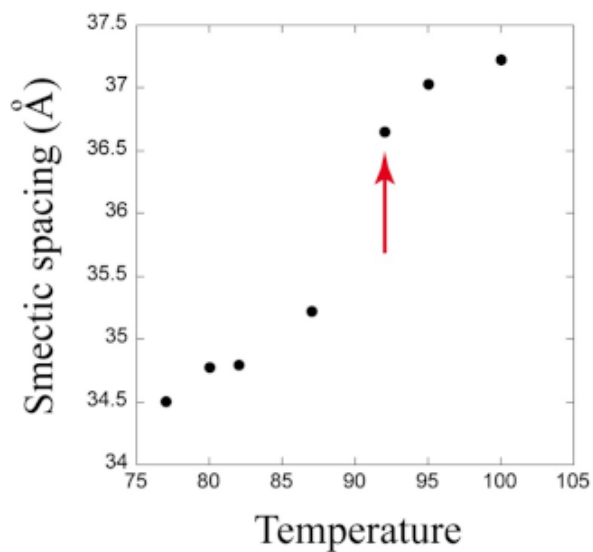


Figure S81. Smectic spacing vs temperature for compound **5**. A transition to a tilted SmC* phase occurs at 92 °C on cooling (red arrow).

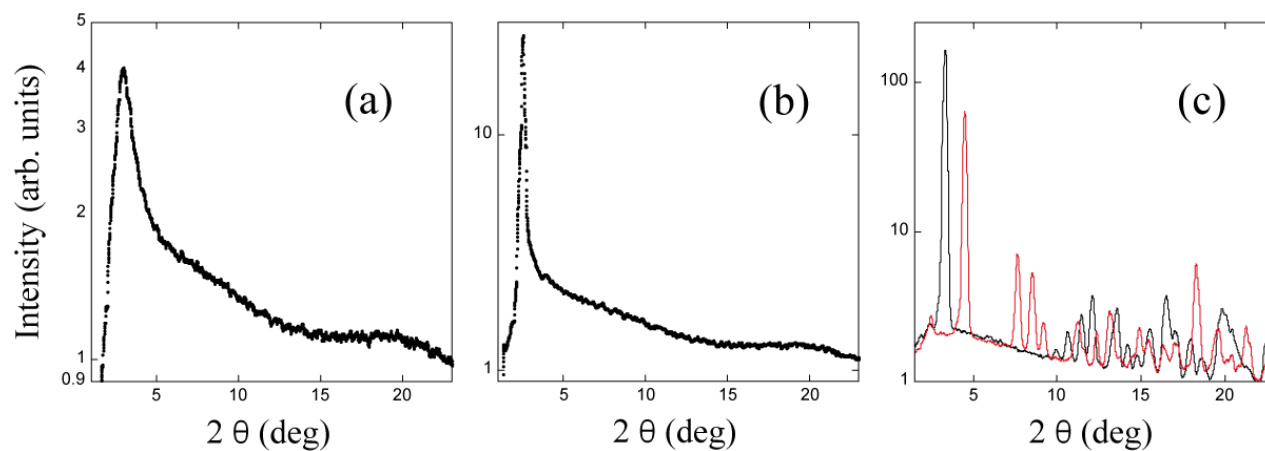


Figure S82. X-ray diffraction patterns of compound **7**. (a) in the isotropic phase. (b) in the interdigitated smectic A phase, where the layer spacing is 35 Å. (c) at 25 °C in the Cr₂ phase, just after cooling (red line), and in the Cr₁ phase after relaxing for a few hours (black line).

References

- ¹ S. Coco, C. Fernández-Mayordomo, S. Falagán, P. Espinet, *Inorganica Chim. Acta.*, 2003, **350**, 366.
- ² T. Kaharu, T. Tanaka, M. Sawada, S. Takahashi, *J. Mater. Chem.* 1994, **4**, 859.
- ³ R. Usón, A. Laguna, J. Vicente, *J. Organomet. Chem.* 1977, **131**, 471.
- ⁴ R. Bayón, S. Coco, P. Espinet, *Chem. Mater.* 2002, **14**, 3515.
- ⁵ Mitsunobu, O. *Synthesis* 1981, 1.